DOI:10.14753/SE.2024.2911

SEMMELWEIS EGYETEM

DOKTORI ISKOLA

Ph.D. értekezések

2911.

HERNYES ANITA

Szív- és érrendszeri betegségek élettana és klinikuma
című program

Programvezető: Dr. Merkely Béla, egyetemi tanár

Témavezető: Dr. Tárnoki Dávid László, egyetemi docens

DOI:10.14753/SE.2024.2911

GENETIC BACKGROUND OF TRAITS CONTRIBUTING TO REDUCED CORONARY BLOOD FLOW

PhD thesis

Anita Hernyes

Doctoral School of Theoretical and Translational Medicine

Semmelweis University

Supervisor: Dávid László Tárnoki, Ph.D

Official reviewers: Dávid Sándor Győri, Ph.D
Edit Várady, Ph.D

Head of the Complex Examination Committee:
Tivadar Tulassay, member of MTA

Members of the Complex Examination Committee:
Kinga Karlinger, member of MTA
Arnold Tóth, Ph.D

Budapest
2024

DOI:10.14753/SE.2024.2911

TABLE OF CONTENTS

DOI:10.14753/SE.2024.2911

DOI:10.14753/SE.2024.2911

List of Abbreviations

4S_hyper	four-segment score of hyperechoic plaques on carotid-femoral ultrasound
4S_hypo	four-segment score of hypoechoic plaques on carotid-femoral ultrasound
4S_mixed	four-segment score of mixed plaques on carotid-femoral ultrasound
4S_mixed/hyper	four-segment score of mixed and/or hyperechoic plaques on carotid-femoral ultrasound (any plaque containing calcification)
4S_PL	four-segment plaque score (any type) on carotid-femoral ultrasound
A	additive genetic effects
ABS	atherosclerosis burden score
ACE	angiotensin-converting enzyme
ACE model	hypothetic (full) model where latent factors A, C and E explain phenotypic variation, frequently used in twin studies – quantitative genetic research. Submodels consist of AE, CE or E model.
ACS	acute coronary syndrome
AHAA/ACC	American Heart Association/ American College of Cardiology
AIC	Akaike Information Criterion – model selection is based on the principle of parsimony: sufficiently good fitting model with least AIC value (thus least explaining factors) is preferred over more complex models.
AIx	augmentation index
AP	augmented pressure
Apo	apolipoprotein
ATB	atherosclerotic burden
BMI	body mass index
B-mode	brightness-mode, frequently used ultrasound imaging method
BP	blood pressure
C	common environmental effects
Ca	calcium
CAC	coronary artery calcification
CACS	coronary artery calcification score
CAD	coronary artery disease
CBF	coronary blood flow
cf-PWV	carotid-femoral pulse-wave velocity

CHD	coronary heart disease
CI	confidence interval
CIMT	carotid intima-media thickness
COL4A1	collagen type IV, alpha1
cov_e	environmental covariance
cov_g	genetic covariance
CPP	coronary perfusion pressure
CT	computed tomography
CV	cardiovascular
CVD	cardiovascular disease
CXCL14	C-X-C Motif Chemokine Ligand 14
DBP	diastolic blood pressure
df	degrees of freedom
DM	diabetes mellitus
DZ	dizygotic
E	unique environmental effects
ECG	electrocardiogram
ENPP1	ectonucleotide pyrophosphatase/phosphodiesterase 1
ESC/ESH	European Society of Cardiology, European Society of Hypertension
EVA	early vascular ageing
FH	familial hypercholesterolemia
GWAS	genome-wide association studies
h^2	heritability
HF	heart failure
HR	heart rate
HT	hypertension
IAP	International Atherosclerosis Project
ICD	implantable cardioverter defibrillator
IHD	ischemic heart disease
IMT	intima-media thickness
IR	insulin resistance
LDL	low-density lipoprotein

LVEDP	left ventricular end-diastolic pressure
MAP	mean arterial pressure
MESA	Multi-Ethnic Study of Atherosclerosis
MGP	matrix ɣ-carboxyglutamic acid protein
MI	myocardial infarction
MMP	matrix metalloproteinase
MZ	monozygotic
NO	nitric oxid
NSTEMI	non-ST-elevation myocardial infarction
PESA	Progression of Early Subclinical Atherosclerosis
Pi	inorganic phosphate
PP	pulse pressure
PWV	pulse-wave velocity
r_A	additive genetic component of tetrachoric correlation
RAAS	renin-angiotensin-aldosterone system
r_C	common environmental component of tetrachoric correlation
r_{DZ}	intra-pair correlation among dizygotic twins
r_e	environmentral correlation
r_g	genetic correlation
r_{MZ}	intra-pair correlation among monozygotic twins
ROC	receiver operating curve
R-R	time interval between two consecutive R waves on ECG.
RT	return time, time difference between first and reflected systolic wave
SBP	systolic blood pressure
SD	standard deviation
SEM	structural equation modeling
SNP	single nucleotide polymorphism
STEMI	ST-elevation myocardial infarction
TPR	total peripheral resistance
TREML-4	triggering receptor expressed on myeloid cells
VSMC	vascular smooth muscle cell
VVC	vascular-ventricular coupling

DOI:10.14753/SE.2024.2911

1. INTRODUCTION

Cardiovascular diseases (CVD) are the leading cause of death world-wide including a wide variety of related pathologies (both atherosclerotic and non-atherosclerotic). However, ischemic heart disease (IHD) and stroke are the two most common diseases among all CVDs which make the use of this term very practical, as risk factors and preventive approaches for these two pathologies overlap [1]. Approximately 85% of strokes are ischemic in origin [2]. Therefore, the majority of mortality today is due to atherosclerosis-related events [3]. Although using the term CVD indeed has practical utility, being an umbrella term, it also causes difficulties in determining the specific pathomechanisms or pathological entities observed in the extensively large variety of existing studies.

1.1. Ischemic heart disease - the most common cause of death

Ischemic heart disease is globally the leading cause of mortality for almost two decades, which manifests clinically as myocardial infarction (MI) or ischemic cardiomyopathy. Estimated prevalence was 1.655/100,000 world-wide in 2017 [4].

Myocardial ischemia is defined as cardiac function disorder due to insufficient blood flow towards the cardiomyocytes which may be due to the narrowing of coronary arteries, thrombotic events leading to obstruction, or less commonly diffuse narrowing of arterioles and other smaller vessels [5]. Acute coronary syndrome (ACS) clinically represents an episode of ischemia which has longer duration than a transient anginal episode and may lead to MI [6]. Entities covered by ACS are traditionally ST-elevation myocardial infarction (STEMI), non-ST-elevation MI (NSTEMI) and unstable angina. However, lately - with the widespread use of the biomarker high-sensitivity Troponin T – most cases of unstable angina would be converted to NSTEMI [7]. Another classification of MI events include Type I. MI caused by the rupture of an atherosclerotic plaque, thrombus formation and stenosis of the coronary lumen. Type II. MI represents other causes than coronary plaque rupture that cause imbalance between myocardial oxygen supply and demand, such as: hypotension, reduced coronary perfusion pressure, systemic hypoxia, anemia, high afterload or tachyarrhythmias [8].

Although Gupta et al. found similar prevalence for both types of MI (however type II MI patients more commonly died due to non-cardiac causes) and several pathomechanisms other than acute atherothrombotic events might cause cardiovascular death [8] – including worsening heart failure (HF) e.g. due to ischemic cardiomyopathy – the exact proportion of these mechanisms is currently not profoundly investigated. Autopsy data suggest that ischaemia might be the most prominent cause of mortality among patients with heart failure, increasing the risk of arrhythmias, worsening HF and sudden death. However, the role, causativity, exact associations and contributions of myocardial stunning and hibernation to mortality remain difficult to ascertain [9]. Another epidemiological study investigating major ischemic heart disease events in hospitalized and non-hospitalized patients found that acute MI was the most common cause of death in both groups. Any other causes were rare in the hospitalized patients, while in the non-hospitalized group, unspecified chronic IHD and atherosclerosis of the native coronary arteries were the other two most common causes. About 60% of IHD deaths occurred pre-hospitally and 60% of these patients have never been hospitalized before because of IHD [10].

In summary, although neither ‘cardiovascular’, nor ‘ischaemic heart diseases’ by definition doesn’t explain the most common pathomechanism of mortality, currently there is no evidence against the widely accepted concept that acute ischemic event from atherosclerotic origin is the most common cause of death.

1.2. Our current understandings of ischemic heart disease pathophysiology

In order to understand the complex pathophysiology of ischemic heart disease it is essential to review the peculiarities of the myocardium’s blood supply. The heart is a special organ because of several reasons: myocardial oxygen extraction rate is permanently close to maximal (70-80% under resting conditions), therefore increasing coronary blood flow is the only way to ameliorate oxygen consumption when the demand is higher. Coronary autoregulation normally allows a wide range of coronary perfusion pressure (CPP) between 60 and 180 Hgmm with corresponding changes in vascular resistance to suffice myocardial oxygen demand.

Coronary perfusion originates from the aortic root. These epicardial arteries will further branch in the myocardium and finally reach the endocardium where they form

plexuses. Physiologically endocardial blood flow is higher than epicardial blood flow (1.2:1) because higher wall stress requires more nutrients. Systolic myocardial contraction impedes left ventricular perfusion by compressing the traversing arterial branches, therefore left ventricular perfusion occurs mainly in diastole. The right ventricle doesn't generate such high pressure – it is perfused predominantly during systole and to a lesser extent during diastole [11,12].

Also, the regular "vascular waterfall" model (blood flows from highest towards lowest pressure) doesn't explain myocardial blood flow. A computer analysis rather suggests that forward flow consists of a proximal "pushing" forward and a distal "suction" backwards wave – later being the more prominent during diastole. Epicardial coronary arteries in this model might serve as reservoirs, where blood is stored until relaxation occurs [13]. In healthy individuals, epicardial arteries mean bare resistance to coronary blood flow (CBF). Smaller pre-arterioles (100-500 μm) are resistive vessels which can dilate or contract adjusting CBF in response to arterial pressure changes (coronary autoregulation) or myocardial nutrient demands (metabolic adaptation). In the intramural microvasculature (<100 μm) there is a significant pressure drop, allowing the oxygen and nutrient uptake of cardiomyocytes [14].

CPP of the left ventricle is calculated as the difference between aortic diastolic and left ventricular end-diastolic pressure (LVEDP) as majority of perfusion occurs during diastole. Reduction of CPP occurs both in coronary artery disease and heart failure making these patients more prone to myocardial ischaemia. Compensatory mechanisms through increased sympathetic drive in systolic heart failure increase aortic diastolic pressure to counterforce the elevated LVEDP as result of decreased ejection fraction. However, increases in systemic blood pressure also increase afterload, promoting cardiac remodeling and leading to the vitious circle of increasing myocardial oxygen demand. Tachycardia also worsens coronary blood flow as it shortens duration of diastole [11,12].

Atherosclerotic coronary artery disease (CAD) not only causes increasing resistance in the epicardial arteries but also worsens microvascular function due to endothelial dysfunction. Although many complications of coronary reperfusion are attributable to distal embolization in smaller arteries and microvascular dysfunction, currently there is a limited understanding of the later's role in adverse outcomes. Therefore, in vivo quantification methods of CBF and microvascular resistance should gain more

importance [14]. As Severino et al. highlight ischemic heart disease pathophysiology is more complex than the conventional conception of atherosclerotic plaque complication limiting CBF. In case of atherosclerotic lesions causing a significant stenosis, proximal resistance increases and distal CPP descreases. Autoregulation may be able to maintain normal CBF at rest, but the dilator reserve is compromised and lack of capacity to adjust higher metabolic demands may result in ischemia due to insufficient blood flow [15].

Chronic coronary artery atherosclerosis can also cause arteriolar remodeling and rarefaction with diminished vasodilator and exaggerated vasoconstrictor (e.g. due to reduced CPP) responses leading to CBF reserve reduction and microvascular dysfunction – a common cause of type II myocardial infarction. Microvascular dysfunction is commonly related to cardiovascular (CV) risk factors such as smoking, hypertension (HT), hyperlipidaemia, diabetes mellitus (DM) or insulin resistance (IR). Increased shear stress due to HT and higher blood flow velocity contribute to impaired endothelium-dependent dilation (or endothelial dysfunction) which was found to be the underlying cause in ~30% of women with IHD in the absence of epicardial coronary artery disease. Furthermore, in some patients, microvascular dysfunction seems to be attributable to impaired myocardial oxygen extraction rather than reduction of myocardial blood flow – a phenomenon which might be explained by reductions in capillary transit time heterogeneity [15,16].

Coronary spasm with or without atherosclerotic lesions, age-related ‘hydraulic modifications’ in coronary arteries – such as loss of endothelial layer integrity, intimal thickening, increasing collagen/elastin ratio leading to arterial stiffness and reduced vascular adaptability can further contribute to reduced CBF and the pathogenesis of IHD [15].

In conclusion, understanding physiological coronary blood flow is essential in understanding how deterioration of coronary perfusion is of key importance in the development of ischemic heart disease – at all levels of the coronary arterial vasculature.

1.3. The conflicting relationship between atherosclerosis, arterial stiffness, hypertension and vascular aging

The pathophysiology of atherosclerosis is complex and its definition consists of both thickening and loss of elasticity of the walls of arteries (which solely is called

arteriosclerosis), and atherosclerotic plaque formation within the arterial intima [17], which aspects are frequently used in a confusing manner. By using the term atherosclerosis, most authors don't specify if they mean it in this broader sense or narrow sense (only referring to atherosclerotic plaque formation) and some authors use this term defining atherosclerosis as atherosclerotic plaque formation in the arterial wall. However, carotid intima-media thickness (CIMT, thickening of the carotid arterial wall) is also commonly used as a surrogate marker for 'atherosclerosis' [18,19]. Reduced distensibility of the arterial wall – also called arterial stiffness – however is rather treated as a distinct entity highlighting the functional changes caused by structural changes in the arterial wall (mainly affecting the elastin/collagen ratio in the extracellular matrix). The illustration of the overlapping definitions is given in *Figure 1*.

It is hypothesized that arterial stiffness may have a causative role in the development of 'atherosclerosis' by endothelial and vascular smooth muscular cells (VSCMs) sensing the hemodynamic changes involved in arterial stiffness and promoting atherosclerotic plaque formation [20,21]. However, many other ideas were suggested: presence of 'atherosclerosis' leads to arterial stiffness, 'atherosclerosis' is both the consequence and - in later phase - the cause of stiffness, or these two aspects co-occur frequently without any causative association. It is also likely that the pathological changes of the arterial wall in the atherosclerotic process - in this sense not narrowed to plaque formation - might cause increased arterial stiffness [20,22,23]. Although separating arterial stiffness from atherosclerosis by definition doesn't seem to be a question worth investigating – understanding the relationship between atheroma formation, arterial stiffening occurring due to atherosclerosis and due to early or 'normal' vascular aging still remains challenging [24]. Hypercholesterolaemia might induce arterial stiffness through higher levels of circulating $CD31^{+}/CD42^{-}$ microparticles and lower levels of endothelial progenitors [25]. Oxidative stress and atherosclerotic plaque calcification are also thought to contribute to arterial stiffness in atherosclerosis [24].

The relationship of elevated blood pressure with arterial stiffness is also conflicting - it was a question of debate for a long time whether HT is a cause or a consequence of arterial stiffness. Breaking down HT to two different types helps understanding their associations: systolic/diastolic HT in midlife due to increased total peripheral resistance (TPR) is alone a cause of increased arterial stiffness without any obligatory changes in

the arterial wall. As intraluminal pressure is higher both during systole and diastole, it results in an increased stress to strain ratio on the viscoelastic aorta which determines its stiffness value. On the other hand, hypertension in the elderly (>70 years) is mainly systolic, while diastolic blood pressure remains normal or low, resulting in elevated pulse pressure. In this case, degenerative changes of the structure and mechanical properties of the arterial wall are the cause of systolic HT. In the stiff aorta both the forward and 'reflected' wave travel faster – and later one would superimpose the blood pressure curve resulting in elevated systolic pressure [26].

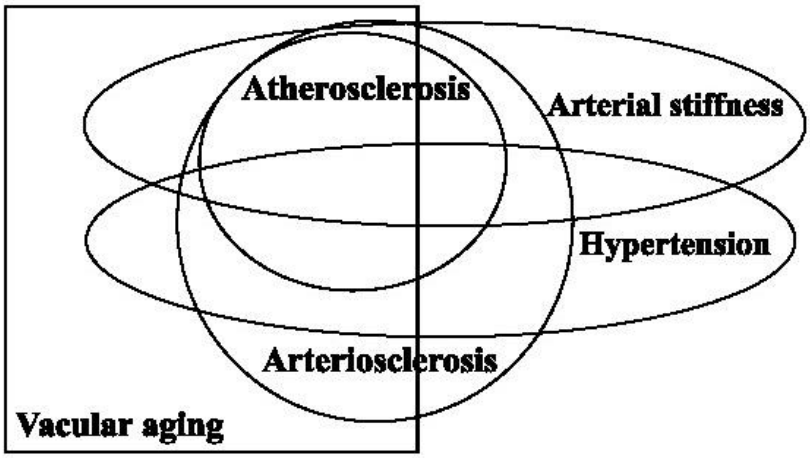

Figure 1. Relationship of frequently used terms in cardiovascular research. Vascular aging might include all pathologies, atherosclerosis is part of arteriosclerosis – definitions and pathomechanisms show overlap, however they also differ.

Normal aging of the vasculature involves structural and morphological changes of the arterial wall, which changes depend on the localization and type of the vessel. Large elastic arteries such as the aorta and carotid arteries tend to increase in diameter, length, intima-media thickness and stiffness. Peripheral arteries, which are more muscular have normally higher stiffness values and show less progression with aging. Pulsatile wall stress alone during a lifetime can cause fatigue and elastin fragmentation. Furthermore, the activity of specific types of matrix metalloprotease (MMP) enzymes increases with aging, which contributes to elastin degradation. The decreased bioavailability of desmosine and isodesmosine – which form crosslinks with elastin – also contributes to the deterioration of elastin functionality [24]. On the other hand, in the tunica media the number of VSMCs decrease and collagen takes place causing medial fibrosis. Collagen

I and III deposition also occurs in the adventitia layer. Collagen crosslinking by non-enzymatic glycation end products increases arterial stiffness further (also the main mechanism observed in diabetic patients). As a result, the elastin-collagen ratio of the extracellular matrix decreases, they become disorganized and the artery loses its distensibility. Calcium deposition and endothelial dysfunction are also known to increase stiffness with aging. Decreased bioavailability of nitrogen-monoxide (NO) results in impaired vasodilation, dysregulated vascular tone and increased arterial stiffness [21,24].

The concept of early vascular aging (EVA) is based on the finding that arterial stiffening is accelerated in people at higher cardiovascular risk and vice versa: people with increased arterial stiffness (for their age and gender) are at higher risk for CV disease, progression or complications. It is widely accepted that large arterial stiffness shows the actual state of cumulative effects of an individual's previous exposure to arterial damages and CV risk factors, thus arterial stiffness might be a 'tissue' biomarker [27,28]. It was also shown that determination of vascular or cardiometabolic age can improve patient compliance rather than CV risk assessment alone, which numerically might sound too low even in high-risk patients [29].

In summary, much huddle in the literature comes from the inconsistent use of definitions. Furthermore, overlaps in definitions, possible overlaps in pathomechanisms and other confounding factors commonly involved in cardiovascular risk (eg, diabetes or aging) seem to further complicate the understanding of arterial stiffness – which is an aspect of both arteriosclerosis and atherosclerosis as well as 'healthy' and early vascular aging. In essential hypertension of middle-aged patients, arterial stiffness can also be increased without morphological changes in the aortic wall.

1.4. Functional and morphological traits of atherosclerosis with emphasis on aortic stiffness, coronary artery calcification and their relation to coronary blood flow

Aortic pulse wave velocity (PWV) and augmentation index (AIx) are two indices for arterial stiffness, both being independent predictors of future CV events [30,31]. Van Popele et al. found strong association between aortic PWV and 'atherosclerosis' at different arterial sites suggesting that aortic PWV could be an indicator of generalized atherosclerosis [22].

Being the largest elastic artery, aorta also contributes to the vascular-ventricular coupling (VVC) effect thus physiologically it dampens pulse pressure oscillation resulting in a more steady-state flow as blood arrives to the smaller peripheral arteries [32]. Reduced distensibility of the aorta implies higher afterload and hypertrophy of the left ventricle, accelerated PWV, increased shear-wall stress and reduction of coronary perfusion thus worsening symptoms of myocardial ischemia in a manner of a vitious circle [33].

Decrease in coronary perfusion is due to the concept of the 'reflected wave' which is produced by altered impedances of the vasculature e.g. at the level of branches or the distal part of the aorta where the wall structure is already of more muscular type. The geometry, number and vasoconstrictive state of arterioles and the microvascular architecture also influence the reflected wave. This reflected wave normally arrives back to the aortic root in late systole-early diastole superimposing the ongoing pressure wave (physiological amplification) and allowing ideal coronary flow. Stiff arteries on the other hand return this wave earlier resulting in higher peak systolic pressure (also causing systolic hypertension) and less optimal coronary blood flow (due to pressure augmentation) [34].

Indeed, multiple studies showed that increased aortic stiffness is associated with a decrease in coronary blood flow (mainly affecting subendocardial flow) during increased left ventricular contraction, in the presence or absence of coronary stenosis and reduced coronary flow reserve after successful revascularisation [35-37]. In contrary, a distensible aorta was associated with higher increase in coronary blood flow after successful percutaneous intervention therapy [38]. In a hydraulic model with the most stiffened aorta coronary blood flow was only 1% of the output of the 'ventricular' pump, while with a more distensible aorta coronary blood flow could be increased up to 18% - although this model lacks the effect of many other in vivo physiological factors, e.g. coronary autoregulation [39].

The relationship between PWV and distensibility can be expressed by the Bramwell-Hill equation:

$$c_o = \sqrt{V \times dP/\rho \times dV} \tag{1.1}$$

where c_o is speed of blood flow, dP is change in pressure causing the change in volume, dV is change in volume and ρ is density of the fluid. Therefore, blood velocity

is inversely related to distensibility (dV/VxdP). The Moens-Korteweg equation, from which the previous was derived describes the relation with another stiffness parameter, the Young's elastic modulus (E) – which expresses the ratio of wall stress and strain.

$$c_o = \sqrt{Eh/2R\rho} \quad (1.2)$$

Here, h is wall thickness and R is radius of vessel lumen. As we can see speed is positively associated with the elastic modulus (therefore positively associated with stiffness and negatively associated with strain or elasticity) [40]. Thus, aortic PWV is considered a direct a measurement of arterial stiffness, representing the arterial wall's mechanical properties.

The gold standard method of measuring aortic stiffness is the non-invasive carotid-femoral pulse-wave velocity (cf-PWV) assessment – which is also recommended to use (Class I; Level of Evidence A). Although, many other measurement methods exist, it is recommended that they should be validated non-invasively, or if this is not possible, they should be validated against a non-invasive device that has been used in prospective trials showing an independent prognostic value of PWV [41].

The importance of pressure augmentation is expressed by the AIx which denotes the proportion of this augmented pressure wave to the magnitude of central pulse pressure (PP). However, AIx is not considered an intrinsic marker of arterial stiffness as it is also influenced by heart rate (HR), PWV and the amplitude of the reflected wave [34]. Given the latest component, AIx is thought to rather represent the vasomotor tone in the peripheral, smaller arteries as contributors to wave reflection. The increased AIx was also shown to reduce coronary flow reserve in revascularized patients [35].

Coronary artery calcification (CAC) assessed by cardiac CT is nonspecific regarding which type of arterial calcification is visualized, however it most commonly represents atherosclerotic 'intimal' calcification. CAC represents the extent of CAD, in general it correlates with the total plaque burden of the coronary arteries. The gold standard method to measure CAC is the Agatson-score, which sums lesions' total calcified area and maximum density of calcification because of its simplicity [42]. Although other methods also exist and additive information such as type, location, extent and volumes of the plaques would be beneficial for describing plaque vulnerability or stability – the Ca (calcium) score is still useful for the CV risk prediciton probably due to its correlation with the extent of underlying disease. Furthermore, it is known that histologically

fibrocalcic plaque type is most heavily calcified, which involves lumen narrowing and patients with very high CAC scores have a high probability for experiencing stress-induced ischaemia. Also, a study found that patients with acute MI had higher calcification area and more coronary segments involved than the control group [42]. Indeed, CAC was found in association with impaired myocardial perfusion and lower myocardial blood flow under stress [43,44].

The exact pathomechanism of vascular calcification is not yet fully understood and is still extensively researched. The original theory that calcification might be a passive degenerative process seems to be overwritten by recent evidence that suggest that it is an active process. It is known that macrocalcification builds up from microcalcification which is facilitated in an elastin-poor environment [45].

Chronic inflammation might induce microcalcification by the apoptosis and necrosis of macrophages together with the compromised clearance of apoptotic bodies which would allow Ca and inorganic phosphate (Pi) to precipitate. Microcalcification in turn promotes further inflammation in a manner of a vicious cycle. In addition, extracellular vesicles produced by macrophages may serve as calcification foci. VSMCs can differentiate to osteochondrocyte-like cells and induce bone formation – however this process is more less frequent in humans [46, 47].

In conclusion, both aortic stiffness and CAC score are independent cardiovascular predictors and both can contribute pathophysiologically to reduced coronary blood flow through the above mentioned mechanisms. Aortic stiffness might also be suggestive of concomitant coronary stiffness causing further impairment of coronary flow reserve and myocardial perfusion. Both methods are acquired non-invasively, giving information indirectly about coronary flow and CV risk, however coronary CT (computed tomography) involves radiation exposure.

1.5. Cardiovascular risk prediction - recommendations and the concept of atherosclerosis burden

It is currently known that CV risk calculation based on the traditional risk factors alone has limitations. Also, patients tend to adhere to lifestyle changes and accept medication more if they are confronted by their vascular or cardiometabolic age, compared to other people in their age and gender group [29].

The term atherosclerotic burden (ATB) is used to describe an individual's overall affection by atherosclerosis considering that it might be generalized and is supposed to express the individual risk of future CV events in a more direct way than traditional risk factors indirectly do. Although measurement of ATB in one single arterial bed is easy to obtain, there is no general consensus on which parameter represents global burden the best [48]. Measurement of carotid IMT for example was recommended, but later removed from the American Heart Association/American College of Cardiology (AHAA/ACC) guidelines possibly because of conflicting study results regarding its additive value to classic risk prediction models [49].

Arterial stiffness is a predictor of CV events and all-cause mortality, also in asymptomatic individuals – therefore it has been proposed to be an early indicator of CV risk [50]. In a scientific statement from the American Heart Association, it is recommended Class II a (reasonable) to determine arterial stiffness in order to provide incremental information beyond standard CVD risk factors in the prediction of future CV events – at evidence level A [41]. However, latest review about current guidelines lists a limited current role of arterial stiffness in the CV risk prediction. Chinese, Korean and Japanese hypertension guidelines recommend the measurement of PWV mainly as indicator of target organ damage. The 2016 European Guidelines on Cardiovascular Disease Prevention in Clinical Practice, 2018 ESC/ECH (European Society of Cardiology, European Society of Hypertension) Guidelines for the Management of Arterial Hypertension and the 2020 International Society of Hypertension Global Hypertension Practice Guidelines acknowledge arterial stiffness as additive information to improve cardiovascular risk, however they do not recommend its routine or systematic use, other guidelines do not mention the measurement of stiffness [51].

Frequently expressed as Agatston score, the coronary artery calcification score (CACS) is a very promising, robust CV risk predictor and it is currently recommended to screen among patients with borderline-intermediate 10-year CV risk (5-20%), or in uncertain cases of indicating statin therapy [52]. CACS is also representative of atherosclerosis burden of the coronary arteries, therefore it is promising ATB marker [48]. The absence of CAC was associated with an excellent 10-year survival rate [53], however, moderate and severe CAC increased the adjusted risk of coronary events by a factor of 7.73 and 9.67, respectively. Prediction of coronary events was also better when

CACS was added to traditional Framingham risk scores, than traditional risk factors alone [54]. The Multi-Ethnic Study of Atherosclerosis (MESA) found CAC to be predictive of broader CV outcomes too, including stroke [55]. Although CAC screening was found to be a cost-effective screening strategy, there are concerns about the right scoring method and radiation exposure also limits its wide-spread use [56].

Although coronary arteries are currently not possible to visualize in a non-harmful non-invasive way, there is overall limited data about the multi-vessel approach to atherosclerosis and its relation to CV risk. However, there is growing interest in screening extracoronal arteries and determining their value in CV risk assessment [57-60]. Based on the International Atherosclerosis Project (IAP) from the ‘60s, a commonly taught approach is that within individuals, the severity of atherosclerosis in one artery does not predict the severity in another artery in autopsy specimens [61]. However, multiple studies ever since found inter-bed correlations between different arterial segments [62-63], moreover, the extension or generalized state of atherosclerotic disease has also been investigated e.g. in the PESA (Progression of Early Subclinical Atherosclerosis) study and found that CAC is seldom present as a monovascular disease [64].

In summary, the concept of atherosclerosis burden theoretically would select one atherosclerotic trait which could give direct evidence of increased CV risk outside the indirect role of traditional risk factors. However, choosing one trait is still a question of debate. Also, current guidelines are careful with recommending screening of atherosclerosis on a population level possibly because of lack of convincing amount of evidence. Aortic PWV and coronary calcification score has some limited role in current guidelines. Aortic stiffness was also proposed to be a marker of generalized atherosclerosis and coronary calcification score is known to reflect the atherosclerotic burden of coronary arteries.

1.6. What is known and unknown about the genetic background of atherosclerosis?

The role of twin studies

Despite great advances and expansive knowledge, being a complex disease, atherosclerosis is still not fully understood. Different stages of the disease include initiation, progression, rupture and calcification of atherosclerotic plaque. In a nutshell,

endothelial dysfunction - especially in the environment of disturbed blood flow - predispose the vessel wall to lipid infiltration, which together with the oxidation of captured low-density lipoprotein (LDL) particles induce a plethora of inflammatory and 'adaptive' response mechanisms including endothelial activation, leukocyte adhesion, macrophage activation, VSMC activation (both forming foam cells), VSMC migration and phenotypic alteration forming a fibrous cap, programmed apoptosis and efferocytosis (clearance of dead macrophage and VSMC cells). A sustained microinflammatory environment together with the imbalance of accumulating oxidized LDL and cholesterol versus their phagocytosis, also the imbalance between cell death versus their clearance can lead to plaque progression. Sustained inflammation can also weaken the fibrous cap by cytokines that inhibit collagen production of VSMCs. If the thrombogenic necrotic core is exposed to the blood in the lumen, coagulation process is initialized and thrombus formation occurs which can further increase the size of the plaque, obstruct the vessel or cause distal embolization [65].

Although atherosclerosis is conventionally thought to be a modern disease, multiple evidence shows that ancient people already had atherosclerosis – including hunter-gatherers [66-68]. Outside the Mendelian monogenic heredity of familial hypercholesterolemia (FH) (and other rare forms such as: Tangier disease, sitosterolaemia, Hutchinson-Gilford progeria sy. and other laminopathies, or familial defective apolipoprotein B) most cases evolve because of polygenic effect summing from multiple frequent single nucleotide polymorphisms (SNP). These SNPs one-by-one are thought to have only subtle effect on disease phenotypes making it difficult to clarify significant genetic pathways. Although there is also difficulty in replicating the results of atherosclerosis genetic studies, assessment of individual polygenic risk score as the earliest moment for assessing future CV risk and introducing preventing strategies might be already on the horizon waiting for standardization [69].

Although up- and downregulation of some specific genes as part of some specific pathways in the development and progression of atherosclerosis were described [70-74], the full image is still not well understood - there are still missing dots connecting discovered genes through pathophysiological pathways to phenotypic variance of atherosclerosis traits. Notably, carotid IMT as 'surrogate for atherosclerosis' was used in a lot of genetic studies raising the question of which atherosclerosis phenotype would

be the best to investigate. Carotid endarterectomy specimens and genetic analysis of plaque cellular components is a more direct way, but the availability of these specimens is limited, many times failing to reach favorable population size. Also, plaque phenotypes might differ regarding their advanced or non-advanced stage, in this regard genetic studies could further refine whether they concentrate on the initial or later stage of any disease e.g. calcification [75]. The question of genetic contribution to the longitudinal changes is also of major importance because it is suggested that any systematic or regional inflammation far from the plaque itself could provoke rapid changes in plaque progression, therefore atherosclerosis might not progress continuously but rather in phases [76].

Even fewer studies concentrate on the genetic background of multivessel or generalized atherosclerosis failing to see the involvement of one vessel as part of a possibly larger picture and the potential importance of atherosclerotic plaque location. It is known that despite the systemic effect of risk factors plaque localization is not random. However, the role of differing haemodinamics and the role of differing ability of the endothelium to express atheroprotective genes are still not confirmed [77]. Although it is quite well-established, that plaques are frequently located near the bifurcations and also some studies have found overlapping and differing genes regarding plaque locations [78-81] - the aspect of plaque location is often overlooked.

Twin studies can have a major role in answering these questions. Classical twin study design is a form of quantitative genetics, where the effect of unobserved genes on the phenotypical population variance can be quantified by using known genetic relationships. Therefore, without knowing the exact genes involved or conducting expensive research methods we can estimate the magnitude of the sum of genetic effects on the expression of given trait, also by using less participants [82-83]. By comparing monozygotic (MZ) to dizygotic (DZ) twins, based on their intra-pair similarities and differences we can estimate the magnitude of contributing genetic vs. common or unique environmental effects on the development of given trait. Twin siblings represent a unique (age-, genome-, upbringing- and major lifestyle-matched) control group – this study model infers less stochastic effects than any other study population. In a classical univariate twin study model we can decompose the total phenotypic variance into variances of genetic versus environmental origin - based on the expected versus observed

within-pair covariance values in the MZ and DZ twins. Model fitting methods are used to find the best explanation to our observations. As a result, heritability estimate of the trait will give the percentage of phenotypic variance attributed to the genotypic variance on the population level [84].

Furthermore, bivariate and multivariate twin models can be used to examine more than one phenotypic trait. In bivariate models, the within-pair covariance and the cross-trait within-person covariance can add valuable information and increase power compared to univariate models, making it possible to calculate both heritability and bivariate heritability (proportion of covariance between two traits explained by genetic factors). Genetic covariance and genetic correlation between traits can provide results comparable to molecular genetic studies, giving reliable estimates about the overlap in sets of genes contributing to associated complex traits [83]. These twin models can help discover and understand the possible common genetic origin of different traits.

Bivariate and multivariate twin models can also be used on longitudinal data giving valuable information e.g. on the age-relatedness of diseases, longitudinal genetic stability of given traits, or also examine developmental starting points and trajectories which are influenced by genetic factors. Moreover, genome-wide association studies (GWAS), epigenetic, gene-environment and longitudinal studies -among others - offer new insights in disease pathways and promise the discovery of novel disease reversal options – all these studies in the ‘omics’ era can also profit from the benefits of twin study subjects [85].

In summary, evidence shows that atherosclerosis is not merely a modern disease. Due to its complex polygenic background we face difficulties in finding significant, replicable genetic pathways. Specification of atherosclerotic traits in regard of location or disease progression state could help establishing common or differing genetic contributors and better understanding of underlying pathomechanisms. Twin studies offer the possibility to investigate the genetic background of given traits on a population level with less stochastic effects than any other study population.

DOI:10.14753/SE.2024.2911

2. OBJECTIVES

Currently three robust and promising CV risk predictor traits were at the center of our research (which are also potentional ATB markers): aortic PWV, aortic AIx and CACS. We were looking for a correlation between CACS and aortic stiffness , however we found higher correlation with the in house developed 4-segment scores of uni-/bilaterality of carotid/femoral atherosclerotic plaques. Our aim was to better understand the underlying genetic factors' contributions to these atherosclerotic phenotypes in multinational and national twin study populations (*Figure 2*).

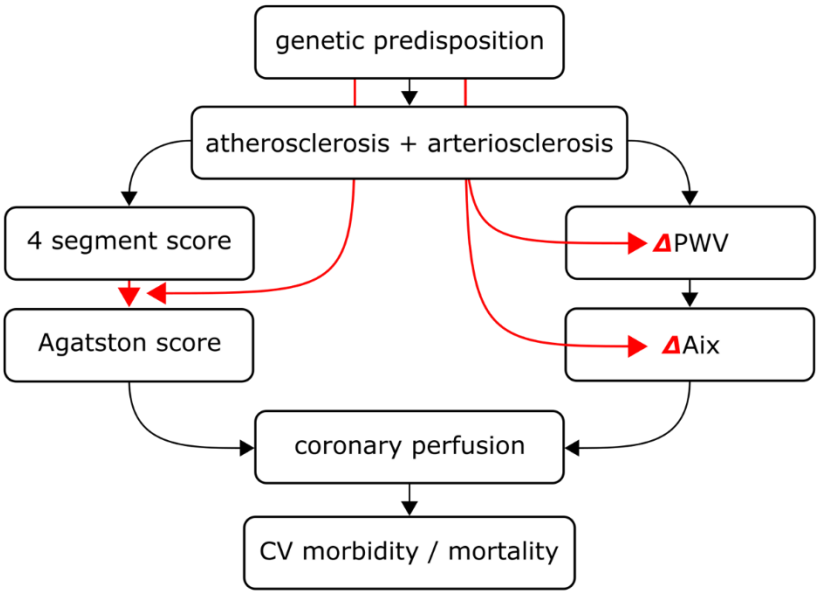

Figure 2. Rationale of our research. We aimed to examine the genetic predisposition to traits contributing to reduced coronary perfusion and increased cardiovascular risk. We examined both the genetic relationship between coronary and extracoronary atherosclerosis and also the longitudinal genetic predisposition to arterial stiffness parameters. Abbreviations: PWV: pulse wave velocity; AIx: augmentation index; CV: cardiovascular. (Own image).

Specific Aim 1: To determine the magnitude of genetic vs environmental contributors to aortic PWV and aortic AIx on the longitudinal run.

Hypothesis: Aortic stiffness as a marker of vascular 'aging' progression with time might be primarily influenced by genetic factors.

Approach: One hundred and eighty-four twin pairs from the Hungarian [86] and Italian Twin Registry [87] were followed up during a time period of 4.4 years. Within-individual/cross-wave, cross-twin/within wave and cross-twin/cross-wave correlations were calculated, bivariate Cholesky models were fitted to calculate additive genetic (A), shared environmental (C) and unique environmental (E) components.

Specific Aim 2: To assess phenotypical and possible genetic correlation between CAC and severity score of carotid/femoral atherosclerosis.

Hypothesis: We hypothesized that an ultrasound-derived trait investigating the carotid and femoral arteries could well represent the severity of extracoronal atherosclerosis, and this trait would correlate with the severity of coronary atherosclerosis as expressed by Agatston score.

Approach: Our in house developed 4-segment score assessing uni/bilaterality of carotid/femoral atherosclerosis correlated best with CACS when hyperechoic (calcified) or mixed plaque score was calculated (4s_mixed/hyper). Age and sex-adjusted bivariate ACE modeling (correlated factors model) was used for the genetic (rA) vs. environmental (rC) decomposition of phenotypic similarity between CACS and 4S_hyper (four-segment score of hyperechoic plaques on carotid-femoral ultrasound) using a liability-threshold structural equation model.

We further decomposed the genetic correlation to investigate underlying co-occurrences in coronary-carotid and coronary-femoral atherosclerosis by concordant and discordant twin pairs showing overlapping or differing patterns.

DOI:10.14753/SE.2024.2911

3. METHODS

3.1 Basic principles of twin statistical methods

This chapter was written based on several different sources [82-83,88-90]. In classic twin studies we use the known genetic relationships to estimate the magnitude of the effect of unknown genes (quantitative genetic study). The sources of phenotypical variance (P) in our study population can be described as the sum of additive (A) and dominant (D) genetic effects, common (C) and unique environmental (E) effects:

$$P = A + D + C + E \quad (3.1.)$$

Additive genetic variance represents the sum of all the alleles that affect the phenotype, while D denotes interactions between alleles that cannot be explained by a lienar model (dominance – if alleles are at the same locus, or epistasis if they are at different loci). The magnitude of C and D usually cannot be calculated in the same model (unless it is extended to a family study design). When dominance is present, the monozygotic intraclass correlation coefficient (r_{MZ}) would be more than twice the dizygotic correlation coefficient (r_{DZ}) – in this case, an ADE model is appropriate.

The simplest form of calculating heritability (h^2) is the Falconer formula,

$$h^2 = 2(r_{MZ} - r_{DZ}) \quad (3.2)$$

which is purely derived from the difference between the intrapair correlation of MZ and DZ twins. The higher the resemblance between MZ twins (compared to DZ twins), the higher the heritability of given trait. In this case, the estimation of common environmental effects is as follows:

$$c^2 = r_{MZ} - h^2 \quad (3.3)$$

The magnitude of unique environmental factors can be calculated as follows:

$$e^2 = 1 - h^2 + c^2 \quad (3.4)$$

However, this simple method has many limitations, such as the lack of ability to test for sex differences, inadequacy for testing multivariate data and the lack of obtaining confidence intervals, thus the result is merely a rough point-estimation.

Therefore, a more advanced method gained ground in twin studies, which is based on model fitting according to the expected and observed covariances in MZ and DZ twins. The expected and observed correlations and covariances can be visualized on a path diagram (*Figure 3*), which is a convenient non-algebraic way to demonstrate a

priori the causal relations of the latent factors (A,C,E or A,D,E) to the observed phenotypic variation – and furthermore can be translated into structural equations.

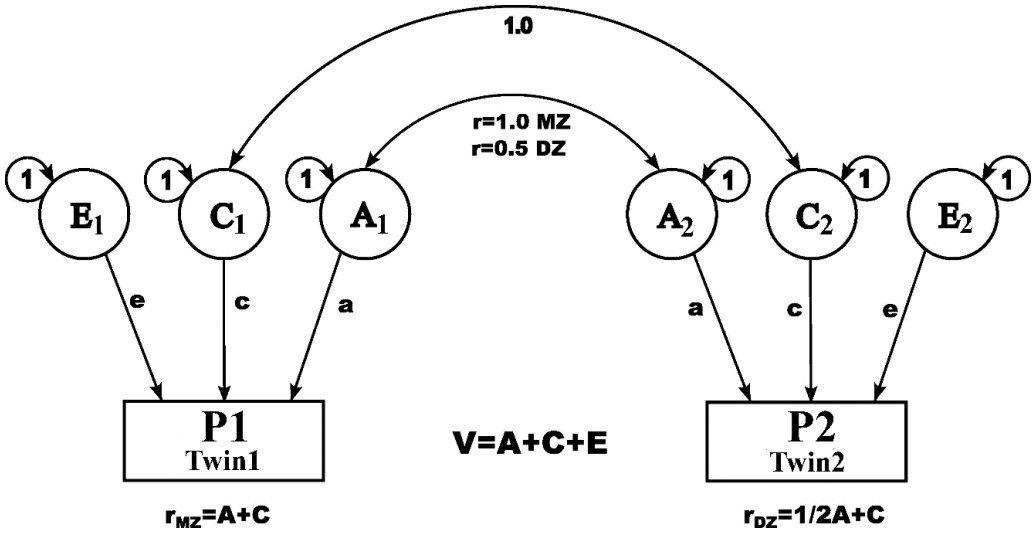

Figure 3. Pathway diagram in univariate twin ACE model: 'A' stands for additive genetic factors, 'C' common environmental factors, 'E' unique environmental factors, 'a' 'c' and 'e' depict the effect (regression coefficients) of these latent variables on the observed trait. The variances of the latent factors A, C and E are fixed at '1', as they are unknown and unmeasurable. This model is also called 'path coefficients model'. An equivalent would be the so called 'variance components model', where the regression coefficients would be fixed at a unit value, and the variances of A, C and E would be calculated (own image).

Path diagrams can be translated into structural equations, which can further be converted into covariance matrices which allows further matrix algebraic operations. Later is useful in the process of model fitting. Prior to model fitting, naturally we need to build models on a hypothetic basis, which in our case are the following:

1) Full ACE model: Latent additive genetic (A), common environmental (C) and unique environmental (E) factors all substantially contribute to the observed phenotypical variance (Vp)
2) AE model: only latent additive genetic (A) and unique environmental factors (E) explain majority of Vp (the influence of common environmental factors is negligible)

DOI:10.14753/SE.2024.2911

3) CE model: only common environmental (C) and unique environmental factors (E) explain majority of Vp (the influence of additive genetic factors is negligible)
4) E model: only unique environmental factors (E) explain Vp (the influence of additive genetic and common environmental factors do not contribute substantially to Vp, they are negligible)

In the ACE path analysis, following path tracing rules we can derive the following tracing routes connecting the two members of a twin pair:

For MZ twins:

1) $P1 \overset{c}{\leftarrow} C1 \overset{1}{\leftrightarrow} C2 \overset{c}{\rightarrow} P2$
2) $P1 \overset{a}{\leftarrow} A1 \overset{1}{\leftrightarrow} A2 \overset{a}{\rightarrow} P2$

Thus, the expected covariance between MZ twins can be expressed as the following equation:

$cov_{MZ}=a^2A1A2+c^2C1C2= a^21x1+c^21x1=a^2+c^2$

For the DZ twins we have the following routes:

1) $P1 \overset{c}{\leftarrow} C1 \overset{1}{\leftrightarrow} C2 \overset{c}{\rightarrow} P2$
2) $P1 \overset{a}{\leftarrow} A1 \overset{0.5}{\leftrightarrow} A2 \overset{a}{\rightarrow} P2$

This will lead us to the following equation:

$cov_{DZ}= 0.5a^2A1A2+c^2C1C2= 0.5a^21x1+c^21x1=0.5a^2+c^2$

For the variance of a given trait P1 we can trace back the following routes to itself:

1) $P1 \overset{a}{\leftarrow} A1 \overset{a}{\rightarrow} P1$
2) $P1 \overset{c}{\leftarrow} C1 \overset{c}{\rightarrow} P1$
3) $P1 \overset{e}{\leftarrow} E1 \overset{e}{\rightarrow} P1$

Therefore, the expected variance of trait P1 (or P2) will be:

$$V_P=a^2+c^2+e^2 \quad (3.5)$$

For the following calculations we imply covariance matrices. We can form the covariance matrix of the observed trait in MZ and DZ twins separately from their original data matrix **A**, where column 1 is Twin 1, column 2 is Twin 2, and phenotypic values from all twin pairs (N) are listed in the raws. For each $a_{i,j}$ element (where i is the number

of raw, j is the number of column) of the matrix we can calculate its deviance from the parameter mean value. If we replace all a_{ij} data with $z_{ij}=a_{ij}-\mu_{ij}$ (where μ_j is the mean value of the j^{th} parameter), we get the matrix **Z**. Phenotypical covariance matrix then is easy to obtain by multiplying matrix **Z** by its transpose **Z'**, multiplied by 1/N-1, e.g. for the sake of simplicity if we would have only 3 twin pairs:

$$\frac{1}{N-1}\mathbf{Z}'\mathbf{Z} = \frac{1}{2}\begin{pmatrix} z11 & z21 & z31 \\ z12 & z22 & z32 \end{pmatrix}\begin{pmatrix} z11 & z12 \\ z21 & z22 \\ z31 & z32 \end{pmatrix} =$$

$$= \frac{1}{2}\begin{pmatrix} (z11)^2+(z21)^2+(z31)^2 & (z11)(z12)+(z21)(z22)+(z31)(z32) \\ (z11)(z12)+(z21)(z22)+(z31)(z32) & (z12)^2+(z22)^2+(z32)^2 \end{pmatrix}$$

$$= \begin{pmatrix} S^2_{zi1} & S_{zi1*zi2} \\ S_{zi1*zi2} & S^2_{zi2} \end{pmatrix} \quad (3.6)$$

Which is then finally the symmetric phenotypical covariance matrix, e.g. **S**, where the diagonal elements represent the trait's variance among Twin1 of twin pairs (S^2_{zi1}) and Twin2 of the twin pairs (S^2_{zi2}), while the elements under and above the diagonal are identical and represent the covariance of the trait in-between the twin pairs.

Therefore, we might also write the observed covariance matrices of MZ and DZ twins in other form:

$$\mathbf{S}_{MZ} = \begin{pmatrix} var(P_{MZ1}) & \\ cov(P_{MZ1}, P_{MZ2}) & var(P_{MZ2}) \end{pmatrix}$$

and

$$\mathbf{S}_{DZ} = \begin{pmatrix} var(P_{DZ1}) & \\ cov\,(P_{DZ1}, P_{DZ2}) & var(P_{DZ2}) \end{pmatrix}$$

The expected variances and covariances are then decomposed by the results of the latent variables (ACE) following the above detailed path tracings: covariance due to additive genetic effects will be the result of the paths linking trait values via A (for MZ twins: $a*1*a=a^2$, for DZ twins: $a*0.5*a=0.5a^2$). The covariance due to C can be derived in similar ways (c^2 for MZ twins and c^2 for DZ twins). Variances would contain all three elements ($a^2+c^2+e^2$). Let us name the expected covariance matrices **Σ**, which has then the following forms:

$$\mathbf{\Sigma}_{MZ} = \begin{pmatrix} a^2+c^2+e^2 & \\ a^2+c^2 & a^2+c^2+e^2 \end{pmatrix} \quad (3.7)$$

and

DOI:10.14753/SE.2024.2911

$$\boldsymbol{\Sigma}_{\mathrm{DZ}} = \begin{pmatrix} a^2 + c^2 + e^2 & \\ \frac{1}{2}a^2 + c^2 & a^2 + c^2 + e^2 \end{pmatrix} \tag{3.8}$$

Naturally, in the reduced AE, CE or E model the value of either c^2 or a^2, or both c^2 and a^2 would be fixed at zero, respectively.

The next step is to fit our expected covariance matrices ($\boldsymbol{\Sigma}_{\mathrm{MZ}}, \boldsymbol{\Sigma}_{\mathrm{DZ}}$) to the observed phenotypical covariances matrices ($\mathbf{S}_{\mathrm{MZ}}$, $\mathbf{S}_{\mathrm{DZ}}$). This requires multiple iterative processes, where the latent variables are estimated and optimized at each step until the best fit is reached (multiple methods exist, but the most commonly used is the maximum likelihood method). SEM (Structural Equation Modeling) programs can analyse data from several different familial relationships, provide measurement errors, and enables to compare the fit of different models. Akaike's extended method enables us to assess model parsimony at the same time (choosing the model with the least number of latent variables without significant loss of fit).

When parameter estimates reach the maximum likelihood, technically, we obtain the least possible misalignment between predicted model and observed data (covariance matrices). Assuming normally distributed data, the maximum likelihood function is defined as:

$$\mathrm{F}_{(\mathrm{ML})} = (\mathrm{s} - \sigma)' \mathbf{W}_{(\mathrm{ML})}^{-1} (\mathrm{s} - \sigma) \tag{3.9}$$

where s is the vector of the observed covariance matrix **S** and σ is the vector of model matrix $\boldsymbol{\Sigma}$, $\mathrm{W}_{(\mathrm{ML})}^{-1}$ is a matrix created by the inverted variances and covariances among the elements in matrix $\boldsymbol{\Sigma}$. While computing each iteration, $\boldsymbol{\Sigma}$ should be inverted each time – it is this value which will define $\mathrm{F}_{(\mathrm{ML})}$ and the aim is to create the least discrepancies between s and σ. The vector s is a data set obtained by the diagonal and lower half elements of matrix **S**, rearranged in the form of only one column. The same stands for vector σ, which contains the non-duplicate elements of matrix Σ:

$$\mathrm{s} = \begin{pmatrix} \mathrm{var}_{\mathrm{PMZ1}} \\ \mathrm{cov}_{\mathrm{PMZ1,2}} \\ \mathrm{var}_{\mathrm{PMZ2}} \end{pmatrix} \qquad \sigma = \begin{pmatrix} a^2 + c^2 + e^2 \\ a^2 + c^2 \\ a^2 + c^2 + e^2 \end{pmatrix}$$

Technically, as there are two different twin groups (MZ and DZ twins), we use the multi-sample analysis of model fitting in the following form:

$$\mathrm{F} = \sum_{\mathrm{g}=1}^{\mathrm{G}} (\mathrm{N_g}/\mathrm{N}) \mathrm{F_g} (\mathbf{S}^{(\mathrm{g})} \boldsymbol{\Sigma}^{(\mathrm{g})} \mathbf{W}^{(\mathrm{g})}) \tag{3.10}$$

Where G is the number groups. Therefore, when two groups of twins are investigated, the number of groups G=2, where g1 refers to the MZ twins and g2 refers to DZ twins. Ng/N is the number of MZ or DZ twin pairs compared to the whole population, Fg the fit function of the given group, while $\mathbf{S}^{(g)}$ is the covariance matrix of the observed phenotypes, $\mathbf{\Sigma}(g)$ is the covariance matrix of the expected model and $\mathbf{W}^{(g)}$ is the weight matrix for group G. Naturally in this case we sum the functions of the two groups.

An example of the iterative minimization method is the so-called Newton-Raphson method. Here we want to assess the unknown parameters (converging to their 'real' value) by starting with a certain chosen value of the latent factors (let us call vector $\Theta^{(1)}$). Using these estimates we get the $F(^{\theta 1})$: the function value of the first iteration process. From the above equation we can calculate the gradient (m dimensional vector g, where m is the number of the latent variables), which is the first order derivative and the Hessian matrix (**H**), which is the second order partial derivates' matrix. From the gradient and the Hessian matrix we get the direction vector d, which will orient to the next estimation of the unknown parameters (which will give a closer approximation):

$$\Theta^2 = \Theta^{(1)} - \mathrm{d}^{(1)} \tag{3.11}$$

where

$$\mathrm{d} = \mathbf{H}^{-1}\mathrm{g}$$

We can continue the iterations until reaching parameter estimation $\mathbf{\Theta}^{(k)}$, where the difference between $\mathbf{\Theta}^{(k)}$ and $\mathbf{\Theta}^{(k-1)}$ or the difference between their F value is negligibly small, so the parameter estimates are close enough to their 'real' value.

After parameter optimization (getting close enough the 'real' value of a, c and e), we can calculate the goodness-of-fit of the model by calculating the χ^2 measure of fit as follows:

$$\chi^2 = (\mathrm{N} - 1)\mathrm{F_k} \tag{3.12}$$

where F_k is the minimal value of the fit function (last iteration).

If the sample is large enough we might be able to compare it to a perfectly fitting ('saturated') model using likelihood ratio χ^2 statistics. Alternatively, comparison of the submodels can be made against the full (ACE) model. When calculating maximum likelihood estimates one parameter is progressively moved away resulting in different models (e.g. removing C from the ACE model will give the AE model). When the χ^2

value of the given model is non-significant ($p>0.05$), the model is consistent with the data. However, when the χ^2 value is significant, the model fits the data poorly - therefore it should be rejected.

The degrees of freedom (df) denotes the number of observed variables (typically sample variances and covariances) minus the number of parameters estimated in the given model. When computing the Akaike's Information Criterion (AIC) we take df (therefore number of parameters) also into account:

$$\mathrm{AIC} = \chi^2 - 2\mathrm{df} \tag{3.13}$$

This method serves to choose the most parsimonious model, meaning that if a simpler model with less parameter doesn't provide significantly worse fit, it should be chosen over the more complex model, because it is preferred that the least latent variables which can explain the population variation should be chosen. The model with the lowest AIC value will correspond to the most parsimonious model. For example, when we compare the AE model to the ACE model, we test whether component C's path coefficient c^2 value is significantly higher than 0 or not – or in other words, we test whether AE model is significantly worse than ACE model or not. When C can be left out, the simpler AE model should be chosen.

The above methods can easily be extended to multiple variables, so it is also possible to analyze multiple traits in the form of looking for genetic and environmental covariance or correlation between two or more traits or e.g. looking for longitudinal genetic origin of stability of one given trait (with multiple measurements). These are called bivariate or multivariate genetic models. The corresponding matrix algebraic representation is similar to that in a univariate model- however, the dimensions are no longer 1 x 1, but n x n (where n is the number of variables).

Figure 4. shows Cholesky model where the within-individual factor loadings (which are equivalent to path coefficients, one-way arrows), are hypothesized to have an overlapping effect on both phenotypical traits. It is important to note, that only one latent factor is hypothesized to have an influence on both traits, however this is not true for the second latent factor. This model fits e.g. longitudinal data well. Additionally, intrapair correlations (or covariations) of the latent variables (= latent factors) in the form of two-way arrows are also demonstrated, which differ among MZ and DZ twins.

DOI:10.14753/SE.2024.2911

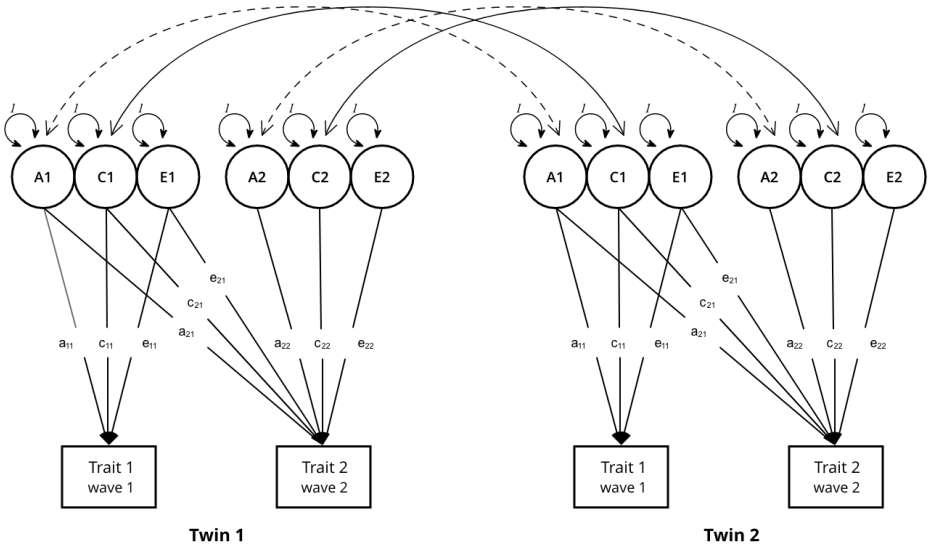

Figure 4. Bivariate Cholesky twin model. Solid lines represent that the covariance between the shared environmental variance components is fixed at 1 for all types of twins. Dashed lines represent a correlation regarding additive genetic effects fixed at 1 for MZ twins and 0.5 for DZ twins. Latent variables have a causative effect on the observed phenotype presuming that variables can partly have an effect both at the first and the second observed phenotype. A: additive genetic effects, C: common environmental effects, E: unique environmental effects (own image).

The Cholesky method is based on the knowledge that any positive definite matrix can be decomposed into a triangular matrix multiplied by its transpose. The aim is to decompose total population phenotypic covariance (matrix) into genetic and environmental components by using the genetically informative data from MZ and DZ twins:

$$\mathbf{C}_\mathrm{P} = \mathbf{A} + \mathbf{C} \tag{3.14}$$

where $\mathbf{A}$ is the additive genetic covariance matrix, $\mathbf{C}$ is the common environmental covariance matrix. Assumed that A is a positive definite matrix, we can decompose it to the triangular matrices:

$$\mathbf{A} = \mathbf{T}\mathbf{T}' \tag{3.15}$$

where

$$\mathbf{A} = \begin{pmatrix} a_{11}^2 & a_{11}a_{21} \\ a_{11}a_{21} & a_{21}^2 + a_{22}^2 \end{pmatrix}$$

from which we can get the value of the factor loadings one by one using the Cholesky method:

$$\mathbf{T} = \begin{pmatrix} a_{11} & 0 \\ a_{21} & a_{22} \end{pmatrix} \text{ and } \mathbf{T}' = \begin{pmatrix} a_{11} & a_{21} \\ 0 & a_{22} \end{pmatrix}$$

If the elements under the diagonal of **A** equal 0, there is no genetic covariance between the two traits - as only diagonal elements would be present, which define the genetic variances of trait 1 and trait 2.

The expected model is very similar to that in the prior univariate model (see 3.7. and 3.8.), however, now we have matrices within the matrices. Eg, the expected model matrices for MZ and DZ covariance between trait 1 and trait 2 are:

$$\boldsymbol{\Sigma}_{MZ1,2} = \begin{pmatrix} \mathbf{A}+\mathbf{C}+\mathbf{E} & \\ \mathbf{A}+\mathbf{C} & \mathbf{A}+\mathbf{C}+\mathbf{E} \end{pmatrix} \quad (3.16)$$

$$\boldsymbol{\Sigma}_{DZ1,2} = \begin{pmatrix} \mathbf{A}+\mathbf{C}+\mathbf{E} & \\ 0.5\%x\%\mathbf{A}+\mathbf{C} & \mathbf{A}+\mathbf{C}+\mathbf{E} \end{pmatrix} \quad (3.17)$$

Where %x% denotes the Kronecker product.

The observed phenotypical matrices are also similar to the univariate model, however now we have covariance matrices among the diagonal elements too:

$$\mathbf{S}_{MZ1,2} = \begin{pmatrix} \mathbf{C}_{P12T1} & \\ \mathbf{C}_{P12T12} & \mathbf{C}_{P12T2} \end{pmatrix} \quad (3.18)$$

$$\mathbf{S}_{DZ1,2} = \begin{pmatrix} \mathbf{C}_{P12T1} & \\ \mathbf{C}_{P12T12} & \mathbf{C}_{P12T2} \end{pmatrix} \quad (3.19)$$

Where $\mathbf{C}_{P12T1}$ is the within-twin covariance matrix of Phenotype 1 and Phenotype 2 in Twin 1, $\mathbf{C}_{P12T2}$ is the within-twin covariance matrix of Phenotype 1 and Phenotype 2 in Twin2 and $\mathbf{C}_{P12T12}$ is the cross-twin covariance matrix of Phenotype 1 and Phenotype 2 in Twin 1 and Twin 2. The observed phenotypes can also be shown in the following forms (*Table 1-2.*):

Table 1. Covariance matrices of two observed traits in twin pairs.

<table>
<tr><td colspan="2" rowspan="2"></td><td colspan="2">Twin 1</td><td colspan="2">Twin 2</td></tr>
<tr><td>p1</td><td>p2</td><td>p1</td><td>p2</td></tr>
<tr><td rowspan="2">Twin 1</td><td>p1</td><td colspan="2" rowspan="2">Within-twin covariance matrix (Twin 1)</td><td colspan="2" rowspan="2">Cross-twin covariance matrix (Twin 1 and 2)</td></tr>
<tr><td>p2</td></tr>
<tr><td rowspan="2">Twin 2</td><td>p1</td><td colspan="2" rowspan="2">Cross-twin covariance matrix (Twin 1 and 2)</td><td colspan="2" rowspan="2">Within-twin covariance matrix (Twin 2)</td></tr>
<tr><td>p2</td></tr>
</table>

DOI:10.14753/SE.2024.2911

Table 2. Covariance matrices of two observed traits in twin pairs.

		Twin 1		Twin 2	
		p1	p2	p1	p2
Twin 1	p1	$VarP_1T_1$			
	p2	$CovP_{12}T_1$	$VarP_2T_1$		
Twin 2	p1	$CovP_1T_{12}$		$VarP_1T_2$	
	p2	$CovP_{12}T_{12}$	$CovP_2T_{12}$	$CovP_2T_{12}$	$VarP_2T_2$

The process of model fitting, parameter optimization and model comparison to choose the most parsimonious one is then similar to the procedures used in univariate models described above.

Additionally, we might calculate genetic (r_g) and environmental correlation. Per definition, correlation between two traits can be obtained by their variances and covariances, e.g.:

$$r_g = \frac{a_{11}a_{21}}{\sqrt{a_{11}^2(a_{21}^2+a_{22}^2)}} \tag{3.20}$$

So far we have discussed the methodologies concerning continuous normally distributed phenotypical data. However, frequently we have to deal with non-continuous e.g. discrete, ordinary, binary or ordered categorical data. In these cases the phenotypical data can usually be presented as frequencies in mxm contingency tables, where m is the number of categories, e.g. as shown in *Table 3*:

Table 3. Contingency table of one (ordered) categorical trait in twins. The contingency table shows the frequencies/proportions (or number) of twin pairs, e.g. f11 is the frequency of twin pairs where both twins fall into category 1 (Cat 1).

		Twin 1		
		Cat 1	Cat 2	Cat 3
Twin 2	Cat 1	f11	f21	f31
	Cat 2	f12	f22	f32
	Cat 3	f13	f23	f33

In the case of these data we can make the assumption that an underlying continuous, normally distributed but unmeasured variable exist, which is called liability.

DOI:10.14753/SE.2024.2911

Another assumption is that our measurements are imprecise measurements of the underlying liability, therefore the different m categories represent distinct parts of the liability distribution curve divided by m-1 thresholds. In other words, liability is the hypothetical distribution of a hypothetical underlying factor, which will define e.g. whether a disease will be present or not.

If we look at only Twin 1, we can take a vector g containing the frequencies of m=3 categories:

$$g = \begin{pmatrix} f11 + f12 + f13 \\ f21 + f22 + f23 \\ f31 + f32 + f33 \end{pmatrix} = \begin{pmatrix} g1 \\ g2 \\ g3 \end{pmatrix}$$

The underlying liability of g is assumed to have the mean value fixed as 0, variance 1, then the threshold can be placed at given z values, which would partition the liability distribution so that it would match our observed frequencies, e.g. let g be:

$$g = \begin{pmatrix} 20 \\ 35 \\ 12 \end{pmatrix}$$

The expected proportion in category i can be calculated by finding the definite integral between the two thresholds (t_i and t_{i-1}) (or between the first threshold and minus infinite/last threshold and positive infinite):

$$\int_{ti-1}^{ti} \emptyset(x)dx \tag{3.21}$$

where $\phi(x)$ denotes the probability density function defined as:

$$\emptyset(x) = \frac{e^{-.5x^2}}{\sqrt{2\pi}} \tag{3.22}$$

where e is Euler's number (approximately equals 2.71828) and π is the Ludolphian number approximating (3.14159). In our example, if we take

$$\int_{-\infty}^{\infty} = 1$$

Then logically, the sum of the elements in g should equal 1. Therefore we can transform the numbers to keep reflecting the same partitions as follows:

$$g = \begin{pmatrix} 20/67 \\ 35/67 \\ 12/67 \end{pmatrix} = \begin{pmatrix} 0.29851 \\ 0.52239 \\ 0.17910 \end{pmatrix}$$

Therefore, from the equation 3.21. and 3.22.

$$\int_{-\infty}^{t1} \frac{e^{-.5x^2}}{\sqrt{2\pi}} dx = 0.29851$$

we can get

$$\frac{\text{erf}\left(\frac{t1}{\sqrt{2}}\right) + 1}{2} = 0.29851$$

where erf refers to error function. From this equation we get:

$$\text{erf}\left(\frac{t1}{\sqrt{2}}\right) = -0.40298$$

Which allows to calculate the z value of the first threshold, t1= -0.52869. Following with similar methods, the z value of the second threshold will be t2= 0.91880. Finally we can demonstrate and check the correctness of these results as follows:

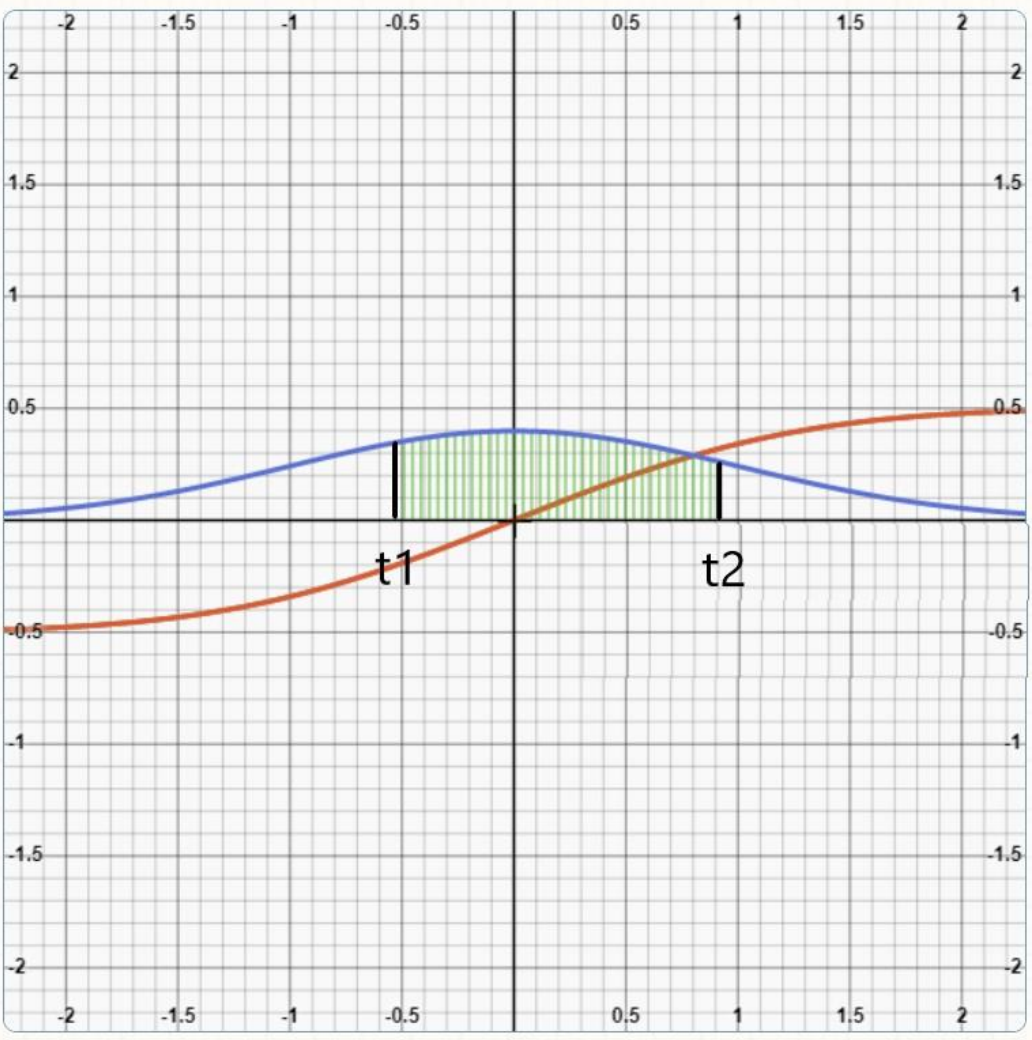

Figure 5. Hypothetical liability distribution. Here t_1 and t_2 denote the two thresholds between categories.

DOI:10.14753/SE.2024.2911

The curve in *Figure 5*. shows the liability distribution of the ordered categorical measurements in Twin1 (vector g contains the frequency of twins in each category), where the first threshold (t1) refers to -0.528969 z score and the second threshold (t2) equals 0.91880 (the x axis shows the z score values). The area under curve marked with color green can be calculated by the integral between t1 and t2, which equals 0.52293, corresponding to 35/67, the second element of vector g. Therefore, the frequencies in Cat1-3 (elements of vector g) match the areas under curve of the normal distributed liability curve, where t1 and t2 represent the margins between the three categories.

Next, if we get back to the contingency table where the frequencies of Twin1 and Twin2 are merged (*Table 3*.), we must continue with the assumption that bivariate normal liability underlies our observations. The correlation between the two twins is yet unknown, however, with this model, we can compute the expected proportions of each cell and the contrary is also true: the observed proprotions in the cells can be used to estimate both thresholds and the correlation. This is called polychoric correlation (or tetrachoric correlation, when the contingency table is of 2x2 dimensions), which can be calculated both in MZ and DZ twins (*Figure 6*).

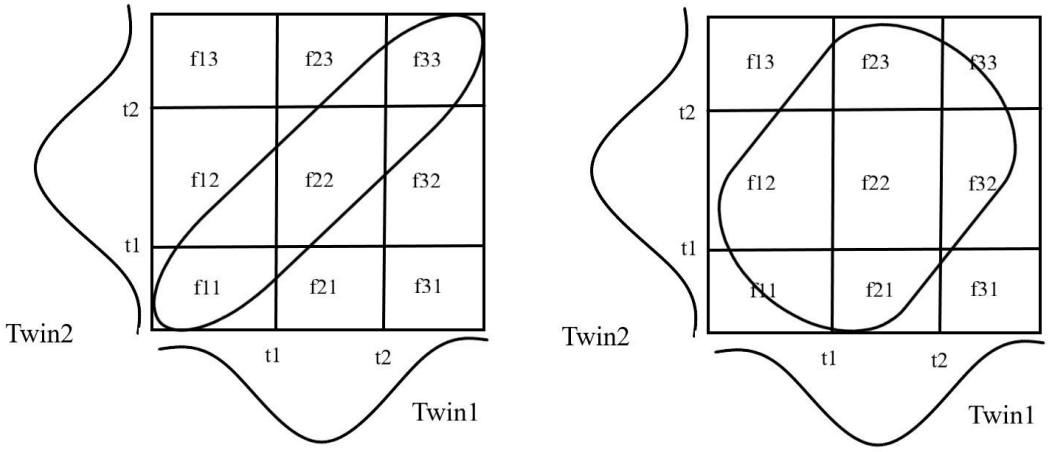

Figure 6. Polychoric correlation between twins. On the left side we see an example of high polychoric correlation where the area of given cell divided by the given part of the ellipse represents the relative proportion of the frequency to the correlation between the two twins. On the right side we see an example of lower polychoric correlation. In both cases there are two underlying normal distributions with given thresholds (t1 and t2). Logically, the higher the frequency in the diagonal elements relative to the other cells, the higher the correlation between the two twins will be.

DOI:10.14753/SE.2024.2911

As *Figure 6*. shows, the polychoric correlation can be estimated knowing the threshold values and the frequencies of the given cells. Let h denote the vector containing the observed frequencies in Cat1-3 of Twin 2:

$$h = \begin{pmatrix} f11 + f21 + f31 \\ f12 + f22 + f32 \\ f13 + f23 + f33 \end{pmatrix} = \begin{pmatrix} h1 \\ h2 \\ h3 \end{pmatrix}$$

In the next step let Y1 denote the liability underlying g and Y2 denote the liability underlying h. The polychoric correlation coefficient between Y1 and Y2 then can be obtained by path tracing, where the latent variable B has the same effect on both vectors:

$$Y1 \overset{b}{\leftarrow} B \overset{b}{\rightarrow} Y2 \text{ and } r^* = b^2$$

where r^* represents the polychoric correlation coefficient. Numerical integration processes can be used to compute the value of r with programs such as Mx.

After calculating r^*_{MZ} and r^*_{DZ} it is also possible to fit models (ACE, AE, CE, E) to the liabilities of the data and choose the most parsimonious one similarly to the previous methods, however df will be much less. The fit function is based on the observed frequency data and the expected proportions of each cells. E.g. the expected proportion of liability in cell f33 is:

$$\int_{t2}^{\infty} \int_{t2}^{\infty} \Phi(L1, L2; 0, \Sigma) dL1 dL2 \qquad (3.23)$$

where Φ is the multinormal probability density function, L1 is the liability of twin1 L2 is the liability of twin 2, 0 is the mean value and Σ is the expected correlation matrix of the two liabilities based on ACE path tracings.

The ‘saturated model’ (meaning that the model fits the data perfectly, therefore predicted frequencies are equal to the observed frequencies) can be calculated as follows:

$$2 \ln L = 2 \sum_{i=1}^{r} \sum_{j=1}^{c} n_{ij} \ln \left(\frac{n_{ij}}{n_{..}}\right) \qquad (3.24)$$

where r denotes rows, c means columns, nij is the frequency of given cell and n.. is the total number of cells.

A significant χ^2 statistic value of the given predicted model vs. the above saturated model would mean a poor fit to the observed data.

Genetic vs. environmental decomposition of comorbidity (or ordinary phenotypical correlation) is also possible to estimate between two or more, multivariate binary or ordinary variables. In this case, e.g. regarding the binary trait of having disease A or not and having disease B or not, a 2x2 contingency table can be written for both

DOI:10.14753/SE.2024.2911

Twin1 and Twin2 (whole twin population), where the cells represent the frequency of twins having both, only one or neither of the diseases (*Table 4*).

Regarding the underlying liabilities L_A for disease A and L_B for disease B, we hypothesize that an individual is affected by disease A, if the liability value exceeds certain threshold t_A, and same applies to disease B. Comorbidity is present when correlation between L_A and L_B is higher than 0. The tetrachoric correlations r^*_{MZ} and r^*_{DZ} can also be calculated separately.

Table 4. Contingency table of comorbity (two diseases) in twins. The cells represent the frequencies of twins with neither disease (f0), only disease A (fA), only disease B (fB) or both diseases (fAB).

Twin 1 and Twin 2			
		Disease A	
		No	Yes
Disease B	No	f_0	f_A
	Yes	f_B	f_{AB}

In the following step we can draw a 4x4 contingency table where both members of the twin pairs are represented separately (*Table 5*).

Table 5. Contingency table of comorbidity in twin pairs. The cell fAB1AB2 e.g. represents the frequency of twin pairs, where both members have the comorbidity of A and B disease.

		Twin 1			
		01	A1	B1	AB1
Twin 2	02	f0102	fA102	fB102	fAB102
	A2	f01A2	fA1A2	fB1A2	fAB1A2
	B2	f01B2	fA1B2	fB1B2	fAB1B2
	AB2	f01AB2	fA1AB2	fB1AB2	fAB1AB2

Each cell's probability can be predicted as a quadruple integral, e.g. the predicted value of cell fAB1AB2 (meaning both members are comorbid):

$$\int_{tA1}^{\infty}\int_{tA2}^{\infty}\int_{tB1}^{\infty}\int_{tB2}^{\infty}\Phi(L_{A1},L_{A2},L_{B1},L_{B2};0,\Sigma)dL_{A1}dL_{A2}dL_{B1}dLB_2 \qquad (3.25)$$

Fitting the predicted cell values by the ACE, AE, CE and E models to the observed cell values and choosing the most parsimonious one is similar to the previous methods: the χ^2 value is compared to the saturated model and the model with the lowest AIC score is chosen.

In summary, basic classical twin statistical methods can be understood based on the univariate model building (ACE, AE, CE and E) in case of one, normally distributed continuous phenotypic trait (because this type of data is easier to handle and univariate analysis is simpler) in MZ and DZ twins. Each model can be visualized by path diagrams, from which structural equations can be made following path tracing rules. After models are created, we estimate the parameters of each model (either latent variables' variances are fixed at 1 so we calculate path coefficients, or path coefficients are fixed at 1 and we calculate latent factor variances), where each unknown variables are approximated iteratively using maximum likelihood functions until the discrepancies between the observed covariance matrices and the expected covariance matrices show least discrepancies. Afterwards, generally the χ^2 value of each model are assessed, and they are compared to each other (either starting with the full ACE model or a 'saturated' perfectly fitting model). Models which fit the data poorly (e.g. show significant difference in their χ^2 value) are rejected and the most parsimonious one is selected based on the lowest AIC value.

The similar logic can be extended to more than one phenotypical trait, however both the observed and the expected covariance matrices will contain other covariance matrices in their elements. The Cholesky method can be used to decompose genetic and environmental covariance matrices to find the corresponding path coefficients.

In case of non-continuous data, contingency tables depicting frequencies in each cell can be used, where the elements of both the columns and rows are regarded as two imprecise measurement of two latent, normally distributed liabilities. Separate MZ and DZ tetrachoric or polychoric correlations can be computed by numerical integration processes. Model building and fitting can also be used by fitting the expected frequencies of cells to the observed frequencies. With similar logic the model can be extended to multiple variables, where polychoric correlation, model building and model fitting are

also possible to conduct. In the following sections we refer back to the twin methods described above.

3.2. SPECIFIC AIM 1

3.2.1. Study participants and measurements

Our first international study participants were twin pairs from Hungary, Italy and the United States. Baseline measurements were conducted between 2009 and 2010 among 760 randomly selected adult twins. Measurements took place in Budapest, Agfalva and Szigethalom (Hungarian Twin Registry), Rome, Padua and Perugia (Italian Twin Registry) and Twins Day Festival in Twinsburg, Ohio, United States. Zigosity was assessed based on self-reported questionnaire [91,92]. Non-white or pregnant participants, twins with arrhythmia were excluded.

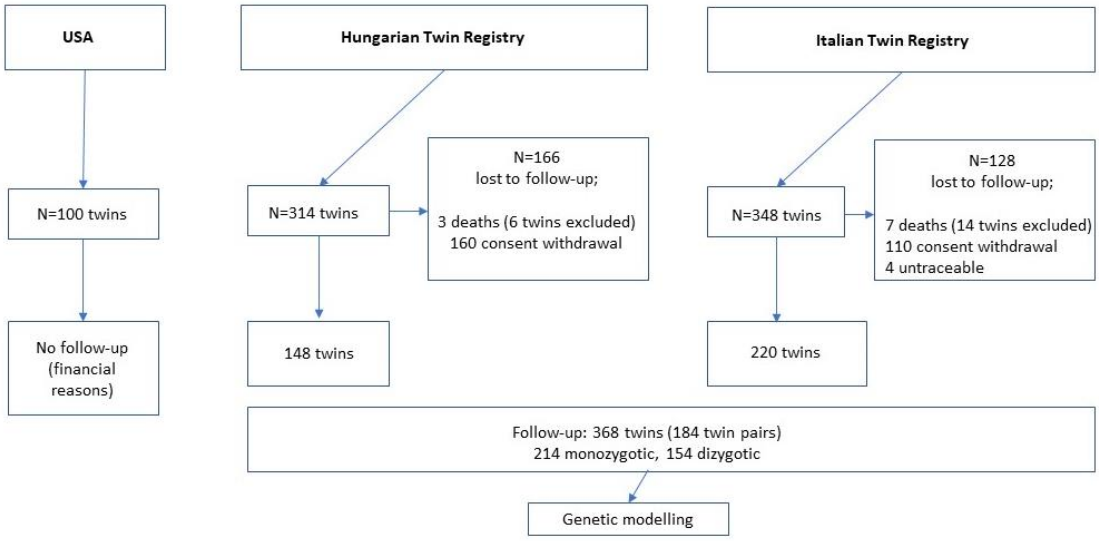

Figure 7. Study flowchart. A total of 394 twin pairs were lost for follow-up. One hundred and forty-eight Hungarian and two hundred and twenty Italian twins participated in the second wave of measurements; therefore, our longitudinal examinations were performed on these 368 twins from which 214 were MZ and 154 were DZ twins.

All participants were invited to a follow-up examination except for the American twins (due to financial reasons). The second wave of visits was organized between 2013 and 2014 with a 4.4 years average follow-up time. Average response rate was 55.6%. In

the final longitudinal analysis 368 twins were included (214 MZ and 154 DZ twins, 148 twin from Hungary and 220 twins from Italy) (*Figure 7*). Measurements of arterial stiffness and blood pressure were performed by the same two operators (A.D.T., D.L.T.) in both waves. Study protocol was approved by the Ethics Committee of the Instituto Superiore de Sanitá. Informed consent was given by all participants and the research was implemented according to the principles of the Declaration of Helsinki.

Participants were asked to fill a self-reported questionnaire about smoking and alcohol drinking habits, chronic diseases, medications and additional clinically relevant conditions. Prior to anthropometric and hemodynamic measurements, all subjects were restricted from smoking for 3 hours, from eating for 1 hour and from drinking alcohol or coffee for 10 hours. Weight measurements were implemented by a validated body consistency monitor (Omron Healthcare Ltd., Kyoto, Japan). For the calculation of BMI (body mass index) we used the following formula:

$$\mathrm{BMI} = \frac{\mathrm{weight\ (kg)}}{\mathrm{height(m^2)}} \tag{3.26}$$

Measurement of brachial and aortic AIx, aortic PWV, brachial and aortic blood pressure (BP), pulse pressures (PP) and mean arterial pressure (MAP) were conducted using a non-invasive, occlusive, oscillometric device (Tensiomed Arteriograph, Medexpert Ltd, Budapest, Hungary). The principle of the device is demonstrated in *Figure 8*.

A brachial cuff inflated at least 35 mmHg above the systolic pressure is used both as a means to create a stop-wave environment and as a sensor to detect central pressure changes (early systolic, late systolic/reflected and diastolic waves) at the upper edge of the cuff - therefore small suprasystolic pressure changes can be recorded and analyzed. Aortic Aix is calculated by the following formula:

$$\mathrm{Aix}(\%) = \frac{P_2 - P_1}{PP} \mathrm{x}100 \tag{3.27}$$

where P_1 represents the amplitude of the first (direct) systolic wave and P_2 is the amplitude of the late (reflected) wave (see also: *Figure 9*).

DOI:10.14753/SE.2024.2911

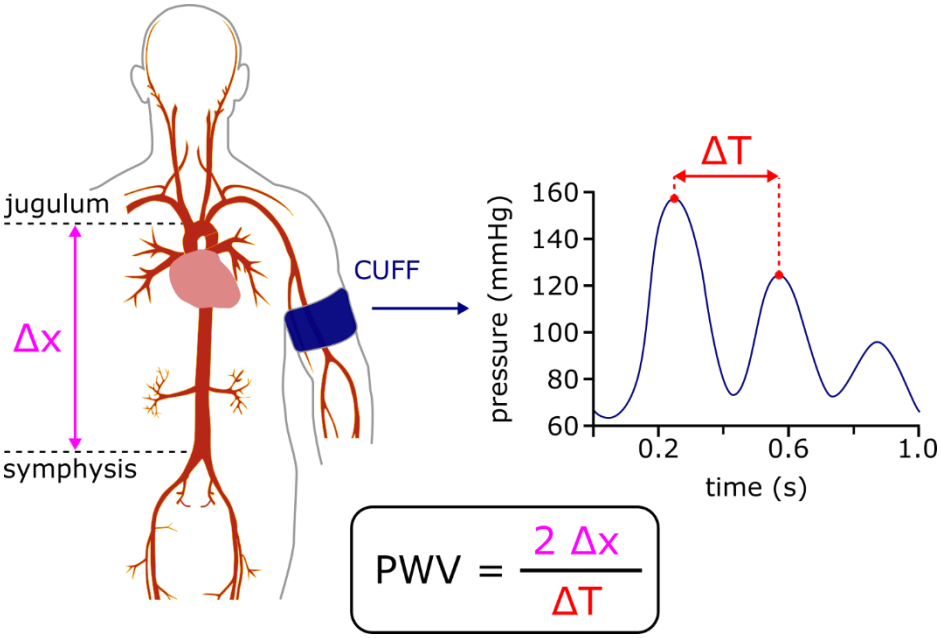

Figure 8. Basic principles of the Arteriograph and measurement method of pulse wave velocity (PWV). Abbreviations: Δx: distance between the jugulum and the symphysis; ΔT: time interval between first and reflected peak systolic values (own image).

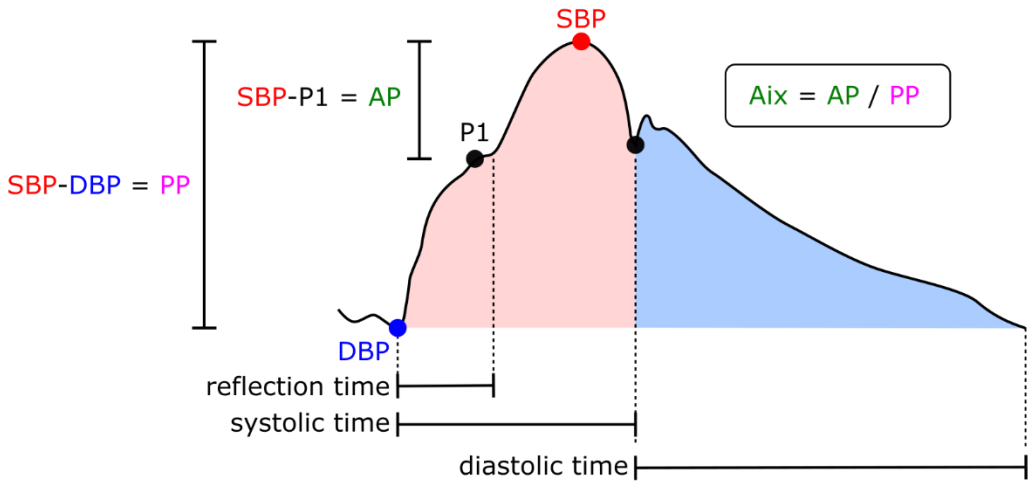

Figure 9. Calculation of the augmentation index (AIx). Abbreviations: SBP: systolic blood pressure; DBP: diastolic blood pressure; AP: augmented pressure wave; PP: pulse pressure (own image).

Central systolic blood pressure (SBP) is calculated using a validated algorithm based on the late systolic wave amplitude and the relationship between brachial and central SBP. Calculation of aortic PWV is based on the physiological wave reflection at the level of the aortic bifurcation (mostly) – therefore the device measures time interval

between first and reflected peak systolic values (return time; RT). Additionally, jugulum-symphysis distance (Jug-Sy) should be measured free-hand as a proxy to aortic length. From these values we get the following equation [93]:

$$\text{aPWV}\left(\frac{\text{m}}{\text{s}}\right) = \frac{\text{Jug}-\text{Sy(m)}}{\text{RT}/2\text{(s)}} \tag{3.28}$$

In order to avoid overestimation, we did not measure the jugulum-symphysis distance on the body surface, but parallel to it. Best-fitting brachial cuff size (small, medium or large) was chosen for each individual on their non-dominant arms. All participants were asked to have at least 10 minutes of rest before the measurement and not to talk or move during the measurements. Quality control was obtained visually (exclusion of signs of improper cuff size or tightness, arrhythmia, tremor or mechanical vibration). At least two measurements were taken from all participants and averaged. If the standard deviation of aortic PWV was >1 m/s we performed an additional third measurement and their median value was used later.

3.2.2. Statistics

For the descriptive statistics we used Intercooled STATA for Windows (version 11.2; StataCorp, College Station, Texas, USA). Arithmetic means and percentage distributions of variables were calculated in different groups of zygosity, country and time of measurements (waves). We compared groups using Student's t-test in case of continuous variables and using Chi-square test in case of frequencies.

For calculating Pearson's correlations on the longitudinal data from the two waves we used bivariate saturated models in the software Mx [94]. For each trait, the following correlations were determined: within-individual/cross wave correlations, cross-twin/within-wave correlations and cross-twin/cross-wave correlation. Within individual correlation between waves is informative about the phenotypical stability over time at the study population's level. A high correlation e.g. would mean similar patterns of changes among the participants rather than no change at all over time. Cross-twin correlations were obtained at wave 1 and wave 2 in MZ and DZ groups. A higher MZ correlation would imply a stronger genetic effect on the given trait at the given time point. With cross twin/cross wave correlations we compared twin 1 at wave 1 to twin 2 at wave 2 and vice versa both in MZ and DZ twins separately. A higher correlation in MZ twins would be suggestive of partly shared genetic factors contributing to phenotypic

expression at wave 1 and wave 2. In case of aortic PWV calculations we adjusted for age, sex, country, changes in MAP and BMI between waves, aortic AIx calculations were adjusted for age, sex, country, changes in heart rate and BMI between waves.

For further twin statistical approaches, we also used the Mx software. Heritability of the traits were calculated at both waves – which by definition means the proportion of total variance explained by genetic variance. Bivariate Cholesky decomposition allowed us to determine bivariate heritability (proportion of phenotypic stability attributable to genetic stability). Both heritability estimates use a pathway model where latent variables: additive genetic effects (A), common environmental effects (C) and unique environmental effects (E) have a causative relationship to the manifest (or phenotypical) variables. For explanation of Cholesky decomposition see *Figure 4*. Genetic modelling started with full ACE decomposition including all three latent variants (in univariate heritability analysis). Sub-models (AE, CE, E) were then compared to the full model by likelihood-ratio chi-square test. When the test wasn't significant, the full model was rejected and the submodel was kept and final results were obtained from the best fitting model based on the lowest Akaike Information Criterion. In bivariate Cholesky modelling the same approach was used.

3.3. SPECIFIC AIM 2.

3.3.1. Study participants and measurements

In the second part of our study 202 adult Hungarian twins (Caucasian ethnic) were enrolled. Subjects were selected from the Hungarian Twin Registry based on their proper clinical history, age and gender. Zigosity was determined using a self-reported questionnaire [91,92]. Only same-sex DZ twins were invited to participate in this study. Inclusion age criteria for females was 40 to 75 years, whilst for males 35 to 75 years. Exclusion criteria were: contraindication of CT-angiography, previous coronary artery revascularization, atrial fibrillation/flutter or frequent irregular or rapid heartbeat within the past 3 months, pacemaker or implantable cardioverter defibrillator (ICD) implantation, active congestive heart failure or known nonischaemic cardiomyopathy, known genetic diseases of atherosclerosis, lipid or lipoprotein metabolism, pregnancy, regular alcohol consumption (>2 units/day), acute infection within three weeks and

conditions possibly lowering compliance during CT scanning. Approximately 90% of twins agreed to participate after notification and sending them detailed study description.

Study measurements were carried out in Budapest, Hungary between April 2013 and July 2014. The study was approved by the national ethics committee (institutional review board number: ETT TUKEB 58401/2012/EKU [828/PI/12]; Amendment-1: 12292/2013/EKU [165/2013]). All participants gave written informed consent and the study was transacted according to the Helsinki Declaration.

All subjects were retained from smoking and eating for 3 hours, drinking coffee or alcohol for 10 hours prior to examinations. Obtainment of anthropometric data (weight, height/BMI) and self-reported questionnaire about lifestyle and medical history were carried out on day one together with cardiac CT. Vascular ultrasound was implemented on the following day by two expert radiologists (A.D.T., D.L.T). Because of missing radiological data we had to exclude six twin pairs resulting in a total number of 190 participant for our analyses.

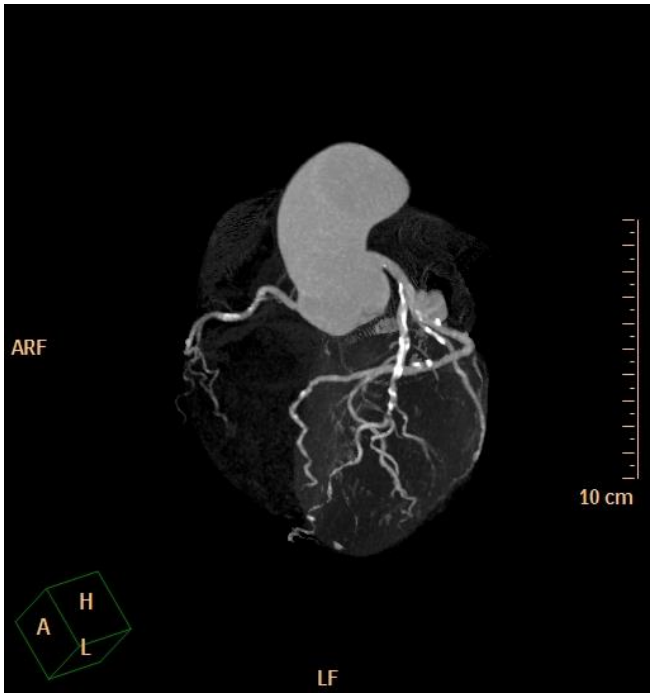

Figure 10. Three-dimensional reconstruction of coronary CT showing extensive calcification mainly in the left anterior descending coronary artery (own image).

Cardiac non-contrast CT examination was performed using ECG (electrocardiogram) triggered, 256-multidetector CT (Brilliance CT, Philips HealthTech, Best, The Netherlands). Per os β-blocker (metoprolol, 100 mg max. dose) was given 1

hour prior to CT scan if any participant had a heart rate was above 65/min. Scans acquisition protocol included 2.0 mm slice thickness, 120 kVp tube voltage and 20-50 mAs tube current depending on BMI. Scans were taken during a single inspiratory breathhold at 78% of the R-R interval (*Figure 10*). The CACS was assessed using commercially available software (Extended Brilliance Workspace; Philips Healthcare) and expressed in Agatston score [95].

Carotid and femoral ultrasound examinations were performed in B-mode (brightness-mode) and color Doppler mode using high frequency (5-10 MHz) linear transducers (Philips HD15, Philips Healthcare, Best, The Netherlands). Carotid arteries were scanned on both sides from the proximal common carotid arteries until the visible proximal 2-3 cm segments of the internal and external carotid arteries. Femoral arteries were visualized also bilaterally from the inguinal ligament until the bifurcation and the proximal 1-2 cm of the deep femoral artery and 3-4 cm of the superficial femoral artery. We considered ≥1.5 mm endoluminal protrusion or >50% focal thickening relative to adjacent intima-media layers plaques (*Figure 11*).

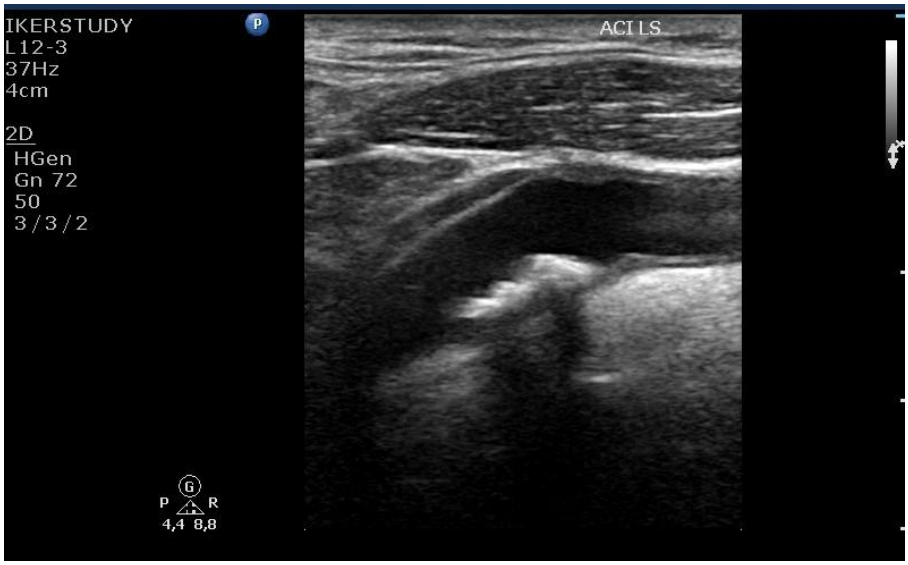

Figure 11. B-mode ultrasound image of a hyperechoic (calcified) plaque in the left internal carotid bulb (own image).

Each plaque was registered, measured, described and categorized based on their echogenicity type. We differentiated hypo-, hyper- and mixed plaque types as described previously [96]. These categories have been validated against histologic specimens

proving that increasing echogenicity correlated with the amount of calcification [97]. Plaque dissemination was assessed by four-segments score summing the number of affected arteries regarding or not regarding plaque type.

3.3.2. Statistics

Study participants demographic characteristics and phenotypic variations were analyzed using the SPSS statistical program (SPSS Statistics 17). Group of MZ and DZ pairs were compared to each other by independent sample's t-test in case of parametric, Mann-Whitney U test in case of nonparametric and Chi-square test in case of binary data. Prevalence of distinct combinations of plaque distribution in the carotid, femoral and coronary arteries were shown in form a Venn diagram. We also assessed the prevalence of the four CAC severity scores among participants with different plaque locations and different plaque dissemination status. We assessed non-adjusted Pearson correlation between four-segment scores and CAC. In order to gain insight into the genetic basis of differing plaque locations we categorized MZ and DZ twins into concordant and discordant twin pair groups.

We used OpenMx library of the R statistical program [98] for the twin statistics. Agatston score of CAC was converted to ordinary values (0: no calcification; 1: mild calcification, CACS 1-100; 2: moderate calcification, CACS 101-400; 3: severe calcification CACS >400). We used age and sex adjustment for each variable. First, we calculated univariate ACE models using a liability-threshold model to estimate heritability for each trait. Full ACE model was compared to the submodel and the most parsimonious solution was chosen using the Akaike Information Criterion.

Age and sex-adjusted polychoric phenotypic correlations between CACS and 4S_hyper were assessed in MZ, DZ and all twins. Age and sex-adjusted bivariate correlated factors model (ACE model) was used for the latent variable decomposition of phenotypic resemblance using liability-threshold structural equation model. Model selection was based on full and reduced model comparison similarly to the univariate analysis.

3.3.3 Additional methods

Additionally, we calculated the phenotypical correlation between CACS and aortic PWV in our second (190 Hungarian twins) population. Aortic PWV measurement was conducted by the same device, same methodology and the same observers as we used in our first, international study population (Tensiomed Arteriograph, Medexpert Ltd, Budapest, Hungary). As CACS in non-normally distributed and cannot be transformed, we used Spearman correlation (SPSS Statistics 17) to assess similarity between the two variables.

The second additional unpublished statistical procedure was a two-step procedure also in our second, Hungarian twin study population (N=190): first, logistic regression models were used to assess significant determinants of CAC and to test whether 4S_hyper, 4S_mixed or PWVao should be included in the models or not. We used binary values of CAC (0: no coronary calicification; 1: >0 coronary calcification score). The algebraic equation of the logistic regression gives the equation, which can predict CAC based on our model:

$$\log\left(\frac{\pi}{1-\pi}\right) = \beta_0 + \beta_1 X_1 + \cdots + \beta_{p-1} X_{p-1} \tag{3.29}$$

or in a different form:

$$\mathrm{Logit}\big(E(y)\big) = \beta_0 + \sum_{i=1}^{p-1} \beta_i X_i \tag{3.30}$$

where β_0 is the estimate of the intercept, β_i are the β estimates of the independent variables, X_i are the actual values of the independent parameters, and y is the dependent parameter (e.g., CAC). In other form, eg:

$$\Pr(y = \text{yes}) = \mathrm{logit}^{-1}(\beta_0 + \sum_{i=1}^{p-1} \beta_i X_i) \tag{3.31}$$

Then secondly, we used a machine learning method to assess the performance of the model for predicting CAC: binary classification was used based on the logistic model, the test and training set was randomly separated (ratio: 0.7:0.3) on our population (cross-validation). The threshold for the probability was assessed based on the ROC curve, where the sum of sensitivity and specificity were maximal (both statistical procedures were conducted by R statistical software, version: 4.2.3).

If we further dive into the hypothesis that twins might have a genetic predisposition to plaque colocalization (the first two affected arterial sights might be either carotid and coronary – phenotype 1, femoral and coronary – phenotype 2 or carotid and femoral –

phenotype 3) and assume that there might be some level of time delay in the manifestation of atherosclerosis phenotypes between the twin pairs we can enroll them in the following categories: 1/clear overlap 2/probable overlap 3/possible overlap 4/contradictory localization 5/not enough information - too early or too advanced state (*Figure 12*). We chose to multiply the number of participants by a weighing number for each category: twin pairs with clear overlap would be multiplied by a weighing number 3, the weighing number in category 2 is 2, and weighing number in category 3 is 1. For contradictory localization we used -1, and in case of category 5 we used number 0. By summing the weighed numbers of twins in categories 1-3 for each phenotypes we approximate and then compare the MZ to the DZ twin resemblance (*Figure 17*).

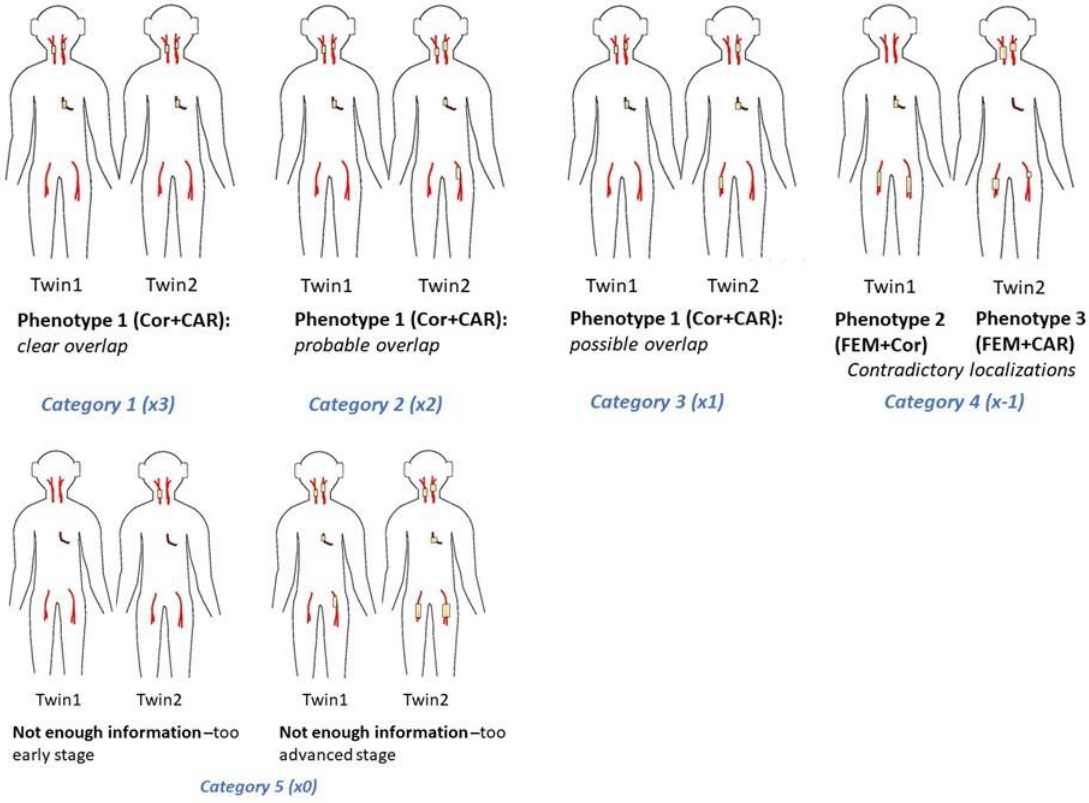

Figure 12. Categorization of twins based on the hypothesis that plaque co-localization (first two affected sites) might be genetically predisposed (own image). We also assumed that some extent of time delay in the manifestation of the phenotypes might be present between the twins. The number of twin pairs falling to each category were then multiplied by a weighing number in order to get intrapair resemblance among the monozygotic and dizygotic twins.

DOI:10.14753/SE.2024.2911

4. RESULTS

4.1. SPECIFIC AIM 1

4.1.1. Demographic, clinical characteristics and measures

Final participants' characteristics at wave 1 and wave 2 are shown below (*Table 6*). The whole study population's mean age was 51.9±12.8 years at baseline, about 1/3 of them were males. Average time of follow-up was 4.4±0.5 years. Comparisons were made regarding zygosity and country groups. At baseline, Italian twins were slightly older, their average follow-up duration also lasted a bit longer, there was a significantly higher percentage of current/ex-smokers among them, however significantly fewer participants received anti-hypertension treatment and their mean heart rate was lower compared to Hungarian twins. We found no significant differences between MZ and DZ twin characteristics. Regarding our two main traits of interest, aortic AIx significantly increased during the follow-up period both in MZ (35 ± 16% at wave 2 vs. 31 ± 15% at wave 1) and DZ (36 ± 15 % at wave 2 vs. 31 ± 15% at wave 1, $p<0.01$) twins. However, no significant changes were found in case of aortic PWV (wave 2 vs. wave 1, 9.3 ± 2.1 vs. 9.2 ± 2.3 m/s, p=0.33 in MZ twins; 9.0 ± 2.0 vs. 9.0 ± 2.1 m/s, p=0.73 in DZ twins).

4.1.2. Longitudinal twin correlations, standardized genetic and environmental components of variances and longitudinal covariances

The intra-individual longitudinal phenotypic correlation of arterial stiffness parameters showed weaker magnitude in case of aortic PWV (r=0.35, 95% confidence interval: CI: 0.25-0.45), but moderate strength in case of aortic AIx (r=0.60, 95% CI: 0.52-0.67) in all participants (*Table 7*). Cross-twin/within wave correlations were significantly higher in MZ (r_{MZ} between 0.35 and 0.6) than in DZ twins (r_{DZ} between 0.15 and 0.48) both at wave 1 and wave 2, indicating a strong genetic influence on the expression of arterial stiffness parameters. However, we can also observe that the difference between MZ and DZ correlations in the case of aortic AIx is not as prominent as in the case of aortic PWV at both waves. Cross-twin/cross-wave correlations were weak-moderate in MZ twins (r= 0.34 for aortic PWV and 0.32 for aortic AIx), however these were stronger than the correlations observed in DZ twins (r= -0.03 for aortic PWV and 0.23 for aortic AI

DOI:10.14753/SE.2024.2911

Table 6: Demographic, clinical characteristics and measures at wave 1 and wave 2 according to zygosity or country.

	Wave 1				Wave 2			
	MZ twins	DZ twins	Hungary	Italy	MZ twins	DZ twins	Hungary	Italy
Participants, N	214	154	148	220	214	154	148	220
Age (years)	51.4 (13.3)	52.5 (12.2)	48.6 (12.9)	54.1 (12.3) *	56.1 (13.4)	57.1 (12.3)	52.7 (12.8)	59.1 (12.4) *
Male sex (%)	35.5 %	33.8%	27.7%	39.5%	-	-	-	-
FU duration (years)	4.4 (0.5)	4.3 (0.6)	4.1 (0.6)	4.6 (0.3) *	-	-	-	-
BMI (kg/m^2)	26.2 (4.5)	26.9 (4.6)	26.6 (5.1)	26.4 (4.1)	26.6 (4.5)	27.1 (4.9)	27.2 (5.3)	26.4 (4.1)
Obesity (%)	19.6%	19.0%	21.6%	17.8%	20.2%	23.4%	27.9%	17.3%*
Ex smoker-current smoker (%)	40.3%	50.0%	29.5%	54.4% *	40.5%	48.3%	28.8%	52.1%*
Hypertension treatment (%)	31.3%	29.8%	37.7%	25.9% *	34.8%	31.5%	44.9%	26.9% *

DOI:10.14753/SE.2024.2911

	Wave 1				Wave 2			
	MZ twins	DZ twins	Hungary	Italy	MZ twins	DZ twins	Hungary	Italy
Cardiovascular disease (%)	7.6%	8.6%	7.5%	8.3%	9.5%	10.6%	9.3%	10.3%
SBP (mmHg)	129 (17)	127 (17)	128 (16)	128 (18)	126 (17)	127 (17)	123 (13)	129 (19)
DBP (mmHg)	77 (11)	76 (10)	77 (12)	77 (10.2)	77 (10)	77 (12)	76 (10)	77 (11)
Heart rate (bpm)	70 (11)	69 (10)	72 (10)	68 (11) *	67 (10)	65 (9)	66 (10)	67 (9)
Mean arterial pressure (mmHg)	94.2 (12.5)	93.0 (12.2)	93.7 (12.4)	93.7 (12.4)	93.1 (11.5)	93.5 (13.1)	91.7 (11)	94.4 (13.0)
Aortic PWV (m/s)	9.2 (2.3)	9.0 (2.1)	9.3 (2.6)	9.0 (2.0)	9.3 (2.1)	9.0 (2.0)	8.7 (1.9)	9.5 (2.1)
Aortic AIx (%)	31 (16)	31 (15)	28 (15)	33 (15)	35 (16)	36 (15)	34 (15)	36 (16)

Abbreviations: MZ, monozygotic; DZ, dizygotic; AIx, augmentation index; BMI, body mass index; DBP, diastolic blood pressure; SBP, systolic blood pressure; FU, follow-up; PWV, pulse wave velocity. Data are expressed as mean (standard deviation) or percentage. *$p<0.05$ (between-country comparison)

DOI:10.14753/SE.2024.2911

Table 7. Longitudinal correlations by zygosity.

	Correlations		
	All twins	**Monozygotic**	**Dizygotic**
Aortic PWV[a]			
Within-individual/cross wave correlations	0.35 (0.25-0.45)		
Cross twin/within wave 1 correlations		0.51 (0.36-0.62)	0.21 (-0.04 to 0.42)
Cross twin/within wave 2 correlations		0.50 (0.34-0.62)	0.15 (-0.10 to 0.37)
Cross twin/Cross wave correlations		0.34 (0.22 – 0.45)	-0.03 (-0.20 to 0.15)
Aortic AIx[b]			
Within-individual/cross wave correlations	0.60 (0.52-0.67)		
Cross twin/within wave 1 correlations		0.56 (0.42-0.67)	0.48 (0.27-0.63)
Cross twin/within wave 2 correlations		0.35 (0.17-0.50)	0.28 (0.06-0.47)
Cross twin/Cross wave correlations		0.32 (0.18-0.44)	0.23 (0.05-0.39)

Abbreviations: PWV, pulse wave velocity; AIx, augmentation index. Values in parentheses indicate 95% confidence intervals. [a]Adjusted by age, sex, country, between-waves changes for MAP and BMI. [b]Adjusted by age, sex, country, between-waves changes for HR and BMI.

DOI:10.14753/SE.2024.2911

Bivariate Cholesky decomposition were fitted to our longitudinal data thus allowing us to determine the contribution of additive genetic (A), common environmental (C) and unique environmental (E) factors to the variances and covariances of aortic PWV and aortic AIx at wave 1 and wave 2 (*Table 8*). A model including only additive genetic and unique environmental factors (AE model) was the best-fitting for both traits. In case of aortic PWV, heritable and unshared environmental factors' contribution to variation proved to be substantially time-independent (h^2=0.51, 95% CI 0.36-0.63 at wave 1; h^2=0.49, 95% CI 0,34-0.62 at wave 2). However, in case of aortic AIx genetic effect decreased whereas environmental contributions increased with time (h^2= 0.57, 95% CI 0.45-0.67 at wave 1; h^2=0.37, 95% CI 0.21-0.51 at wave 2).

Genetic factors contributed in a high percentage (genetic covariance: cov_g=0.88, 95%CI: 0.61-1.00) to the longitudinal covariance of aortic PWV. In turn, genetic factors explained only a lesser proportion of longitudinal covariance of aortic AIx (cov_g=0.55, 95% CI 0.35-0.70). Environmental covariation and correlation also appeared as a contributors of intermediate importance (cov_e= 0.45, 95% CI 0.30-0.65; r_e= 0.52, 95% CI 0.38-0.64). However, genetic correlations were moderate-substantial in both cases (r_g=0.64, 95% CI 0.42-0.85 for aPWW and r_g=0.70, 95% CI 0.52-0.87). We also calculated that after removing covariates, genetic covariance changed from 0.55 to 0.82 in case of aortic AIx, whereas in case of aortic PWV it changed from 0.88 to 0.98 – thus covariates (age, sex, country, between-waves changes for HR and BMI in case of AIx; age, sex, country, between-waves changes for MAP and BMI) had a greater influence on longitudinal covariance in case of aortic AIx, than aortic PWV (result not showed in table).

DOI:10.14753/SE.2024.2911

Table 8. Standardized genetic and environmental components of variance and longitudinal covariance of aortic pulse wave velocity and aortic augmentation index, as estimated from best fitting models.

	Standardized variance/covariance components		**Model fit indices[a]**			
	A	E	χ^2	ΔDF	P	AIC
Aortic PWV[b]						
Aortic PWV wave 1	0.51 (0.36-0.63)	0.49 (0.37-0.64)				
Aortic PWV wave 2	0.49 (0.34-0.62)	0.51 (0.38-0.66)				
Aortic wave PWV wave 1/ wave 2	0.88 (0.61-1.00)	0.12 (0.00-0.39)	1.92	3	0.59	-4.09
	Genetic correlation, r_g 0.64 (0.42-.85)	Environmental correlation, r_e 0.08 (0.00-0.26)				
Aortic AIx[c]						
Aortic AIx wave 1	0.57 (0.45-0.67)	0.43 (0.33-0.55)				
Aortic AIx wave 2	0.37 (0.21-0.51)	0.63 (0.49-0.79)				
Aortic AIx wave 1/wave 2	0.55 (0.35-0.70)	0.45 (0.30-0.65)	5.23	3	0.16	-0.77
	Genetic correlation, r_g 0.70 (0.52-0.87)	Environmental correlation, r_e 0.52 (0.38-0.64)				

Values given in parentheses indicate 95% confidence intervals. Abbreviations: A, additive genetic variance; E, unshared environmental variance; AIx, augmentation index; PWV, pulse wave velocity; $\chi 2$ = (-2log-likelihood sub-model)- (-2log-likelihood full model); ΔDF = (DF sub-model) - (DF full model); AIC: Akaike Information Criterion = $\chi 2$-2 ΔDF. aFull model was ACE. bAdjusted by age, sex, country, between-waves changes for mean arterial pressure (MAP) and BMI. cAdjusted by age, sex, country, between-waves changes for heart rate (HR) and BMI.

To further investigate aortic AIx heritability, augmented pressure (AP) and pulse pressure (PP) were analyzed separately (*Table 9*). Our results showed that genetic effect influencing both AP and PP decreased with time (0.30 at wave 2 and 0.48 at wave 1 for AP and 0.39 at wave 2 and 0.42 for PP), with AP showing a slightly greater diminishment and being more influenced by environmental factors in the longitudinal run. However, the genetic vs environmental covariances between waves were still rather similar in the case of AP (cov_g=0.45, 95% CI 0.23-0.64; cov_e=0.55, 95% CI 0.36-0.77), while the longitudinal covariance of PP was mainly due to bivariate heritability (cov_g=0.68, 95% CI 0.42-0.92; cov_e=0.32, 95% CI 0.08-0.58).

Table 9. Standardized genetic and environmental components of variance and longitudinal covariance of augmented pressure and pulse.

	Standardized variance/covariance components	
	A	E
Augmented pressure (AP)		
AP wave 1	0.48 (0.34-0.60)	0.52 (0.40-0.66)
AP wave 2	0.30 (0.13-0.46)	0.70 (0.54-0.87)
AP wave 1/wave 2	0.45 (0.23-0.64)	0.55 (0.36-0.77)
	Genetic correlation r_g 0.65 (0.40-0.89)	Environmental correlation r_e 0.51 (0.36-0.63)
Pulse pressure (PP)		
PP wave 1	0.42 (0.27-0.54)	0.58 (0.46-0.73)
PP wave 2	0.39 (0.23-0.52)	0.61 (0.48-0.77)
PP wave 1/wave 2	0.68 (0.42-0.92)	0.32 (0.08-0.58)
	Genetic correlation r_g 0,69 (0.44-0.95)	Environmental correlation r_e 0.22 (0.05-0.38)

Values given in parentheses indicate 95% confidence intervals. Adjusted by age, sex, country, between-waves changes for heart rate (HR) ad BMI.

4.2. SPECIFIC AIM 2

4.2.1. Descriptive statistics and phenotypic analyses

Second part of this thesis was conducted among 190 asymptomatic twin adults from the Hungarian twin registry (*Table 10*).

Table 10. Characteristics of the twin participants.

	Total	MZ	DZ	P
Zygosity	190	120	70	
Male (n,%)	72 (37.89)	48 (40)	24 (34.29)	.43
Age (mean, SD)	56.84±9.33	55.46±9.75	59.16±8.11	.01
BMI (kg/m2) (mean, SD)	27.57±4.65	27.85±4.46	27.08±4.95	.27
Hypertension (n,%)	79 (41.58)	50 (41.67)	29 (41.43)	.96
Diabetes (n,%)	14 (7.37)	10 (8.33)	4 (5.71)	.52
Dyslipidaemia (n,%)	83 (43.68)	49 (40.83)	34 (48.57)	.26
Smoking (n,%)	70 (36.84)	44 (36.67)	26 (37.14)	.89
Coronary plaque occurrence (CACS>0) (n,%)	74 (38.95)	44 (36.67)	30 (42.86)	.39
Carotid plaque occurrence (n,%)	89 (46.84)	54 (45.00)	35 (50.00)	.51
Femoral plaque occurrence (n,%)	71 (37.37)	38 (31.67)	33 (47.14)	.03
Carotid/femoral and coronary plaque co-occurrence (n,%)	65 (34.21)	39 (32.50)	26 (37.14)	.51
Carotid+femoral+coronary plaque co-occurrence (all 3) (n,%)	32 (16.84)	16 (13.33)	16 (22.86)	.09
4S_PL >1 (n,%)[1]	119 (62.63)	76 (63.33)	43 (61.43)	.79
4S_hypo >1 (n,%)[2]	71 (37.37)	46 (38.33)	25 (35.71)	.72
4S_mixed >1 (n,%)[2]	61 (34.21)	39 (32.5)	22 (31.43)	.88
4S_hyper >1 (n,%)[2]	75 (37.5)	44 (34.9)	31 (41.9)	.36
4S_mixed/hyper >1 (n,%)[2]	98 (51.58)	58 (48.33)	40 (57.14)	.38

1: Four-segment score consists of the number of arterial locations that are affected by atherosclerotic plaque (right/left carotid/femoral artery). 4S_PL refers to any plaque-type detected by ultrasound. 2: 4S_hypo refers to the four-segment score of hypoechoic plaques, 4S_mixed refers to the four-segment score of mixed plaques and 4S_hyper refers to the four-segment score of hyperechoic plaques. MZ: monozygotic, DZ: dizygotic twins, CACS: coronary artery calcification score, SD: standard deviation

DOI:10.14753/SE.2024.2911

The average age in study population was 56.84 ± 9.33 years, 37.89% were males. MZ twins were slightly younger and had more femoral atherosclerotic plaque occurrence than DZ twins – however, femoral atherosclerosis was relatively more common among DZ twins. Otherwise, there were no significant differences between the MZ and DZ groups.

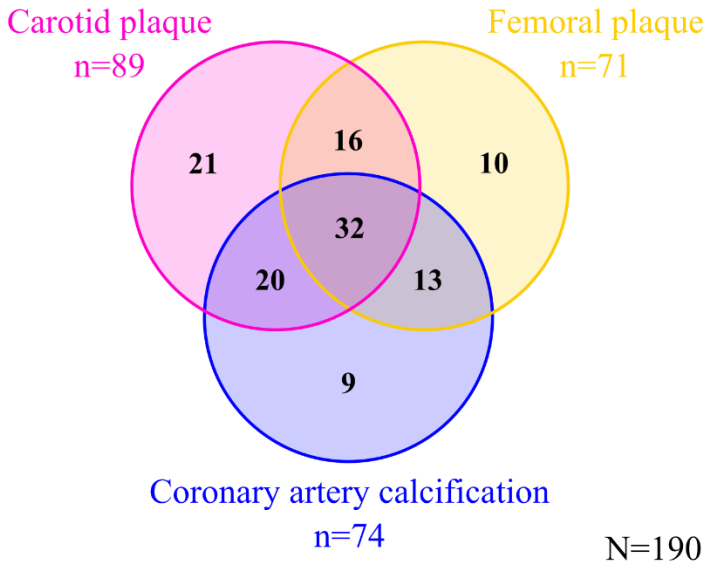

Figure 13. The Venn-diagram showing frequency of overlaps between atherosclerosis localizations in our study participants (own image).

Multi-territorial distribution of atherosclerosis can be demonstrated best by a Venn-diagram (*Figure 13*). Among the three investigated vascular territories, coronary atherosclerosis without other manifestation was the rarest (7.4% of people with atherosclerosis, 4.7% of all participants). Among participants with carotid atherosclerosis 58% had co-occurrent coronary calcification and 63% of people with femoral atherosclerosis had concomitant CAC. From all participants with atherosclerosis 26.4% had more generalized atherosclerosis affecting all three investigated segments. Seventeen percent of individuals with CAC had no sign of atherosclerosis in their carotid arteries, only in the femoral arteries. Sixty-nine (36%) study participants had no sign of atherosclerosis.

DOI:10.14753/SE.2024.2911

Demonstration of how these plaque localizations and co-occurrences distribute among the MZ and DZ twins is more difficult to show in a didactic way. Detailed lists of concordant and discordant twin pairs are presented in Tables 15-18.

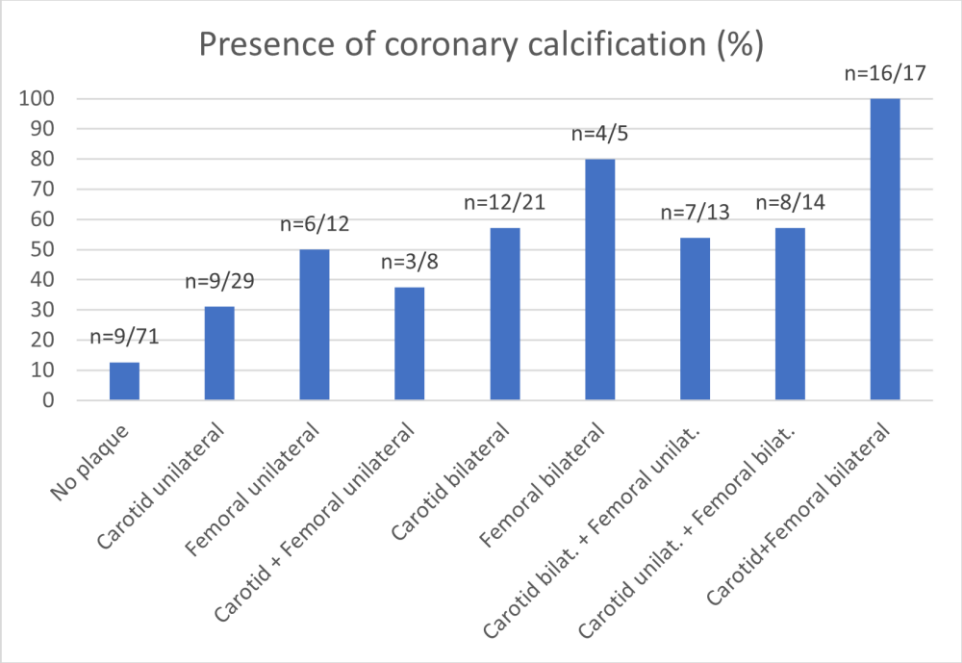

Figure 14. Prevalence of coronary calcification in participants with different distributions of plaque location in the carotid and femoral arteries.

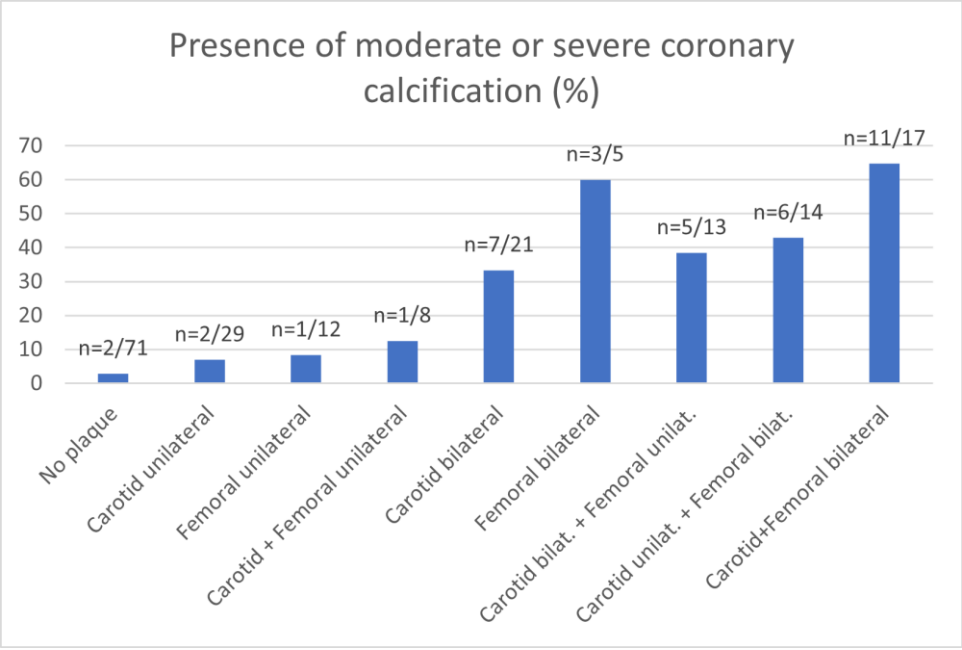

Figure 15. Prevalence of moderate or severe coronary calcification in participants with different distributions of plaque location in the carotid and femoral arteries.

DOI:10.14753/SE.2024.2911

Table 11. Relationship between coronary artery calcification severity and ultrasound findings.

	CAC severity			
	0 (n=116)	1-100 (mild) (n=36)	100-400 (moderate) (n=22)	>400 (severe) (n=16)
Localization of plaques on ultrasound:				
No plaque /4S_PL=0/ (n,%)	62 (87.32)	7 (9.86)	2 (2.82)	0 (0.00)
Unilateral Carotid /4S_PL=1/ (n,%)	20 (68.97)	7 (24.14)	1 (3.45)	1 (3.45)
Unilateral Femoral /4S_PL=1/ (n,%)	6 (50.00)	5 (41.67)	1 (8.33)	0 (0.00)
Unilateral Carotid and Femoral /4S_PL=2/ (n,%)	5 (62.50)	2 (25.00)	1 (12.50)	0 (0.00)
Bilateral Carotid /4S_PL=2/ (n,%)	9 (42.86)	5 (23.81)	4 (19.05)	3 (14.29)
Bilateral Femoral /4S_PL=2/ (n,%)	1 (20.00)	1 (20.00)	1 (20.00)	2 (40.00)
Bilateral Carotid and unilateral Femoral /4S_PL=3/ (n,%)	6 (46.15)	2 (15.38)	2 (15.38)	3 (23.08)
Bilateral Femoral and unilateral Carotid /4S_PL=3/ (n,%)	6 (42.86)	2 (14.29)	4 (28.57)	2 (14.29)
Bilateral Carotid and bilateral Femoral /4S_PL=4/ (n,%)	1 (0.06)	5 (29.41)	6 (35.29)	5 (29.41)
Generalized state according to ultrasound findings:				
Total plaque number (Mean Rank)*	73.03	111.00	136.95	163.22

DOI:10.14753/SE.2024.2911

	CAC severity			
	0 (n=116)	1-100 (mild) (n=36)	100-400 (moderate) (n=22)	>400 (severe) (n=16)
Total plaque number > Median (n,%)	33 (38.37)	20 (23.26)	17 (19.77)	16 (18.60)
Total plaque number ≤ Median (n,%)	83 (80.58)	16 (15.53)	4 (3.88)	0 (0.00)
4S_PL > Median (n,%)	27 (35.06)	17 (22.08)	18 (23.38)	15 (19.48)
4S_PL ≤ Median (n,%)	89 (78.76)	19 (16.81)	4 (3.54)	1 (0.88)
4S_hypo > Median (n,%)	35 (49.30)	14 (19.72)	10 (14.08)	12 (16.90)
4S_hypo ≤ Median (n,%)	81 (68.07)	22 (18.49)	12 (10.08)	4 (3.36)
4S_mixed > Median (n,%)	19 (31.15)	16 (26.23)	13 (21.31)	13 (21.31)
4S_mixed ≤ Median (n,%)	97 (75.19)	20 (15.50)	9 (6.98)	3 (2.32)
4S_hyper > Median (n,%)	24 (32.88)	18 (24.66)	16 (21.92)	15 (20.55)
4S_hyper ≤ Median (n,%)	92 (78.63)	18 (15.38)	6 (5.13)	1 (0.85)

Four-segment score consists of the number of arterial locations that are affected by atherosclerotic plaque (right/left carotid/femoral artery). 4S_PL refers to any plaque-type detected by ultrasound. 4S_hypo refers to the four-segment score of hypoechoic plaques, 4S_mixed refers to the four-segment score of mixed plaques and 4S_hyper refers to the four-segment score of hyperechoic plaques, CAC: coronary artery calcification. *According to Kruskall-Wallis H independent samples' test.

Our next question of interest was how ultrasound findings associate with CAC severity (*Table 11*). First, we compared anatomical localization, uni- and bilaterality of carotid/femoral atherosclerosis to CACS presence and severity (see also *Figure 14* and 15.), next we compared the four-segments scores regarding or not regarding plaque types (generalized state and severity).

The mean rank of total carotid+femoral plaque number seems to correlate well with severity of CAC. However, relatively large percentage of people (38.37%) with higher total plaque number than the median had zero CAC score. Hyperechoic (4S_hyper) or mixed plaque score (4S_mixed) above the median co-occurred with positive CAC in 67-69%, and 41-42% meant moderate or severe CAC. Hypoechoic (4S_hypo) or any type of plaque scores (4S_PL) above the median were 50-64% associated with positive CACS, 30-42% with moderate or severe CACS, demonstrating that the presence of peripheral calcification is somewhat more predictive of CAC. However, for ruling out CAC, total plaque number ≤ the median or 4S_PL ≤ the median seems to be better, than the differentiated plaque type scores (78-80% vs. 68-78%).

Table 12. Results of non-adjusted Spearman correlation between coronary artery calcifications score (CACS) and the four-segment plaque scores.

N=190	CACS	P
4S_PL (four-segment plaque score regardless of plaque type)	0.557	<0.01
4S_hypo (four-segment plaque score of hypoechoic plaques)	0.289	<0.01
4S_mixed (four-segment plaque score of mixed plaques)	0.444	<0.01
4S_hyper (four-segment plaque score of hyperechoic plaques)	0.551	<0.01
4S_mixed/hyper (four-segment score of plaques that are either mixed or hyperechogenic)	0.604	<0.01

4S_PL: four-segment plaque score as seen on ultrasound (right/left, carotid/femoral involvement) regardless of plaque-type. 4S_hypo: four-segment plaque score of hypoechoic plaques. 4S_mixed: four-segment plaque score of mixed plaques. 4S_hyper: four-segment plaque score of mixed plaques. 4S_mixed/hyper: four-segment score of plaques that are either mixed or hyperechogenic.

In the next step we calculated Spearman correlation between CACS and four-segment plaque scores and demonstrated that the distribution state of any calcification

in the carotid/femoral arteries correlated with CACS best (0.604, p<0.01, *Table 12*). However, to stick with the visual classification system treating mixed and hyperechoic plaques as different entities we chose not to merge them in the later genetic calculation, and 4s_hyper was chosen as it showed better correlation than 4s_mixed (0.551 vs 0.444, p<0.001).

4.2.2. Univariate and bivariate analyses, decomposition of concordance and discordance in plaque localization.

Univariate twin statistical analyses allow us to decompose any investigated trait to determine the contribution of underlying additive genetic (A), common environmental (C) and unique environmental (E) effects (*Table 13*). Best fitting model was chosen for each trait. We found moderate heritability for both CAC (h=0.67, 95%CI: 0.35-1) and 4S-hyper (0.69, 95% CI: 0.38-1). On the other hand, dissemination of hypoechoic plaques is mainly influenced by unique environmental factors (E=1). The 4-segment score of mixed plaque type is influenced both by genetic and unique environmental factors (h=0.49, 95% CI: 0-0.76; E= 0.50, 95%CI: 0.24-1).

Regarding the two traits that showed both high-moderate phenotypic correlation and high-moderate heritability one-by-one we performed a bivariate genetic analysis between CAC and 4S_hyper using a liability-threshold model (*Table 14*). Best-fitting model was AE model showing strong age- and sex adjusted genetic correlation between the two traits (0.86, 95%CI: 0.42-1). Polychoric adjusted phenotypic correlation was 0.48 (95%CI: 0.30-0.63) which was lower than the unadjusted correlation (0.604, p<0.01, *Table 7*.) thus demonstrating an important role of age and gender – however, the MZ correlation was higher than the DZ correlation (0.54, 95%CI 0.31-0.72 for MZ twins vs. 0.44, 95%CI 0.14-0.68 for DZ twins) also underpinning the significance of genetic influences on the similarity of traits.

As four-segments score were derived from carotid and/or femoral atherosclerosis showing better phenotypical correlation than either carotid-coronary or femoral-coronary atherosclerosis would, we sought to demonstrate how atherosclerotic plaques co-localize in MZ and DZ study participants to have an insight into the genetic background of atherosclerotic plaque localizations (*Table 15-18*).

DOI:10.14753/SE.2024.2911

Table 13. The results of univariate analyses of the investigated traits.

		Goodness-of-fit indices					Parameter estimates (95% CI)		
Trait	**Model**	AIC	-2LL	df	DiffLL	P-value	A	C	E
CAC	ACE	337.2	311.9	11	Ref.	Ref.	0.67 (0.16, 1)	0 (0, 0.38)	0.34 (0, 0.67)
	AE*	334.6	311.9	10	0	1	0.67 (0.35, 1)	-	0.34 (0, 0.65)
	CE	340.1	317.5	10	-5.5	0.02	-	0.43 (0.15, 0.66)	0.57 (0.35, 0.85)
	E	346.2	326.1	9	-14.1	0.00	-	-	1
	Sat.	346.9							
4S_hypo	ACE	408.7	378.2	13	Ref.	Ref.	0 (0, 0.41)	0.18 (0, 0.45)	0.82 (0.55, 1)
	AE	406.9	379.2	12	-0.9		0.13 (0, .45)	-	0.87 (0.56, 1)
	CE	406.0	378.2	12	0	1	-	0.18 (0, 0.45)	0.82 (0.55, 1)
	E*	404.9	379.7	11	-1.5	0.47	-	-	1
	Sat.	419.7							
4S_mixed	ACE	342.7	312.2	13	Ref.	Ref.	0.49 (0, 0.76)	0 (0, 0.49)	0.50 (0.24, 1)
	AE*	340.0	312.2	12	0	1	0.49 (0, 0.76)	-	0.50 (0.24,1)
	CE	342.4	314.6	12	-2.4	0.13	-	0.32 (0.02, 0.57)	0.68 (0.43, 0.98)
	E	344.2	319.0	11	-6.8	0.03	-	-	1
	Sat.	355.0							
4S_hyper	ACE	363.4	332.9	13	Ref.	Ref.	0.69 (0.19, 1)	0 (0.38, 1)	0.31 (0, 0.63)
	AE*	360.7	332.9	12	0	1	0.69 (0.38, 1)	-	0.31 (0, 0.63)

DOI:10.14753/SE.2024.2911

		Goodness-of-fit indices					Parameter estimates (95% CI)		
Trait	**Model**	AIC	-2LL	df	DiffLL	P-value	A	C	E
	CE	366.6	338.8	12	-5.8	0.02	-	0.41 (0.13, 0.63)	0.59 (0.37, 0.87)
	E	371.9	346.8	11	-13.9	0.00	-	-	1
	Sat.	371.9							

Calculations adjusted for age and sex. *: best-fitting model. Values in parentheses express 95% confidence intervals. Abbreviations: AIC, Akaike's Information Criteria; BIC, Bayesian Information Criteria; -2LL, -2 log-likelihood (deviance); df, degree of freedom; diffLL, difference in minus 2*log-likelihoods of the base and comparison models; A, additive genetic effects; C, common environmental effects; E, unique environmental effects.

Table 14. The results of the bivariate analysis between coronary artery calcification (CAC) and 4-segment hyperechoic plaque score (4S_hyper).

Traits	Adjust	Model	Model fit (p)	Model fit (AIC)	A	C	E
CAC and 4S_hyper	Age and sex	ACE	-	-81.9	0.99	0	0.13
		AE*	0.98	-87.8	0.86 (0.42, 1)	-	0.14 (0, 0.58)
		CE	0.01	-77.4	-	0.42	0.58
		E	0	-67.1	-	-	1
	Phenotypic correlation						
		All (95% CI)		MZ (95% CI)		DZ (95% CI)	
CAC and 4S_hyper	Age and sex	0.48 (0.30, 0.63)		0.54 (0.31, 0.72)		0.44 (0.14, 0.68)	

*: best-fitting model. AIC: Akaike's Information Criteria. A: additive genetic effect, C: common environmental effect, E: unique environmental effect.

In *Table 15*, we listed MZ twins who had coronary calcification in a descending order regarding CACS severity and grouped them into concordant and discordant pairs (concordant: both twins have CAC; discordant: only one of them has CAC). We color-coded the overlapping anatomical localizations and found that all CAC concordant MZ twins had at least one overlapping concomitant plaque localization. Out of these 17 twin pairs 13 twin pairs had also carotid atherosclerosis (76%) and 8 twin pairs had concomitant femoral atherosclerosis (47%). However, from these 8 twin pairs, only 4 had femoral-coronary atherosclerosis without overlapping concomitant carotid atherosclerosis (24%) - and these were rather among lower CACS values. MZ twin pairs discordant to CAC were fewer (n=11), had less extended CAC and less atherosclerosis on ultrasound except for one twin pair. In the latter case one twin had moderate atherosclerosis, while the other twin didn't have any atherosclerosis manifestation (*Table 15*, CAC Discordants, first MZ twin pair).

We grouped the remaining MZ twin pairs without CAC regarding their ultrasound atherosclerosis manifestations (*Table 16*). Fourteen MZ twin pairs were free from atherosclerosis in all investigated arterial beds, while 11 MZ twin pairs were discordant (only one twin had carotid and/or femoral atherosclerosis) and the remaining

DOI:10.14753/SE.2024.2911

10 twin pairs had mostly mild atherosclerosis in both twins – all of them had overlapping localization: 7 twin pairs had concordant carotid atherosclerosis, three twin pairs had concordant femoral atherosclerosis.

DOI:10.14753/SE.2024.2911

Table 15. Ultrasound findings of MZ (monozygotic) twins concordant and discordant to CAC (coronary artery calcification).

MZ	CAC Concordants:		CAC Disc	
	MZ Twin 1+ (More Severe)	MZ Twin 2+	MZ Twin1+	MZ Twin 2−
Mean CACS: 728.65	CAR.bil.o.	CAR.bil.o.	CAR.bil + FEM.bil.	-
	CACS: 1233	CACS: 224.3	CACS: 195.8	-
Mean CACS: 726.25	CAR.bil.o.	CAR.bil. + FEM.uni	CAR.uni.o.	CAR.uni.o.
	CACS: 971	CACS: 481.5	CACS: 19.71	-
Mean CACS: 556.86	CAR.bil. + FEM.uni	FEM.bil. + CAR.uni	-	CAR.uni.o.
	CACS: 822.86	CACS: 290.87	CACS: 10	-
Mean CACS: 533.02	FEM.bil.o.	FEM.bil. + CAR.uni	FEM.bil. + CAR.uni	FEM.uni.o.
	CACS: 675.83	CACS: 390.21	CACS: 7	-
Mean CACS: 499.885	CAR.bil + FEM.bil.	CAR.bil.o.	CAR.bil.o.	CAR.uni + FEM.uni
	CACS: 525.64	CACS: 474.13	CACS: 5.1	-
Mean CACS: 356.04	CAR.uni.o.	CAR.bil.o.	-	-
	CACS: 407.54	CACS: 304.54	CACS: 3.5	-
Mean CACS: 330.28	CAR.bil. + FEM.uni	CAR.bil. + FEM.uni	-	CAR.Bil.o.
	CACS: 466.98	CACS: 193.59	CACS: 2.5	-
Mean CACS: 319.5	CAR.bil. + FEM.uni	CAR.bil. + FEM.bil.	CAR.bil.o.	CAR.uni. + FEM.uni
	CACS: 360	CACS: 279	CACS: 2.23	-
Mean CACS: 254.95	CAR.bil. + FEM.bil.	CAR.uni.	-	FEM.uni.o.
	CACS: 413.58	CACS: 96.32	CACS: 2	-
Mean CACS: 193.35	CAR.uni.o.	FEM.bil. + CAR.uni	-	-
	CACS: 262.2	CACS: 124.5	CACS: 1.11	-
Mean CACS: 138.5	CAR.bil. + FEM.bil.	CAR.bil. + FEM.bil.	FEM.uni.o.	-
	CACS: 195	CACS: 82	CACS: 0.64	-
Mean CACS: 134.225	CAR.bil.o.	CAR.bil.o.		
	CACS: 259.54	CACS: 8.91		

DOI:10.14753/SE.2024.2911

MZ	CAC Concordants:		CAC Disc	
	MZ Twin 1+ (More Severe)	MZ Twin 2+	MZ Twin1+	MZ Twin 2−
Mean CACS: 124.1	FEM.bil.o.	FEM.bil. + CAR.uni		
	CACS: 209	CACS: 39.2		
Mean CACS: 71.85	CAR.uni.o.	CAR.uni.o.		
	CACS: 91.88	CACS: 51.82		
Mean CACS: 68.465	CAR.bil.o.	CAR.uni.		
	CACS: 80.7	CACS: 56.23		
Mean CACS: 39.5	FEM.uni.o.	FEM.uni.o.		
	CACS: 78	CACS: 1		
Mean CACS: 36	CAR.Bil. + FEM.bil.	FEM.uni.		
	CACS: 68.19	CACS: 3.81		

CACS: coronary artery calcification score; CAR: carotid artery; FEM: femoral artery; bil.: bilateral; uni: unilateral; o: only. Overlapping localizations are highlighted with the same color (orange or blue).

Table 16. Ultrasound findings of MZ (monozygotic) twins without CAC, grouped as: at least one of them has atherosclerotic plaque seen on ultrasound / none of them has.

MZ	0 CAC Concordants		0 CAC Concordants	
			0 US Concordants	
	MZ twin 1 (+)	MZ twin 2 (+/-)	MZ twin 1 (-)	MZ twin 2 (-)
	CAR.uni	-	-	-
	CAR.uni. + FEM.uni	-	-	-
	CAR.uni	CAR.uni	-	-
	CAR.uni	-	-	-
	CAR.bil.+ FEM.uni.	FEM.uni.o.	-	-
	CAR.bil.o.	CAR.uni.	-	-
	CAR.uni.	-	-	-

DOI:10.14753/SE.2024.2911

MZ	0 CAC Concordants		0 CAC Concordants	
			0 US Concordants	
	MZ twin 1 (+)	MZ twin 2 (+/-)	MZ twin 1 (-)	MZ twin 2 (-)
	CAR.bil.o.	CAR.bil.o.	-	-
	CAR.uni.	CAR.uni.	-	-
	FEM.Bil.	FEM.uni.	-	-
	CAR.uni	-	-	-
	CAR.bil.	CAR.uni.	-	-
	CAR.bil.	CAR.uni.	-	-
	CAR.bil.	-	-	-
	CAR.uni.	-		
	CAR.bil. + FEM.uni.	CAR.uni. + FEM.uni.		
	CAR.uni.	-		
	CAR.bil. + FEM.uni.	-		
	CAR.uni	CAR.uni		
	CAR.bilat.fem.uni.	-		
	FEM.uni.	-		

CAC: coronary artery calcification; CACS: coronary artery calcification score; CAR: carotid artery; FEM: femoral artery; bil.: bilateral; uni: unilateral; o: only. Overlapping localizations are highlighted with the same color (orange or blue).

DOI:10.14753/SE.2024.2911

Table 17. Ultrasound findings of DZ (dizygotic) twins concordant and discordant to CAC (coronary artery calcification).

DZ	CAC Concordants:		CAC Discordants:	
	DZ Twin 1+ (More Severe)	**DZ Twin 2+**	**DZ Twin 1+**	**DZ Twin 2−**
Mean CACS: 990.3	CAR.bil. + FEM.bil.	FEM.bil. + CAR.uni	FEM.bil. + CAR.uni	CAR.uni + FEM.uni
	CACS: 1248	CACS: 732.6	CACS: 728.44	-
Mean CACS: 877.5	CAR.bil. + FEM.bil	CAR.uni + FEM.uni	CAR.bil. + FEM.bil.	FEM.bil. + CAR.uni
	CACS: 1467	CACS: 288	CACS: 334.4	-
Mean CACS: 252.85	FEM.bil.o.	CAR.bil. + FEM.bil.	CAR.bil. + FEM.bil.	CAR.uni
	CACS: 413.4	CACS: 92.3	CACS: 202	-
Mean CACS: 221.65	CAR.bil + FEM.bil.	CAR.uni + FEM.uni	CAR.bil.o.	-
	CACS: 438.21	CACS: 5.09	CACS: 196	-
Mean CACS: 170.1	CAR.bil + FEM.bil.	CAR.bil. + FEM.bil.	-	-
	CACS: 256.92	CACS: 83.25	CACS: 189.3	-
Mean CACS: 86.46	FEM.uni	CAR.uni	-	CAR.uni
	CACS: 149.25	CACS: 23.68	CACS: 145.6	-
Mean CACS: 73.2	CAR.bil. + FEM.bil.	CAR.bil. + FEM.uni.	FEM.bil.o.	FEM.bil. + CAR.uni
	CACS: 79.63	CACS: 66.76	CACS: 62.69	-
Mean CACS: 68.74	FEM.bil. + CAR.uni.	CAR.bil. + FEM.uni	CAR.uni.	CAR.bilat + FEM.uni
	CACS: 114.91	CACS: 22.57	CACS: 61	-
			CAR.uni + FEM.uni	-
			CACS: 14.34	-
			-	-
			CACS: 14	-
			FEM.uni	-
			CACS: 11	-
			CAR.bil.o.	FEM.bil. + CAR.uni
			CACS: 6.36	-
			-	CAR.bil. + FEM.uni
			CACS: 3.02	-

CACS: coronary artery calcification score; CAR: carotid artery; FEM: femoral artery; bil.: bilateral; uni: unilateral; o: only. Overlapping localizations are highlighted with the same color (yellow or blue). Contradictory localizations are highlighted with red color.

Table 18. Ultrasound findings of DZ twins without CAC, grouped as: at least one of them has atherosclerotic plaque seen on ultrasound / none of them has.

DZ	0 CAC Concordants		0 CAC Concordants	
			0 US Concordants	
	DZ Twin 1	DZ Twin 2	DZ Twin 1	DZ Twin 2
	CAR.bil.o.	-	-	-
	CAR.uni.	-	-	-
	FEM.bil. + CAR.uni	CAR.bil. + FEM.bil.	-	-
	FEM.uni	-	-	-
	FEM.bil. + CAR.uni	-	-	-
	FEM.bil.o.	CAR.uni. + FEM. Uni	-	-
			-	-

CAC: coronary artery calcification; CACS: coronary artery calcification score; CAR: carotid artery; FEM: femoral artery; bil.: bilateral; uni: unilateral; o: only. Overlapping localizations are highlighted with the same color (yellow or blue).

Next, we listed and grouped the DZ twin pairs with the same logic (*Table 17-18*). Eight DZ twin pairs were CAC concordant, they rather had severe atherosclerosis both in the coronary arteries both on ultrasound. One pair had contradictory plaque localization: one twin had femoral-coronary and the other had carotid-coronary atherosclerosis. There were 13 CAC discordant DZ twin pairs. Contrary to the MZ twins, they had more frequent moderate-severe CAC (46% of discordant DZ twins vs 9% of discordant MZ twins). In this group we also found a contradictory plaque localization: one twin had only mild coronary atherosclerosis and the other twin had more severe carotid-femoral atherosclerosis without CAC (*Table 17*, CAC discordants, last twin pair).

Seven DZ twin pairs were free from atherosclerosis, four twin pairs were discordant for atherosclerosis and the remaining two DZ twin pairs had concordant moderate carotid-femoral atherosclerosis without CAC (*Table 18*).

4.2.3. Additional results

Additionally, the Spearman correlation between CACS and aortic PWV was calculated in order to assess phenotypical resemblance between the two traits (*Table 19*).

Table 19. Spearman correlation between aortic PWV (pulse-wave velocity) and CACS (coronary artery calcification score).

	Correlation with CACS	p
Aortic PWV	0.394	<0.01

In order to assess significant determinators of CACS we conducted logistic regression with model containing the following parametes: age, sex, 4S_hyper, 4S_mixed. In additional model containing age, sex, 4S_hyper, 4S_mixed and aoPWV – later parameter did not reach statistical significance (p=0.08) thus we left it out.

After creating a model with significant contributors to CAC (*Table 20*), machine learning methods were used for training on 70% of the data, which was cross-validated on the other 30% of the data giving the following results on the receiver operating curve (ROC, *Figure 16*.) and diagnostic values of model (*Table 21*).

The ROC curve shows that choosing 0.4 value as threshold we get the highest sensitivity and specificity values. The area under curve is 0.89 indicating that our model components inserted to Formula 3.31. is a good predictor for coronary artery calcification.

Table 20. Logistic regression model parameters significantly determining coronary calcification. Aortic pulse-wave velocity did not reach statistical significance thus it was left out from the model. 4S_hyper: 4-segment score of hyperechoic plaques, 4S_mixed: 4-segment score of mixed plaques.

Coefficients	**Estimate**	**St. error**	**Z value**	**P**	**Log odds**	**Log odds (2,5%)**	**Log odds (97.5%)**
Intercept	-9.38	1.85	-5.08	<0.01	0.00	0.00	0.00
Sex	1.26	0.42	2.97	<0.01	3.51	1.57	8.33
Age	0.13	0.03	4.33	<0.01	1.14	1.08	1.22
4S_hyper	0.68	0.23	2.95	<0.01	1.97	1.28	3.16
4S_mixed	0.56	0.23	2.42	0.02	1.75	1.13	2.80
Model fit parameters: null deviance: 254.03 (df = 189), residual deviance: 170.18 (df = 185), AIC: 180.18							

DOI:10.14753/SE.2024.2911

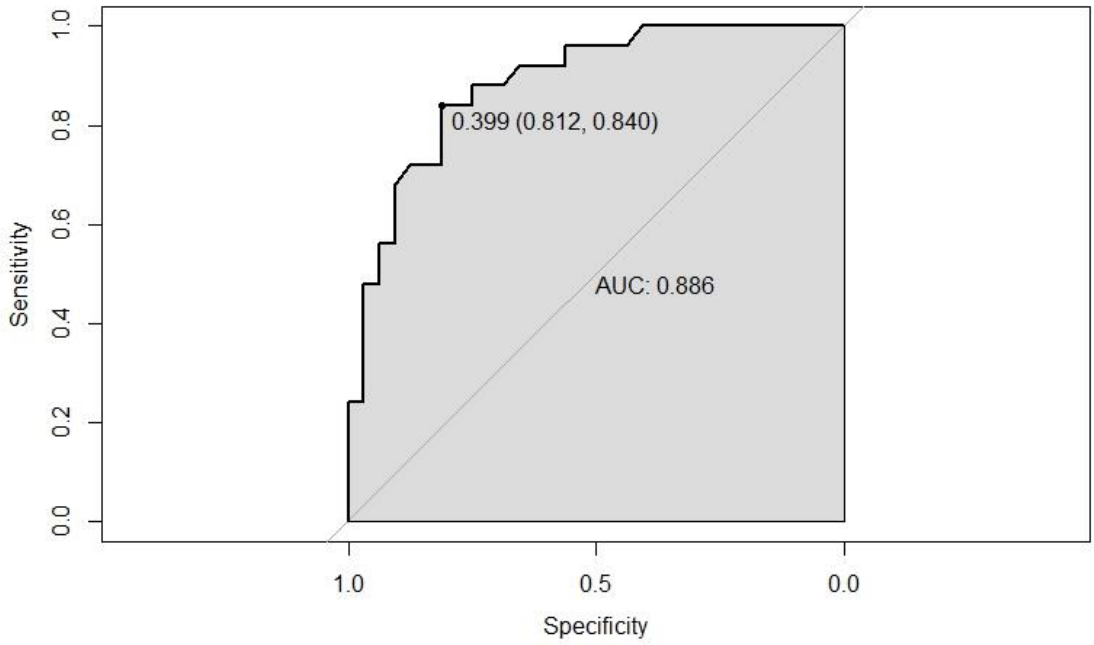

Figure 16. Receiver operating curve of model (including sex, age, 4S_hyper and 4S_mixed parameters) predicting CAC. Area under curve (AUC) is 0.89. Threshold value of 0.4 gives highest sensitivity (0.81) and specificity (0.84) values.

Other diagnostic values of our model show good overall accuracy (0.83, 95%CI: 0.70-0.91), with relatively weak negative predictive value (0.78) – however using different threshold or prediction of moderate/severe calcification state would give us even better negative predictive value (not demonstrated).

Table 21. Diagnostic values of model (containing sex, age, 4S_hyper and 4S_mixed) predicting the presence of coronary calcification.

	Value	95% confidence interval	p value
Sensitivity	0.81		
Specificity	0.84		
Positive predictive value	0.87		
Negative predictive value	0.78		
Accuracy	0.83	0.70-0.91	<0.01

Although previously in Tables 15-18. we listed all twin pairs and their plaque localisations one by one which could give us an impression on MZ twins having higher resemblance than DZ twins regarding their traits, we thought that a different

approach (*Figure 12*) could demonstrate this difference in a more illustrative way (*Figure 17*).

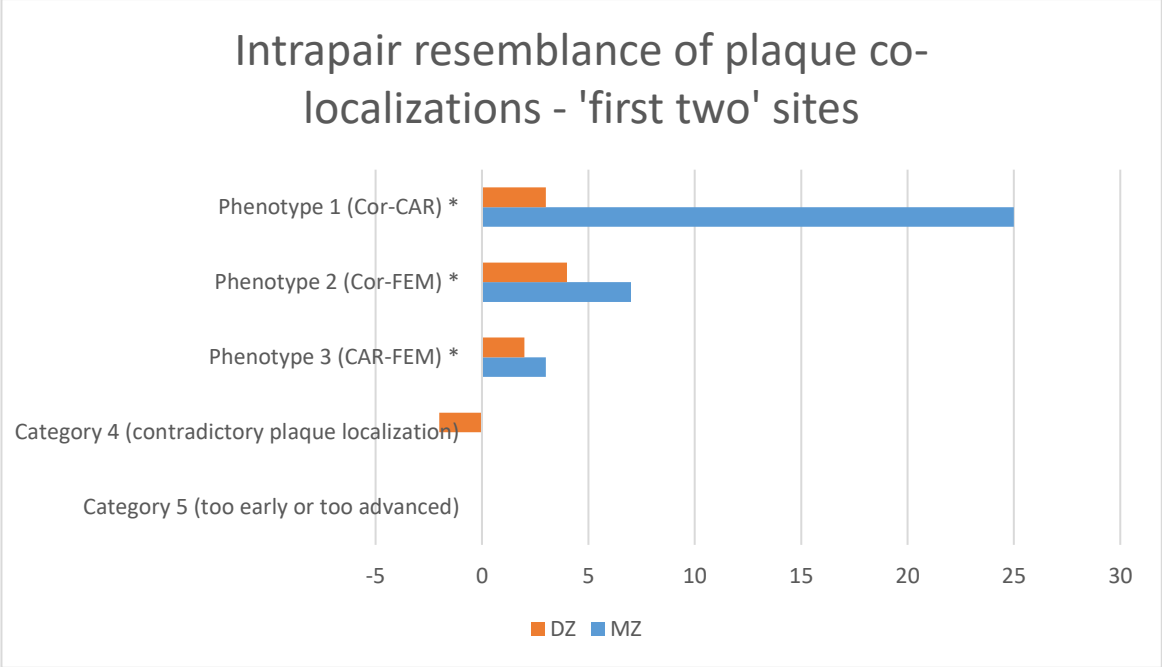

Figure 17. Graphics of the intrapair resemblance of plaque co-localizations in monozygotic (MZ) and dizygotic (DZ) twins. *: Number of twin pairs falling to category 1 (clear overlap) were multiplied by weighing number 3, number of twin pairs with probable overlap (category 2) were multiplied by 2 and number of twin pairs with possible overlap (category 3) were multiplied by 1 and all the weighted numbers of each category were summed up. Category 4 was multiplied by -1 and category 5 was multiplied by 0. Abbreviations: Cor: coronary atherosclerosis; CAR: carotid atherosclerosis, FEM: femoral atherosclerosis.

Figure 17 demonstrates the higher resemblance of MZ twins especially in regard of Phenotype 1 (coronary-carotid co-localization of atherosclerosis) – which was most frequently present as a clear overlap in MZ twins. Phenotype 2 (coronary-femoral co-localisation) was the second most common atherosclerosis manifestation showing also higher resemblance in the MZ twins. Contradictory plaque localization was not present in the MZ twins, only in the DZ twins. Notably, twin pairs falling into category 5 multiplied by zero are eliminated from this figure – not to disturb the display – however, majority of twin pairs fell into this category.

5. DISCUSSION

The topic of our twin research covers genetic vs. environmental contributions to various CV phenotypes related to chronic or acute changes in CBF – which involved longitudinal changes in arterial stiffness parameters, development of 4-segment scores (based on carotid-femoral ultrasound, potential extracoronal ATB marker), cooccurrence of carotid-coronary and femoral-coronary atherosclerosis traits. The investigated parameters are also verified or promising CV risk factors partially through reducing CBF. Aortic stiffness is known to cause acceleration of the reflected wave arriving back to the aortic root in systole instead of diastole thus limiting blood flow to the coronary arteries. Agatston score was found to correlate with the extent of CAD, associated with decreased coronary diameter and lower dilatory reserve capacity. Even in genetic atherosclerosis studies there is a missing gap - atherosclerosis phenotype specification especially in regard of generalized state and localization of atheromas. As we previously discussed, IMT is frequently treated as a surrogate for atherosclerosis, while arterial stiffness is often treated as a distinct entity – although they are both different aspects of arterio- and atherosclerosis. Our aim was to investigate the genetic patterns of CV traits in twins to gain insights into the genetic vs. environmental background of pathomechanisms indirectly leading to reduced CBF.

Our first specific aim was to assess the genetic contribution to longitudinal changes in arterial stiffness parameters such as aortic PWV and aortic AIx. Most importantly, we found that during a 4.4 year follow-up the longitudinal covariance of both parameters are in larger part genetically driven (genetic covariance for aortic PWV was cov_g=0.88 and cov_g=0.55 for aortic AIx).

Previous studies confirmed moderate heritability of aortic PWV and aortic AIx (40-50.1% for aortic PWV and 41-48.7% for AIx), meaning that the phenotypic variance is near half attributable to the genotypic variance of the study population [99-101]. Our cross-sectional heritability estimates were similar for aortic PWV (h^2=0.51 at wave 1 and h^2= 0.49 at wave 2), also showing substantial longitudinal genetic stability and moderate percentage of overlapping genes (r_g=0.64). Regarding aortic AIx, heritability at wave 1 was slightly higher (h^2=0.57) and heritability at wave 2 was lower (h^2=0.37) compared to previous heritability estimates possibly due to distinct methodological concepts.

In previous studies about the longitudinal changes of aortic PWV, follow-up for 25 years in asymptomatic adults found different rates of arterial stiffening acceleration between genders and also between different SBP groups [102]. On the contrary, during a follow-up of two years, aortic PWV values in young adults showed moderate-high tracking stability [103]. Our statistics included adjustment for age, sex, longitudinal changes in MAP and BMI. However, regarding the adjusted and unadjusted cov_g values, we saw only subtle effects of these covariates on the longitudinal run of aortic PWV (adjusted cov_g= 0.88; unadjusted cov_g= 0.98). Thus, here we demonstrated a major role of genetic contribution to longitudinal variations in aortic PWV. In contrary, Huang et al. (2021) found a diminishing role of genes on the longitudinal run in a young twin population [104]. This difference could be due to the distinct age groups and different method to measure arterial stiffness.

Taken together with our results we might suggest that arterial stiffening show a more age-related longitudinal genetic stability pattern in older patients, whereas early or accelerated vascular ageing could be more influenced by environmental factors. This idea is supported by the finding that before the age of 50 aortic AIx is more influenced by age than aortic PWV, while after the age of 50 aortic PWV is more influenced by age [41]. Similar to our results, Cecelja et al. found 55% heritability of aortic PWV progression, which was correlated with arterial dilation but not with wall thickness [105].

We acknowledged as a limitation that aortic PWV measured at the brachial arterial site by Arteriograph could less accurately reflect the central elasticity. One study found that the correlation of PWV measured by Arteriograph with stiffness measured by Sphygmocor was only 0.54-0.59 in healthy individuals [106], but another study found no significant difference between these two methods and found that body surface measurement for calculating aortic length was critical in measurement accuracy [107]. It is not unequivocal how changes in body parameters over time might have affected the calculations at the brachial site, however adjustment for BMI assured that our results were independent from changes in BMI. Duration of follow-up might have not been long enough to show differential genetic contributions in case of aortic PWV. Another limitation is that our population was not large enough to take optimal/suboptimal treatment of hypertension, untreated hypertension, or different types of antihypertensive

medication – as environmental factors – into account. We used the actual MAP value as a covariate influencing the actual PWV value.

In regard of aortic AIx we found substantial, however less genetic longitudinal stability and a higher overlapping environmental effect (r_e= 0.52) on the longitudinal phenotypic changes, which was also a novel finding. This result is in line with previous observations about higher sensitivity of aortic AIx to pathophysiological factors and pharmaceutics than aortic PWV. For example, ß-adrenerg isoprenaline reduced aortic AIx without changing aortic PWV, which was mainly due to changes in HR, SBP and diastolic blood pressure (DBP) [108]. Indeed it is known, that reflection sites (related to DBP and height), aortic PWV, amplitude of reflected wave, duration and pattern of left ventricular ejection (including heart rate and ventricular contractility) influence the value of aortic AIx [40]. Although still largely genetically influenced, aortic AIx might show more responsiveness to therapy or lifestyle changes and epigenetic influences are also possible contributors to the expression of novel genes longitudinally.

As a limitation we could not observe the forward and reflected wave components contributing to aortic AIx, although these traits have been linked to distinct genes and proteins [109]. However, in a sensitivity analysis we found that the augmented pressure wave is less genetically driven, than the pulse pressure (covg=0.45 for AP and covg=0.68 for PP).

Exponential interest in the genetic basis of arterial stiffness could be observed in the later years. Observed genetic influences include genetic polymorphisms associated with the RAAS (renin-angiotensin-aldosterone system), endothelial physiology, inflammation, matrix metalloproteases, elastin and others: ß-adrenergic receptor gene, G-protein β3 subunit, osteopontin, fetuin-A, or ectonucleotide pyrophosphatase/phosphodiesterase 1 (ENPP1) [33, 109]. Cecelja et al. investigating female twins found significant correlation between the expression levels of ENPP1 and COL4A1 (collagen type IV, alpha 1) in lymphoblastoid cell lines (among 52 genes previously associated with arterial stiffness phenotype) and longitudinal changes of aortic PWV, which could act synergistically [110]. The authors also suggested different mechanisms contributing to arterial stiffness at different vascular ages, which might partially explain differing results from cross-sectional GWAS studies.

In conclusion, our results suggest that aortic PWV is a more rigid parameter, which reflects the arterial wall's mechanistic properties better and as such – its longitudinal variance is under strong genetic control. The differences in distinct age groups in broader studies might highlight the importance of early vascular aging. AIx is dependent on many other physiological factors which could also be used as a therapeutical intervention point to lower negative consequences on coronary blood flow.

Our second specific aim was to establish a phenotypical and a possible genetic correlation between CACS and a candidate extracoronary ATB marker. Altough aortic stiffness was shown to correlate both with coronary atherosclerosis [111,112] and numerous extracoronary vessels – thus was proposed to be an indicator of generalized atherosclerosis [22] – we found only moderate phenotypic correlation between aortic PWV and CAC ($r=0.39$, $p<0.01$ – result not published). The in-house developed 4-segment score which represents the presence and dissemination state of sclerotic plaques in the carotid and femoral arteries showed stronger correlation with with CAC ($r=0.604$ for 4S_mixed/hyper and $r=0.551$ for 4S_hyper). We also found a substantial genetic overlap between the expression of 4S_hyper and CACS ($r_A=0.86$).

Previous studies found that combination of carotid and femoral ultrasound could better predict CACS than using only carotid ultrasound [113,114]. It is unclear which specific carotid-femoral ultrasound trait would best predict CACS, however we used similar approach as some other authors did. Yerly et al. used the term atherosclerosis burden score (ABS), which most likely corresponds to our 4S_PL score, summing the 'bifurcations' with atherosclerotic plaques [113]. Jarauta et al. used the term 'number of territories with plaque' – which was not further specified, could also represent similar characteristic, as 4S_PL used by us [115]. We further broke down this score according to plaque types and found different proportions of heritability to each one of them ($h^2=0$ for 4S_hypo; $h^2=0.49$ for 4S_mixed; $h^2=0.69$ for 4S_hyper). We found similar magnitude of phenotypic correlation for both 4S_PL and CACS ($r=0.557$), and 4S_hyper and CACS ($r=0.551$). We also confirmed that carotid and femoral ultrasound could predict coronary calcification with high accuracy (0.83, CI: 0.70-0.91 – result not published). Interestingly, we found that bilateral atherosclerosis in carotid or femoral arteries was also more indicative of more severe CAC than the combination of unilateral carotid and femoral atherosclerosis (in both cases the 4S_PL is 2).

Being a cross-sectional study and regarding atherosclerotic plaque progression a slow, longitudinal process, we cannot undoubtedly conclude that the formation and dissemination status of hypoechoic plaques is less heritable than the later, hyperechoic (calcified) plaque type. However, our results suggest that the process of plaque calcification might be indeed in larger part, genetically determined – moreover in a systemic or generalized manner. The mechanism of atherosclerotic plaque formation is still not fully understood. Interesting insight is that some authors suggest that atheroma formation and more extensive calcification might even be two different entities with some overlap between them [116]. Furthermore, other authors approach calcification as an evolutionary, immunobiological process, which serves as a mechanical barrier towards injurious stimuli [117]. It is possible however, that the irreversibility and "terminal state" of calcification in the atherosclerotic plaque progression make it more likely that twin pairs – who else way might have different rates of atherosclerosis progression – would resemble more in regard of this trait. Therefore, this irreversible state could explain higher heritability estimates in a cross-sectional design. Future longitudinal twin studies can help elucidate this question.

Co-heredity of coronary atherosclerosis with other arterial segments' atherosclerotic involvement hasn't been investigated in twins yet. We found high contribution of genetic factors to the correlation between CAC and 4S_hyper. Although four-segment approach permits better phenotypic correlation, our study is limited in the capability of treating carotid and femoral atherosclerosis as different entities because of relatively small sample size. However, demonstrating plaque dissemination patterns in MZ and DZ twins (Tables 15-18, Figures 12, 17.), we suggest that dissemination route of atherosclerosis is rather a genetically predisposed than a merely stochastic process. Although a high percentage of our study population had either more extended or too early atherosclerosis to investigate this question, we observed that carotid-coronary co-occurrence in MZ twins without femoral atherosclerosis findings was more common than femoral-coronary co-occurrence without carotid atherosclerosis - suggesting two distinct underlying genotype. This highlights the importance of adding femoral ultrasound screening to carotid ultrasound. Important to bare in mind – some individuals with coronary atherosclerosis might be missed by screening their carotid and femoral arteries – however on a population level our results suggest that these patients would be only 4-

5%, while carotid-femoral ultrasound could find around 87% of patients with CAC (*Figure 13*). The positive predictive value of our model including age, sex, 4S_hyper and 4S_mixed was also 87% (*Table 21*).

There is limited information about the genetics of multi-vessel atherosclerosis. Lucatelli et al. found major genetic correlation (r_g=0.77) between carotid and femoral atherosclerosis in a twin study population [79]. The Tampere Vascular study found site-specific genes only for aorta and femoral artery, but not for carotid arteries [80]. A substudy of the Rotterdam study found that the joint effect of three SNPs associated not only with calcification in the coronaries, but also with calcification in the carotid arteries and the aorta [81], which is in line with our results.

Another Tampere study investigated more thoroughly the overlapping and differing gene up- and downregulations in aortic, carotid and femoral arteries. Osteopontin was the single most upregulated gene compared to healthy individuals and it was highly upregulated in all investigated arterial beds, possibly playing a role in calcification and plaque progression. Furthermore, Apolipoprotein-D (ApoD) was down-regulated in every arterial segments. They also found differences between these arterial beds. Most significant differences were between aortic and carotid plaques (especially ApoD and C-X-C motif chemokine ligand 14, CXCL14, genes were down-regulated in the former location). Many other upregulated genes were related to inflammation and lipid transport. Apolipoprotein C1 was significantly upregulated especially in the carotid arteries. Enzyme encoding genes from the matrix-metalloprotease family were also significantly upregulated in all plaques compared to the control group. Furthermore, 50.4% of Ingenuity Canonical Pathways and 41.2% of Gene Ontology terms overlapped between all three locations, however differences were also observed. These were mostly related to the leukocyte activity of arterial wall, for example pathways that influence adhesion and diapedesis of agranulocytes [82]. These valuable results are partly in line with our findings and demonstrate differing locus minoris resistenciae of the arterial walls in distinct regions which might be a key explanation to individual differences in atherosclerosis plaque locations.

The above study is also suggestive of the validity of the other interpretation of our finding, namely that calcification is a more generalized and rather uniformly genetically driven process, which might not be arterial site-specific. Several other results

show that intra-individual inter-arterial correlation is highest among calcified plaque type, also supporting this idea [118-123].

Genetic basis of atherosclerotic calcification was extensively studied in the coronary arteries. Genes found to be involved (among others) are insertion-deletion polymorphism of the ACE (angiotensin-converting enzyme) gene [124], ApoE ε3/2 ε3/3 ε4/3 genotypes [125], MMP3 genotype [26], polymorphisms in the MGP (matrix Y-carboxyglutamic acid protein) gene [127], and TREML-4 (triggering receptor expressed on myeloid cells) gene involved in inflammatory processes [128]. The process of vascular calcification is still not fully understood. Research shows that extracellular vesicles release microcalcification which more easily confluence into macrocalcification in a collagen-poor environment [45,129-131]. Calcium-phosphate imbalance and trabecular bone formation are also thought to play a role due to the plasticity of mesenchymal cell highlighting the role of genes involved in ossification [132-134].

Despite the limitations of our study (cross-sectional design, relatively small sample size), our results support the proposal that carotid-femoral ultrasound could help re-group patients' CV risk and might help pre-select patients who would possibly benefit from CAC screening. Nowadays therapeutic options are available for extensively calcified arteries including double-wire technique, rotational and orbital atherectomy [135].

We also observed that CACS and aortic PWV are only moderately correlated, while the extracoronary large vessel 4-segment plaque scores showed better phenotypical correlation and might represent generalized state of atherosclerosis better. We do not propose to use arterial stiffness as a surrogate marker for atherosclerosis (in the sense of atheroma formation).

Highlighting the genetic background of multivessel atherosclerosis and plaque calcification, we found good correspondence with the results of broader genetic studies. Using carotid-femoral ultrasound could be a reasonable method for assessing extracoronay atherosclerosis burden. With the good phenotypical and genetical correlation with CACS we underpin the validity of examining cost-benefit studies of 4-segment scores' screening in the future. We also believe that our twin studies generate further research, which will help better understanding of the complex pathophysiology of atherosclerosis. Especially longitudinal studies about the dissemination route of

multivessel atherosclerosis would fill missing gaps. Future investigations of common (e.g. osteopontin) or differing gene expressions in dinstinct ahterosclerolerosis phenotypes might possibly help elucidate some of the reproducibility problems in genetic studies. Further development of polygenic risk scores for distinct atherosclerosis phenotypes could be the most individual and most effective way to start early prevention or raise surveillance of CV diseases.

DOI:10.14753/SE.2024.2911

6. CONCLUSIONS

In our international and national twin studies we investigated the longitudinal and cross-sectional heritability and genetic association patterns of four important and promising CV risk factors leading to reduced coronary blood flow, also potentially describing atherosclerosis burden (ATB): aortic PWV and aortic AIx (rigidity markers of the aorta), CACS and four-segment scores derived from carotid-femoral ultrasound. Our most prominent and novel findings are the following:

(1) Both aortic PWV and aortic AIx phenotypes are moderately genetically determined. Substantial genetic covariation contribute to the longitudinal expression of both these traits during a 4.4-year follow-up period.

(2) The variance components analyses showed that longitudinal changes in aortic AIx - although mainly genetically determined – are partly more sensitive to environmental factors, some of which are continuously influencing the value of aortic AIx. Therefore, therapeutics aiming to reduce aortic AIx might be more effective than in the case of aortic PWV.

(3) CACS phenotypically correlated well with both four-segment plaque score (4S_PL) and four-segment score of hyperechoic plaques (4S_hyper).

(4) Calcified plaque score of carotid/femoral arteries and CACS showed both strong-moderate heritability and we found a substantial overlap in the genetic factors contributing to these traits – therefore, our results suggest that having a high 4S_hyper score makes people more prone to have a higher CACS mainly due to genetic factors.

(5) Our results highlight the importance of genetic factors in the etiology of atherosclerosis and support both the idea of polygenic risk score assessment as earliest screening, both the idea that combined ultrasound screening of carotid and femoral atherosclerosis may have better potential use based on the good phenotypical and genetical correlation with CAC. Our proposed genetic predisposition of atherosclerosis dissemination route in multivessel atherosclerosis might generate further longitudinal studies.

DOI:10.14753/SE.2024.2911

7. SUMMARY

The polygenic background of common atherosclerotic phenotypes is not fully understood especially in regard of disease progression and multi-vessel localization.

Our first aim was to investigate the genetic contribution to the longitudinal manifestations of arterial stiffness parameters such as aortic pulse-wave velocity (PWV) and augmentation index (AIx). The second aim was to investigate the phenotypic and genetic associations of coronary artery calcification score (CACS) with carotid/femoral atherosclerosis assessed by ultrasound.

Repeated measure of aortic PWV and aortic AIx (TensioMed Arteriograph) were conducted during a follow-up of 4.4 years in 368 Italian and Hungarian twins (214 monozygotic, MZ; 154 dizygotic, DZ). Bivariate Cholesky models were implemented to decompose influences on phenotypic variances and covariances. Agatston score (non-enhanced CT) and 4-segments scores of uni/bilateral carotid/femoral atherosclerosis (B mode ultrasound) was evaluated in 120 MZ and 70 DZ Hungarian twins. We calculated heritability of plaque types and estimated both the phenotypic and genetic correlations of calcified plaques (CACS and 4S_hyper: 4-segment hyperechoic plaque score).

Aortic PWV showed moderate genetic continuity (h^2= 0.51, [95% CI 0.36-0.63] at wave 1; h^2=0.49 [95% CI 0.34-0.62] at wave 2), with genes explaining 0.88 [95% CI 0.61-1.00] covariance between the longitudinal values. Aortic AIx showed diminishing genetic contribution over time (h^2=0.57 [95% CI 0.45-0.67] at wave 1 and h^2=0.37 [95%CI 0.21-0.51] at wave 2), with relatively less but still substantial effect of genes on the longitudinal covariance (cov_g=0.55 [95% CI 0.35-0.70]). CACS and 4S_hyper were moderately heritable (0.67 [95% CI 0.37–1] and 0.69 [95% CI 0.38–1], respectively). The 4-segment score of hypoechoic plaques showed no heritability, mixed plaque type showed intermediate heritability (h2=0.50 [95% CI 0–0.76]). Age and sex adjusted phenotypic correlation between CACS and 4S_hyper was 0.48 [95% CI 0.30–0.63]. Genetic correlation between these two traits was 0.86 [95% CI: 0.42–1].

We conclude that there is a substantial role of genetic covariance in the longitudinal expression of arterial stiffness parameters. Highly overlapping genetic factors contribute to atherosclerotic calcification in the coronary, carotid and femoral arteries.

DOI:10.14753/SE.2024.2911

8. ÖSSZEFOGLALÁS

Az atherosclerosis fenotípusok poligénes háttere nem teljesen tisztázott, különösen a betegség progresszióját, illetve több ér együttes megbetegedését tekintve.

Első célkitűzésünk az volt, hogy artériás stiffness paraméterek longitudinalis genetikai hátterét vizsgáljuk: az aorta pulzushullám sebesség (PWV), valamint az augmentációs index (AIx) paramétereket. Második célkitűzésünk a koronária kalcifikáció score-ral (CACS) korreláló carotis-femoralis ultrahang fenotípus kiválasztása, illetve ezen korreláció genetikai hátterének vizsgálata volt.

Ismételt aorta PWV és AIx méréseket (TensioMed Arteriograph) végeztünk átlagosan 4.4 év különbséggel 368 olasz, illetve magyar ikerben (214 monozigóta - MZ, 154 dizigóta - DZ). Bivariáns Cholesky módszerrel bontottuk szét a kovarianciákat közös genetikai illetve környezeti eredetre. Natív CT-n állapítottuk meg az Agatston score-t, valamint B módú ultrahang vizsgálat során számítottunk 4-szegmens score-okat az uni/bilateralis carotis/femoralis atherosclerosis felmérésére 120 MZ és 70 DZ magyar ikerben. Kiszámítottuk a különböző plakktípusok örökletességét, illetve a meszes plakkok közötti genetikai korrelációt (CACS és 4S_hyper – 4 szegmens echodenz plakk score).

Az aorta PWV közepes genetikai folytonosságot mutatott az örökletességet tekintve (h^2= 0.51, [95% CI 0.36-0.63] az első méréskor; h^2=0.49 [95% CI 0.34-0.62] a második időpontban); a kovarianciát pedig nagymértékben a gének határozták meg: 0.88 [95% CI 0.61-1.00]. Az AIx tekintetében csökkenő jelentősége volt az örökletességnek: h^2=0.57 [95% CI 0.45-0.67] az első méréskor; h^2=0.37 [95%CI 0.21-0.51] a második méréskor. Az echoszegény 4S plakk score nem mutatott örökletességet, a kevert típusú plakk score közepes örökletességet adott (h2=0.50 [95% CI 0–0.76]). A CACS és echodenz 4S plakk score közötti, életkorra és nemre korrigált korreláció 0.48 [95% CI 0.30–0.63] volt, mely korreláció nagy részét egymással átfedő géneknek tulajdoníthatjuk (0.86 [95% CI: 0.42–1]).

Következtetéseink tehát, hogy jelentős részben genetikai kovariancia áll az aorta stiffness paraméterek hosszabb távon követett kifejeződésének hátterében, valamint döntően egymással átfedő genetikai hatások állnak a koszorúerek, a carotisok, valamint a femoralisok meszes plakkjainak együttes előfordulása hátterében.

9. REFERENCES

1. Timmis A, Vardas P, Townsend N, Torbica A, Katus H, De Smedt D, Gale CP, Maggioni AP, Petersen SE, Huculeci R, Kazakiewicz D, de Benito Rubio V, Ignatiuk B, Raisi-Estabragh Z, Pawlak A, Karagiannidis E, Treskes R, Gaita D, Beltrame JF, McConnachie A, Bardinet I, Graham I, Flather M, Elliot P, Mossialos EA, Weidinger F, Achenbach S. European Society of Cardiology: Cardiovascular Disease Statistics 2021. Eur Heart J. 2022; ehab892.
2. Guzik A, Bushnell C. Stroke Epidemiology and Risk Factor Management. Continuum (Minneap Minn). 2017;23:15-39.
3. Torres N, Guevara-Cruz M, Velázquez-Villegas LA, Tovar AR. Nutrition and Atherosclerosis. Arch Med Res. 2015; 46(5):408-26.
4. Khan MAB, Hashim MJ, Mustafa H, Baniyas MY, Al Suwaidi SK, AlKatheeri R, Alblooshi FM, Almatrooshi ME, Alzaabi ME, Al Darmaki RS, Lootah SN. Global epidemiology of ischemic heart disease: Results from the global burden of disease study. Cureus. 2020;12(7): e9349.
5. U.S. National Library of Medicine. Myocardial ischemia - mesh - NCBI. National Center for Biotechnology Information. [Internet] 1993 [Updated: 1993; Cited: February 13, 2023]. Available from https://www.ncbi.nlm.nih.gov/mesh/68017202.
6. U.S. National Library of Medicine. Acute coronary syndrome - mesh - NCBI. National Center for Biotechnology Information. [Internet] 2008 [Updated: 2008; Cited: February 13, 2023]. Available from https://www.ncbi.nlm.nih.gov/mesh/68054058.
7. Braunwald E, Morrow DA. Unstable angina: is it time for a requiem? Circulation. 2013;127(24): 2452–2457.
8. Gupta S, Vaidya SR, Arora S, Bahekar A, Devarapally SR. Type 2 versus type 1 myocardial infarction: A comparison of clinical characteristics and outcomes with a meta-analysis of observational studies. Cardiovasc Diagn Ther. 2017;7(4): 348–358.
9. S Ørn, K Dickstein. How do heart failure patients die? Eur Heart J Suppl. 2022;4(suppl_D):D59–D65.

10. Grey C, Jackson R, Schmidt M, Ezzati M, Asaria P, Exeter DJ, Kerr AJ. One in four major ischaemic heart disease events are fatal and 60% are pre-hospital deaths: A national data-linkage study (ANZACS-qi 8). Eur Heart J. 2015;38(3):172-180.
11. Carabello BA. Understanding coronary blood flow. Circulation. 2006;113(14):1721–1722.
12. Heward SJ, Widrich J. Coronary Perfusion Pressure. In: StatPearls [Internet]. Treasure Island (FL): StatPearls Publishing; 2023 Jan-. [Updated 2023 Mar 16; Cited: 2023. Apr 13]. Available from: https://www.ncbi.nlm.nih.gov/books/NBK551531/
13. Davies JE, Whinnett ZI, Francis DP, Manisty CH, Aguado-Sierra J, Willson K, Foale RA, Malik IS, Hughes AD, Parker KH, Mayet J. Evidence of a dominant backward-propagating "suction" wave responsible for diastolic coronary filling in humans, attenuated in left ventricular hypertrophy. Circulation. 2006;113(14):1768–1778.
14. Vijayan S, Barmby DS, Pearson IR, Davies AG, Wheatcroft SB, Sivananthan M. Assessing Coronary Blood Flow Physiology in the Cardiac Catheterisation Laboratory. Curr Cardiol Rev. 2017;13(3):232-243.
15. Severino P, D'Amato A, Pucci M, Infusino F, Adamo F, Birtolo LI, Netti L, Montefusco G, Chimenti C, Lavalle C, Maestrini V, Mancone M, Chilian WM, Fedele F. Ischemic Heart Disease Pathophysiology Paradigms Overview: From Plaque Activation to Microvascular Dysfunction. Int J Mol Sci. 2020;21(21): 8118.
16. Østergaard L, Kristiansen SB, Angleys H, Frøkiær J, Michael Hasenkam J, Jespersen SN, Bøtker HE. The role of capillary transit time heterogeneity in myocardial oxygenation and ischemic heart disease. Basic Res Cardiol. 2014;109(3):409.
17. U.S. National Library of Medicine. Atherosclerosis. National Center for Biotechnology Information. [Internet] 1993 [Updated: 1993; Cited: February 13, 2023]. Available from https://www.ncbi.nlm.nih.gov/mesh?Db=mesh&Cmd=DetailsSearch&Term=%22Atherosclerosis%22%5BMeSH%2BTerms%5D

18. Sibal L, Agarwal SC, Home PD. Carotid intima-media thickness as a surrogate marker of cardiovascular disease in diabetes. Diabetes Metab Syndr Obes. 2011;4:23-34.
19. Bots ML, Grobbee DE. Intima Media Thickness as a Surrogate Marker for Generalised Atherosclerosis. Cardiovasc Drugs Ther. 2002;16:341–351.
20. Hansen L, Taylor WR. Is increased arterial stiffness a cause or consequence of atherosclerosis? Atherosclerosis. 2016;249:226-7.
21. Kohn JC, Lampi MC, Reinhart-King CA. Age-related vascular stiffening: Causes and consequences. Front Genet. 2015;6:112.
22. van Popele NM, Grobbee DE, Bots ML, Asmar R, Topouchian J, Reneman RS, Hoeks AP, van der Kuip DA, Hofman A, Witteman JC. Association between arterial stiffness and atherosclerosis. Stroke. 2001;32(2): 454–460.
23. Maedeker JA, Stoka KV, Bhayani SA, Gardner WS, Bennett L, Procknow JD, Staiculescu MC, Walji TA, Craft CS, Wagenseil JE. Hypertension and decreased aortic compliance due to reduced elastin amounts do not increase atherosclerotic plaque accumulation in Ldlr-/- mice. Atherosclerosis. 2016;249:22–29.
24. Vatner SF, Zhang J, Vyzas C, Mishra K, Graham RM, Vatner DE. Vascular Stiffness in Aging and Disease. Front Physiol. 2021;12:762437.
25. Pirro M, Schillaci G, Paltriccia R, Bagaglia F, Menecali C, Mannarino MR, Capanni M, Velardi A, Mannarino E. Increased ratio of CD31+/CD42- microparticles to endothelial progenitors as a novel marker of atherosclerosis in hypercholesterolemia. Arterioscler Thromb Vasc Biol. 2006;26(11): 2530–2535.
26. Smulyan H, Mookherjee S, Safar ME. The two faces of hypertension: role of aortic stiffness. J Am Soc Hypertens. 2016;10(2):175–183.
27. Laurent S, Boutouyrie P, Cunha PG, Lacolley P, Nilsson PM. Concept of Extremes in Vascular Aging. Hypertension. 2019;74(2):218–228.
28. Laurent S. Defining vascular aging and cardiovascular risk. J Hypertens. 2012;30 Suppl:S3–S8.

29. Grover SA, Jekki H, Kaouache M, Lowensteyn I. Gambling With Cardiovascular Disease Risk Models: How to Choose and How to Use. Can J Cardiol. 2021;37(5):786–789.
30. Vlachopoulos C, Aznaouridis K, O'Rourke MF, Safar ME, Baou K, Stefanadis C. Prediction of cardiovascular events and all-cause mortality with central haemodynamics: a systematic review and meta-analysis. Eur Heart J. 2010;31(15):1865-71.
31. Vlachopoulos C, Aznaouridis K, Stefanadis C. Prediction of cardiovascular events and all-cause mortality with arterial stiffness: a systematic review and meta-analysis. J Am Coll Cardiol. 2010;55(13):1318-27.
32. O'Rourke MF, Yaginuma T, Avolio AP. Physiological and pathophysiological implications of ventricular/vascular coupling. Ann Biomed Eng. 1984;12(2):119-34.
33. Alvim RO, Santos PCJL, Bortolotto LA, Mill JG, Pereira AC. Arterial stiffness: Pathophysiological and genetic aspects. Int J Cardiovasc Sci. 2017;30(05):433-441.
34. Shirwany NA, Zou M. Arterial stiffness: a brief review. Acta Pharmacol Sin. 2010;31:1267–1276.
35. Tritakis V, Tzortzis S, Ikonomidis I, Dima K, Pavlidis G, Trivilou P, Paraskevaidis I, Katsimaglis G, Parissis J, Lekakis J. Association of arterial stiffness with coronary flow reserve in revascularized coronary artery disease patients. World J Cardiol. 2016;8(2):231-9.
36. Ohtsuka S, Kakihana M, Watanabe H, Sugishita Y. Chronically decreased aortic distensibility causes deterioration of coronary perfusion during increased left ventricular contraction. J Am Coll Cardiol. 1994;24(5):1406-14.
37. Watanabe H, Ohtsuka S, Kakihana M, Sugishita Y. Coronary circulation in dogs with an experimental decrease in aortic compliance. J Am Coll Cardiol. 1993;21(6):1497-506.
38. Leung MC, Meredith IT, Cameron JD. Aortic stiffness affects the coronary blood flow response to percutaneous coronary intervention. Am J Physiol Heart Circ Physiol. 2006;290(2):H624-30.

39. Bouvrain Y, Lévy B. "Windkessel" et débit coronaire ["Windkessel" and coronary debit]. Arch Mal Coeur Vaiss. 1981;74(6):635-9.
40. Laurent S, Cockcroft J, Van Bortel L, Boutouyrie P, Giannattasio C, Hayoz D, Pannier B, Vlachopoulos C, Wilkinson I, Struijker-Boudier H. Expert consensus document on arterial stiffness: Methodological issues and clinical applications. Eur Heart J. 2006;27(21):2588–2605.
41. Townsend RR, Wilkinson IB, Schiffrin EL, Avolio AP, Chirinos JA, Cockcroft JR, Heffernan KS, Lakatta EG, McEniery CM, Mitchell GF, Najjar SS, Nichols WW, Urbina EM, Weber T. American Heart Association Council on Hypertension. Recommendations for Improving and Standardizing Vascular Research on Arterial Stiffness: A Scientific Statement From the American Heart Association. Hypertension. 2015;66(3):698-722.
42. Mori H, Torii S, Kutyna M, Sakamoto A, Finn AV, Virmani R. Coronary Artery Calcification and its Progression: What Does it Really Mean? JACC Cardiovasc Imaging. 2018;11(1):127-142.
43. Wenning C, Vrachimis A, Pavenstädt HJ, Reuter S, Schäfers M. Coronary artery calcium burden, carotid atherosclerotic plaque burden, and myocardial blood flow in patients with end-stage renal disease: A non-invasive imaging study combining PET/CT and 3D ultrasound. J Nucl Cardiol. 2021;28(6):2660-2670.
44. Wang L, Jerosch-Herold M, Jacobs DR Jr, Shahar E, Detrano R, Folsom AR. MESA Study Investigators. Coronary artery calcification and myocardial perfusion in asymptomatic adults: the MESA (Multi-Ethnic Study of Atherosclerosis). J Am Coll Cardiol. 2006;48(5):1018-26.
45. Hutcheson JD, Goettsch C, Bertazzo S, Maldonado N, Ruiz JL, Goh W, Yabusaki K, Faits T, Bouten C, Franck G, Quillard T, Libby P, Aikawa M, Weinbaum S, Aikawa E. Genesis and growth of extracellular-vesicle-derived microcalcification in atherosclerotic plaques. Nat Mater. 2016;15(3):335-43.
46. Kawtharany L, Bessueille L, Issa H, Hamade E, Zibara K, Magne D. Inflammation and Microcalcification: A Never-Ending Vicious Cycle in Atherosclerosis? J Vasc Res. 2022;59(3):137-150.

47. Canet-Soulas E, Bessueille L, Mechtouff L, Magne D. The Elusive Origin of Atherosclerotic Plaque Calcification. Front Cell Dev Biol. 2021;9:622736.
48. Roquer J, Ois A. Atherosclerotic Burden and Mortality. In: Preedy VR, Watson RR (eds) Handbook of Disease Burdens and Quality of Life Measures. New York: Springer; 2010. p. 902-903.
49. Øygarden H. Carotid Intima-Media Thickness and Prediction of Cardiovascular Disease. J Am Heart Assoc. 2017;6(1):e005313.
50. Bonarjee VVS. Arterial Stiffness: A Prognostic Marker in Coronary Heart Disease. Available Methods and Clinical Application. Front Cardiovasc Med. 2018;5:64.
51. Rey-García J, Townsend RR. Large Artery Stiffness: A Companion to the 2015 AHA Science Statement on Arterial Stiffness. Pulse. 2021;9:1-10.
52. Cheong BY, Wilson JM, Spann SJ, Pettigrew RI, Preventza OA, Muthupillai R. Coronary artery calcium scoring: An evidence-based guide for Primary Care Physicians. J Int Med. 2020;289(3): 309–324.
53. Blaha M, Budoff MJ, Shaw LJ, Khosa F, Rumberger JA, Berman D, Callister T, Raggi P, Blumenthal RS, Nasir K. Absence of coronary artery calcification and all-cause mortality. JACC: Cardiovasc Imaging. 2009;2(6): 692–700.
54. Detrano R, Guerci AD, Carr, JJ, Bild DE, Burke G, Folsom AR, Liu K, Shea S, Szklo M, Bluemke, DA, O'Leary DH, Tracy R, Watson K, Wong ND, Kronmal RA. Coronary calcium as a predictor of coronary events in four racial or ethnic groups. N Engl J Med. 2008;358(13): 1336–1345.
55. Gibson AO, Blaha MJ, Arnan MK, Sacco RL, Szklo M, Herrington DM, Yeboah J. Coronary artery calcium and incident cerebrovascular events in an asymptomatic cohort. The MESA Study. JACC Cardiovasc Imaging. 2014; 11:1108-15.
56. Greenland P, Blaha MJ, Budoff MJ, Erbel R, Watson KE. (2018) Coronary Calcium Score and Cardiovascular Risk. J Am Coll Cardiol, 72(4):434-447.
57. Xie JX, Shaw LJ. Arterial calcification in cardiovascular risk prediction. Circ Cardiovasc Imaging. 2015;8(12): e003843.

58. Duvall WL, Vorchheimer DA. Multi-bed vascular disease and atherothrombosis: scope of the problem. J Thromb Thrombolysis. 2004;17(1):51-61.

59. Bos D, Leening MJ, Kavousi M, Hofman A, Franco OH, van der Lugt A, Vernooij MW, Ikram MA. Comparison of atherosclerotic calcification in major vessel beds on the risk of all-cause and cause-specific mortality. Circ Cardiovasc Imaging. 2015;8(12): e003843.

60. Prati F, Biccirè FG, Budassi S. Present and future of coronary risk assessment. Eur Heart J Supplements. 2021;23 (Supplement_E).

61. Solberg LA, Strong JP. Risk factors and atherosclerotic lesions. A review of autopsy studies. Arteriosclerosis. 1983;3(3): 187–198.

62. Odink AE, van der Lugt A, Hofman A, Hunink MG, Breteler MM, Krestin GP, Witteman JC. Association between calcification in the coronary arteries, aortic arch and carotid arteries: the Rotterdam study. Atherosclerosis. 2007;193(2):408-13.

63. Razzouk L, Rockman CB, Patel MR, Guo Y, Adelman MA, Riles TS, Berger JS. Co-existence of vascular disease in different arterial beds: Peripheral artery disease and carotid artery stenosis--Data from Life Line Screening(®). Atherosclerosis. 2015;241(2):687-91.

64. Fernández-Friera L, Peñalvo JL, Fernández-Ortiz A, Ibañez B, López-Melgar B, Laclaustra M, Oliva B, Mocoroa A, Mendiguren J, Martínez de Vega V, García L, Molina J, Sánchez-González J, Guzmán G, Alonso-Farto JC, Guallar E, Civeira F, Sillesen H, Pocock S, Ordovás JM, Sanz G, Jiménez-Borreguero LJ, Fuster V. Prevalence, Vascular Distribution, and Multiterritorial Extent of Subclinical Atherosclerosis in a Middle-Aged Cohort: The PESA (Progression of Early Subclinical Atherosclerosis) Study. Circulation. 2015;131(24):2104-13.

65. Jebari-Benslaiman S, Galicia-García U, Larrea-Sebal A, Olaetxea JR, Alloza I, Vandenbroeck K, Benito-Vicente A, Martín C. Pathophysiology of Atherosclerosis. Int J Mol Sci. 2022;23(6):3346.

66. Allam AH, Thompson RC, Wann LS, Miyamoto MI, Nur El-Din Ael-H, El-Maksoud GA, Al-Tohamy Soliman M, Badr I, El-Rahman Amer HA,

Sutherland ML, Sutherland JD, Thomas GS. Atherosclerosis in ancient Egyptian mummies: the Horus study. JACC Cardiovasc Imaging. 2011;4(4):315-27.

67. Thompson RC, Allam AH, Lombardi GP, Wann LS, Sutherland ML, Sutherland JD, Soliman MA, Frohlich B, Mininberg DT, Monge JM, Vallodolid CM, Cox SL, Abd el-Maksoud G, Badr I, Miyamoto MI, el-Halim Nur el-Din A, Narula J, Finch CE, Thomas GS. Atherosclerosis across 4000 years of human history: the Horus study of four ancient populations. Lancet. 2013;381(9873):1211-22.
68. Murphy WA Jr, Nedden DD, Gostner P, Knapp R, Recheis W, Seidler H. The iceman: discovery and imaging. Radiology. 2003;226:614–629.
69. Aragam KG, Natarajan P. Polygenic scores to assess atherosclerotic cardiovascular disease risk. Circ Res. 2020;126(9): 1159–1177
70. Frueh J, Maimari N, Homma T, Bovens SM, Pedrigi RM, Towhidi L, Krams R. Systems biology of the functional and dysfunctional endothelium, Cardiovasc Res. 2013;99(2):334–341.
71. Michel T, Vanhoutte PM. Cellular signaling and NO production. Pflugers Arch. 2010;459(6):807-16.
72. Ren K, Xu XD, Yu XH, Li MQ, Shi MW, Liu QX, Jiang T, Zheng XL, Yin K, Zhao GJ. LncRNA-modulated autophagy in plaque cells: a new paradigm of gene regulation in atherosclerosis? Aging (Albany, NY). 2020;12(21):22335-22349.
73. Lu Y, Thavarajah T, Gu W, Cai J, Xu Q. Impact of miRNA in Atherosclerosis. Arterioscler Thromb Vasc Biol. 2018;38(9):e159-e170.
74. Kuznetsova T, Prange KHM, Glass CK, de Winther MPJ. Transcriptional and epigenetic regulation of macrophages in atherosclerosis. Nat Rev Cardiol. 2020;17(4):216-228.
75. Sakamoto A, Virmani R, Finn AV. Coronary artery calcification: recent developments in our understanding of its pathologic and clinical significance. Curr Opin Cardiol. 2018;33(6):645-652.
76. Libby P. The changing landscape of atherosclerosis. Nature. 2021;592(7855):524-533

77. Libby P, Ridker PM, Hansson GK. Progress and challenges in translating the biology of atherosclerosis. Nature. 2011;473(7347):317-25.

78. Lucatelli P, Fagnani C, Tarnoki AD, Tarnoki DL, Sacconi B, Fejer B, Stazi MA, Salemi M, Cirelli C, d'Adamo A, Fanelli F, Catalano C, Maurovich-Horvat P, Jermendy AL, Jermendy G, Merkely B, Molnar AA, Pucci G, Schillaci G, Farina F, Meneghetti G, Baracchini C, Medda E. Genetic influence on femoral plaque and its relationship with carotid plaque: An international twin study. The Int J Cardiovasc Imaging. 2017;34(4): 531–541.

79. Levula M, Oksala N, Airla N, Zeitlin R, Salenius J-P, Järvinen O, Venermo M, Partio T, Saarinen J, Somppi T, Suominen VP, Virkkunen J, Hautalahti J, Laaksonen R, Kähönen M, Mennander A, Kytömäki L, Soini JT, Parkkinen J, Pelto-Huikko M, Lehtimäki T. Genes involved in systemic and arterial bed dependent atherosclerosis – tampere vascular study. PloS ONE. 2012;7(4): e33787.

80. Bos D, Ikram MA, Isaacs A, Verhaaren BF, Hofman A, Duijn CMV, Witteman JC, Lugt AVD, Vernooij MW. Genetic Loci for Coronary Calcification and Serum Lipids Relate to Aortic and Carotid Calcification. Circ Cardiovasc Genet. 2013;6(1): 47–53.

81. Sulkava M, Raitoharju E, Levula M, Seppälä I, Lyytikäinen L-P, Mennander A, Järvinen O, Zeitlin R, Salenius J-P, Illig T, Klopp N, Mononen N, Laaksonen R, Kähönen M, Oksala N, Lehtimäki T. Differentially expressed genes and canonical pathway expression in human atherosclerotic plaques – tampere vascular study. Sci Rep. 2017;7(1): 41483.

82. Posthuma D, Beem AL, de Geus EJ, van Baal GC, von Hjelmborg JB, Iachine I, Boomsma DI. Theory and practice in quantitative genetics. Twin Res. 2003;6(5):361-76.

83. de Vries LP, van Beijsterveldt TCEM, Maes H, Colodro-Conde L, Bartels M. Genetic Influences on the Covariance and Genetic Correlations in a Bivariate Twin Model: An Application to Well-Being. Behav Genet. 2021;51(3):191-203.

84. Steves CJ, Spector TD, Jackson SH. Ageing, genes, environment and epigenetics: what twin studies tell us now, and in the future. Age Ageing. 2021;41(5):581-6.

85. van Dongen J, Slagboom PE, Draisma HH, Martin NG, Boomsma DI. The continuing value of twin studies in the omics era. Nat Rev Genet. 2012;13(9):640–653.

86. Tarnoki AD, Tarnoki DL, Forgo B, Szabo H, Melicher D, Metneki J, Littvay L. The Hungarian Twin Registry update: Turning from a voluntary to a population-based registry. Twin Res Hum Genet. 2019;22(6):561–566.

87. Medda E, Toccaceli V, Fagnani C, Nisticò L, Brescianini S, Salemi M, Ferri M, D'Ippolito C, Alviti S, Arnofi A, Stazi MA. The Italian Twin Registry: An update at 18 years from its inception. Twin Res Hum Genet. 2019;22(6):572–578.

88. Rijsdijk FV, Sham PC. Analytic approaches to twin data using structural equation models. Brief Bioinform. 2002;3(2):119-33.

89. Cavanaugh JE, Neath AA. The Akaike Information Criterion: Background, derivation, properties, application, interpretation, and refinements. WIREs Comput Stat. 2019;11(3):e1460.

90. Neale M, Cardon L. Methodology for the Study of Twins and Families. In: NATO ASI Series, vol 67. Dordrecht: Springer; 1992. p. 10-52,71-125, 131-182,231-257, 289-303.

91. Heath AC, Nyholt DR, Neuman R, Madden PA, Bucholz KK, Todd RD, Nelson EC, Montgomery GW, Martin NG. Zygosity diagnosis in the absence of genotypic data: An approach using latent class analysis. Twin Res. 2003;6(1): 22–26.

92. Kyvik KO, Green A, Beck-Nielsen H. The new danish twin register: Establishment and analysis of twinning rates. Int J Epidemiol. 1995;24(3): 589–596.

93. Horvath IG, Nemeth A, Lenkey Z, Alessandri N, Tufano F, Kis P, Gaszner B, Cziraki A. Invasive validation of a new oscillometric device (Arteriograph) for measuring augmentation index, central blood pressure and Aortic Pulse Wave Velocity. 2010;J Hypertens, 28(10):2068–2075.

94. Neale MC, Boker SM, Xie G, Maes HH. Mx: Statistical Modeling. VCU Box 900126, Richmond, VA 23298: Department of Psychiatry; 2003. 83-107 p.

95. Agatston AS, Janowitz WR, Hildner FJ, Zusmer NR, Viamonte M, Detrano R. Quantification of coronary artery calcium using ultrafast computed tomography. J Am Coll Cardiol. 1990;15(4):827–832.

96. Kobayashi E, Ono J, Hirai S, Yamakami I, Saeki N, Yamaura A. Detection of Unstable Plaques in Patients with Carotid Stenosis Using B-Mode Ultrasonography. Interv Neuroradiol. 2000;6(Suppl. 1):165–170.

97. European Carotid Plaque Study Group. Carotid Artery Plaque Composition—Relationship to Clinical Presentation and Ultrasound B-Mode Imaging. Eur J Vasc Endovasc Surg. 1995;10:23–30.

98. Neale MC, Hunter MD, Pritikin JN, Zahery M, Brick TR, Kirkpatrick RM, Estabrook R, Bates TC, Maes HH, Boker SM. OpenMx 2.0: Extended Structural Equation and Statistical Modeling. Psychometrika. 2015;81:535–549.

99. Mitchell GF, DeStefano AL, Larson MG, Benjamin EJ, Chen MH, Vasan RS, Vita JA, Levy D. Heritability and a genome-wide linkage scan for arterial stiffness, wave reflection, and mean arterial pressure. Circulation. 2005;112(2): 194–199.

100. Tarnoki AD, Tarnoki DL, Stazi MA, Medda E, Cotichini R, Nisticò L, Fagnani C, Lucatelli P, Boatta E, Zini C, Fanelli F, Baracchini C, Meneghetti G, Osztovits J, Jermendy G, Préda I, Kiss RG, Metneki J, Horvath T, Karlinger K, Racz A, Lannert A, Molnar AA, Littvay L, Garami Z, Berczi V, Schillaci G. Heritability of central blood pressure and arterial stiffness: a twin study. J Hypertens. 2012;30(8):1564-71.

101. Seidlerová J, Bochud M, Staessen JA, Cwynar M, Dolejšová M, Kuznetsova T, Nawrot T, Olszanecka A, Stolarz K, Thijs L, Wojciechowska W, Struijker-Boudier HA, Kawecka-Jaszcz K, Elston RC, Fagard R, Filipovský J. Heritability and intrafamilial aggregation of arterial characteristics. J Hypertens. 2008;26(4): 721–728.

102. AlGhatrif M, Strait JB, Morrell CH, Canepa M, Wright J, Elango P, Scuteri A, Najjar SS, Ferrucci L, Lakatta EG. Longitudinal trajectories of arterial

stiffness and the role of blood pressure: the Baltimore Longitudinal Study of Aging. Hypertension. 2013;62(5):934-41.

103. Ye C, Pan Y, Xu X, Su S, Snieder H, Treiber F, Kapuku G, Wang X. Pulse wave velocity in elastic and muscular arteries: tracking stability and association with anthropometric and hemodynamic measurements. Hypertens Res. 2016;39(11):786-791.

104. Huang Y, Su S, Snieder H, Treiber F, Kapuku G, Wang X. Decreased heritability and emergence of novel genetic effects on pulse wave velocity from youth to young adulthood. Sci Rep. 2021;11(1).

105. Cecelja M, Jiang B, Keehn L, Hussain T, Silva Vieira M, Phinikaridou A, Greil G, Spector TD, Chowienczyk P. Arterial stiffening is a heritable trait associated with arterial dilation but not wall thickening: A longitudinal study in the Twins UK cohort. Eur Heart J. 2018;39(24): 2282–2288.

106. Ring M, Eriksson MJ, Zierath JR, Caidahl K. Arterial stiffness estimation in healthy subjects: A validation of oscillometric (Arteriograph) and tonometric (SphygmoCor) techniques. Hypertens Res. 2014;37(11):999–1007.

107. Rajzer MW, Wojciechowska W, Klocek M, Palka I, Brzozowska-Kiszka M, Kawecka-Jaszcz K. Comparison of aortic pulse wave velocity measured by three techniques: Complior, SPHYGMOCOR and Arteriograph. J Hypertens. 2008;26(10): 2001–2007.

108. Lemogoum D, Flores G, Van den Abeele W, Ciarka A, Leeman M, Degaute JP, van de Borne P, Van Bortel L. Validity of pulse pressure and augmentation index as surrogate measures of arterial stiffness during beta-adrenergic stimulation. J Hypertens. 2004;22(3):511–517.

109. Lacolley P, Challande P, Osborne-Pellegrin M, Regnault V. Genetics and pathophysiology of arterial stiffness. Cardiovasc Res. 2008;81(4):637–648.

110. Cecelja M, Jiang B, Mangino M, Spector TD, Chowienczyk PJ. Association of Cross-Sectional and Longitudinal Change in Arterial Stiffness With Gene Expression in the Twins UK Cohort. Hypertension. 2016;67(1):70-76.

111. van Popele NM, Mattace-Raso FU, Vliegenthart R, Grobbee DE, Asmar R, van der Kuip DA, Hofman A, de Feijter PJ, Oudkerk M, Witteman JC. Aortic

stiffness is associated with atherosclerosis of the coronary arteries in older adults: the Rotterdam Study. J Hypertens. 2006;24(12):2371-6.

112. Hofmann B, Riemer M, Erbs C, Plehn A, Navarrete Santos A, Wienke A, Silber RE, Simm A. Carotid to femoral pulse wave velocity reflects the extent of coronary artery disease. J Clin Hypertens (Greenwich). 2014;16(9):629-33.
113. Yerly P, Marquès-Vidal P, Owlya R, Eeckhout E, Kappenberger L, Darioli R, Depairon M. The atherosclerosis burden score (ABS): a convenient ultrasound-based score of peripheral atherosclerosis for coronary artery disease prediction. J Cardiovasc Transl Res. 2015;8(2):138-47.
114. Colledanchise KN, Mantella LE, Bullen M, Hétu, MF, Abunassar JG, Johri AM. Combined femoral and carotid plaque burden identifies obstructive coronary artery disease in women. J Am Soc Echocardiogr. 2020;33(1):90–100.
115. Jarauta E, Laclaustra M, Villa-Pobo R, Langarita R, Marco-Benedi V, Bea AM, León-Latre M, Casasnovas JA, Civeira F. Three Dimensional Carotid and Femoral Ultrasound is not Superior to Two Dimensional Ultrasound as a Predictor of Coronary Atherosclerosis Among Men With Intermediate Cardiovascular Risk. Eur J Vasc Endovasc Surg. 2020;59(1):129-136.
116. Henein M, Nicoll R. Atherosclerosis and extensive arterial calcification: the same condition? Int J Cardiol. 2010;14;141(1):1-2.
117. Sage AP, Tintut Y, Demer LL. Regulatory mechanisms in vascular calcification. Nat Rev Cardiol. 2010;7(9):528-536.
118. Helck A, Bianda N, Canton G, Yuan C, Hippe DS, Reiser MF, Gallino A, Wyttenbach R, Saam T. Intra-Individual Comparison of Carotid and Femoral Atherosclerotic Plaque Features with in Vivo MR Plaque Imaging. Int J Cardiovasc Imaging. 2015;31:1611–1618.
119. Zhao Q, Cai Z, Cai J, Zhao X, Li F, Yuan C. Correlation of Coronary Plaque Phenotype and Carotid Atherosclerotic Plaque Composition. Am J Med Sci. 2011;342:480–485.
120. Arad Y, Spadaro LA, Roth M, Scordo J, Goodman K, Sherman S, Lledo A, Lerner G, Guerci AD. Correlations Between Vascular Calcification and

Atherosclerosis: A Comparative Electron Beam CT Study of the Coronary and Carotid Arteries. J Comput Assist Tomogr. 1998;22:207–211.

121. Lin TC, Wright CM, Criqui MH, Allison MA. Superior Mesenteric Artery Calcification Is Associated with Cardiovascular Risk Factors, Systemic Calcified Atherosclerosis, and Increased Mortality. J Vasc Surg. 2018;67:1484–1490.

122. Allison MA, Criqui MH, Wright CM. Patterns and Risk Factors for Systemic Calcified Atherosclerosis. Arterioscler Thromb Vasc Biol. 2004;24:331–336.

123. Moreyra E, Moreyra C, Tibaldi MA, Crespo F, Arias V, Lepori AJ, Moreyra EA. Concordance and Prevalence of Subclinical Atherosclerosis in Different Vascular Territories. Vascular. 2020;28(3):285–294.

124. Pfohl M, Athanasiadis A, Koch M, Clemens P, Benda N, Häring HU, Karsch KR. Insertion/Deletion Polymorphism of the Angiotensin I-Converting Enzyme Gene Is Associated With Coronary Artery Plaque Calcification As Assessed by Intravascular Ultrasound. J Am Coll Cardiol. 1998;31:987–991.

125. Kardia SLR, Haviland MB, Ferrell RE, Sing CF. The Relationship Between Risk Factor Levels and Presence of Coronary Artery Calcification Is Dependent On Apolipoprotein E Genotype. Arterioscler Thromb Vasc Biol. 1999;19, 427–435.

126. Pöllänen PJ, Lehtimäk, T, Ilveskoski E, Mikkelsson J, Kajander OA, Laippala P, Perola M, Goebeler S, Penttilä A, Mattila KM, Syrjäkoski K, Koivula T, Nikkari ST, Karhunen PJ. Coronary Artery Calcification Is Related to Functional Polymorphism of Matrix Metalloproteinase 3: The Helsinki Sudden Death Study. Atherosclerosis. 2002;164:329–335.

127. Farzaneh-Far A, Davies JD, Braam LA, Spronk HM, Proudfoot D, Chan S-W, O'shaughnessy KM, Weissberg PL, Vermeer C, Shanahan CM. A Polymorphism of the Human Matrix γ-Carboxyglutamic Acid Protein Promoter Alters Binding of an Activating Protein-1 Complex and Is Associated with Altered Transcription and Serum Levels. J Biol Chem. 2001;276:32466–32473.

128. Sen SK, Boelte KC, Barb JJ, Joehanes R, Zhao X, Cheng Q, Adams L, Teer JK, Accame DS, Chowdhury S, Singh LN; NISC Comparative Sequencing

Program; CHARGE Consortium, Kavousi M, Peyser PA, Quigley L, Priel DL, Lau K, Kuhns DB, Yoshimura T, Johnson AD, Hwang SJ, Chen MY, Arai AE, Green ED, Mullikin JC, Kolodgie FD, O'Donnell CJ, Virmani R, Munson PJ, McVicar DW, Biesecker LG. Integrative DNA, RNA, and Protein Evidence Connects TREML4 to Coronary Artery Calcification. Am J Hum Genet. 2014;95:66–76.

129. New SEP, Goettsch C, Aikawa M, Marchini JF, Shibasaki M, Yabusaki K, Libby P, Shanahan CM, Croce K, Aikawa E. Macrophage-Derived Matrix Vesicles. Circ Res. 2013;113:72–77.

130. Kapustin AN, Davies JD, Reynolds JL, Mcnair R, Jones GT, Sidibe A, Schurgers LJ, Skepper JN, Proudfoot D, Mayr M, Shanahan CM. Calcium Regulates Key Components of Vascular Smooth Muscle Cell–Derived Matrix Vesicles to Enhance Mineralization. Circ Res. 2011;109(1):e1–e12.

131. Anderson HC. Matrix Vesicles and Calcification. Curr Rheumatol Rep. 2003;5(3):222–226.

132. Fuery MA, Liang L, Kaplan FS, Mohler ER. Vascular Ossification: Pathology, Mechanisms, and Clinical Implications. Bone. 2018;109:28–34.

133. Otsuka F, Sakakura K, Yahagi K, Joner M, Virmani R. Has Our Understanding of Calcification in Human Coronary Atherosclerosis Progressed? Arterioscler Thromb Vasc Biol. 2014;34(4):724–736.

134. Speer MY, Giachelli CM. Regulation of Cardiovascular Calcification. Cardiovasc Pathol. 2004;13(2):63–70.

135. Farag M, Costopoulos C, Gorog DA, Prasad A, Srinivasan M. Treatment of Calcified Coronary Artery Lesions. Expert Rev. Cardiovasc Ther. 2016;14(6):683–690.

DOI:10.14753/SE.2024.2911

10. BIBLIOGRAPHY OF THE CANDIDATE'S PUBLICATIONS RELATED TO THIS DISSERTATION

1. Pucci G, Tarnoki AD, Medda E, Tarnoki DL, Littvay L, Maurovich-Horvat P, Jermendy AL, Godor E, Fejer B, Hernyes A, Lucatelli P, Fanelli F, Farina F, Baracchini C, Meneghetti G, Jermendy G, Merkely B, Schillaci G, Fagnani C, Stazi MA. Genetic and environmental determinants of longitudinal stability of arterial stiffness and wave reflection: a twin study. J Hypertens. 2018; 36(12):2316-2323. (**IF: 4.209)**
2. Hernyes A, Piroska M, Fejer B, Szalontai L, Szabo H, Forgo B, Jermendy AL, Molnar AA, Maurovich-Horvat P, Jermendy G, Merkely B, Tarnoki DL, Tarnoki AD. Overlapping Genetic Background of Coronary Artery and Carotid/Femoral Atherosclerotic Calcification. Medicina (Kaunas). 2021; 57(3):252. (**IF: 2.948**)

11. BIBLIOGRAPHY OF THE CANDIDATE'S PUBLICATIONS UNRELATED TO THIS DISSERTATION

1. Tarnoki AD, Szalontai L, Fagnani C, Tarnoki DL, Lucatelli P, Maurovich-Horvat P, Jermendy AL, Kovacs A, Molnar AA, Godor E, Fejer B, Hernyes A, Cirelli C, Fanelli F, Farina F, Baracchini C, Meneghetti G, Gyarmathy AV, Jermendy G, Merkely B, Pucci G, Schillaci G, Stazi MA, Medda E. Genetic and environmental factors on heart rate, mean arterial pressure and carotid intima media thickness: a longitudinal twin study. Cardiol J. 2019; 28(3):431-438. (IF: **3,487**)
2. Medda E, Fagnani C, Alessandri G, Baracchini C, Hernyes A, Lucatelli P, Pucci G, Tarnoki AD, Tarnoki DL, Stazi MA. Association between personality profile and subclinical atherosclerosis: The role of genes and environment. Int J Cardiol. 2020; 316(1):236-239. (IF: **4.164**)
3. Forgo B, Tarnoki AD, Tarnoki DL, Kovacs DT, Szalontai L, Persely A, Hernyes A, Szily M, Littvay L, Medda E, Szabo A, Kozak LR, Rudas G, Sas A, Sepsi M, Kostyal L, Olah C. Are the Variants of the Circle of Willis Determined by Genetic or Environmental Factors? Results of a Twin Study and Review of the Literature. Twin Res Hum Genet. 2018; 21(5):384-393. (IF: **1.159**)
4. Forgo B, Medda E, Hernyes A, Szalontai L, Tarnoki DL, Tarnoki AD. Carotid Artery Atherosclerosis: a Review on Heritability and Genetics. Twin Res Hum Genet. 2018; 21(5):333-346. (IF: **1.159**)
5. Jokkel Z, Piroska M, Szalontai L, Hernyes A, Tarnoki DL, Tarnoki AD. Twin and family studies on epigenetics of autoimmune diseases (Chapter 9) in: Li S, Hopper JL (eds) Twin and Family Studies of Epigenetics. Academic Press, Cambridge; 2021. pp.169-191.
6. Szabo H, Hernyes A, Piroska M, Ligeti B, Fussy P, Zoldi L, Galyasz S, Makra N, Szabo D, Tarnoki AD, Tarnoki DL. Association between Gut Microbial Diversity and Carotid Intima-Media Thickness. Medicina (Kaunas). 2021; 57(3):195. (IF: **2.948**)
7. Alijanpourotaghsara A, Strelnikov D, Piroska M, Szalontai L, Forgo B, Jokkel Z, Persely A, Hernyes A, Kozak LR, Szabo A, Maurovich-Horvat P, Tarnoki AD, Tarnoki DL. Genetic and Environmental Effects on the Development of

White Matter Hyperintensities in a Middle Age Twin Population. Medicina (Kaunas). 2022; 10;58(10):1425. (IF: **2.948***)

8. Strelnikov D, Alijanpourotaghsara A, Piroska M, Szalontai L, Forgo B, Jokkel Z, Persely A, Hernyes A, Kozak LR, Szabo A, Maurovich-Horvat P, Tarnoki DL, Tarnoki AD. Heritability of Subcortical Grey Matter Structures. Medicina (Kaunas). 2022; 58(11):1687. (IF: **2.948***)
9. Szabo H, Piroska M, Hernyes A, Zoldi L, Juhasz J, Ligeti B, Makra N, Szabo D, Bikov A, Kunos L, Tarnoki AD, Tarnoki DL. The Relationship between Atherosclerosis and Gut Microbiome in Patients with Obstructive Sleep Apnoea. Applied Sciences. 2022; 12(22):11484. (IF: **2.838***)

* expected impact factor value

Publications in Hungarian:

1. Hernyes A, Fejér B, Szabó H, Szalontai L, Persely A, Fekete M, Szily M, Jokkel Zs, Debreceni R, Gyulai K, Szabó G, Zöldi L, Tárnoki ÁD, Tárnoki DL. Az arteria carotis communis intima-media complex sajátosságainak vizsgálata ultrahanggal – Technikai megfontolások és korrelációk egyéb atherosclerosisra utaló változókkal. Magyar Radiológia Online. 2019; 10(3):1-10.
2. Tarnoki AD, Hernyes A, Szabo H, Tarnoki DL. Genetika, epigenetika és a mikrobiom szerepe a nőgyógyászati betegségek hátterében: Ikerkutatások tapasztalatai. Magyar Nőorvosok Lapja. 2019; 82(5): 268-272
3. Fekete M, Erdei M, Dienes A, Persely A, Szily M, Bitai Z, Hernyes A, Stazi MA, Medda E, Fagnani C, Bérczi V, Tarnoki DL, Tarnoki AD. A pajzsmirigy ultrahang-elasztográfiás vizsgálata ikreken. Magyar Radiológia Online. 2019; 10(1): 5/1-10.
4. Persely A, Szily M, Dienes A, Fekete M, Hernyes A, Karlinger K, Kim E, Sung J, Bekesy-Szabo A, Rudas G, Tarnoki DL, Tarnoki AD. Az elsődleges üres sella háttere – genetika vagy környezet? Magyar Radiológia Online. 2022; 13(4): 2.
5. Mihaly G, Persely A, Hernyes A, Szabó G, Zoldi L, Beszedics B, Jokkel Z, Piroska M, Tárnoki DL, Tárnoki ÁD. Carotis-atherosclerosis ultrahangos

fenotípusainak radiomikai vizsgálata a demencia tükrében. Magyar Radiológia Online. 2023; 14(1):4/1-12.

DOI:10.14753/SE.2024.2911

12. ACKNOWLEDGEMENTS

I would like to express gratitude for the continuous support and positive reinforcements of my supervisor dr. med. habil. Tárnoki Dávid László, PhD and his twin brother dr. med. habil. Tárnoki Ádám Domonkos, PhD. Since 2014, their encouragement and mentoring were an irremissible help in my scientific career and the achievement of all our foregoing results.

I also would like to thank dr. Littvay Levente, dr. Horváth Tamás PhD, Prof. Dr. Joohon Sung (Seoul, South-Korea) and dr. Piroska Márton for sharing ideas, brainstorming about twin study designs, and helping me both in the better understanding and the implementation of twin statistics. I also thank the work of all members of the Hungarian Twin registry, the other PhD students and all the TDK students involved in our research group.

During my two Erasmus+ granted journeys in South-Korea and the United States I learned a lot about the structure and functioning of population-based twin registries, potentials and limitations of twin studies, overseas practices of vascular radiological procedures including intraoperative transcranial Doppler and MR-ultrasound fusion imaging. Special thanks to dr. Garami Zsolt (Houston, TX, US) who advocated these opportunities.

In the past years, all members of our research group were motivating, supportive and our co-operation involved a special mix of collegial and amicable relationships.

My parents, friends and relatives always upheld me. Special thanks to my grandfather Solti Péter, who planted the curiosity towards biology, medical discoveries and scientific attitude.

Finally, I would like to thank dr. Maurovich-Horvat Pál, DSc, PhD, MPH for devoting time and energy to help improve my writing style and for supporting the research work of the Hungarian Twin Registry. Also special thanks to Prof. Dr. Bérczi Viktor DSc, PhD, and Prof. Dr. med. habil. Karlinger Kinga CSc. who supported the establishment of the registry from the beginning.

The studies described in this PhD thesis were supported by research grants from Balassi Institute, Hungarian Scholarship Office and Italian Cultural Institute,

DOI:10.14753/SE.2024.2911

Semmelweis University, Directorate of International Relations and University of Padua, EFSD New Horizons Programme (letter of advice date: 04/12/2013).